GEOWISSENSCHAFTLICHE MITTEILUNGEN

Heft Nr. 69, 2004

Evolving Space Geodesy Techniques

Papers presented at the

EGS XXVII General Assembly, Nice, France, 2002

Veröffentlichung des
Instituts für Geodäsie und Geophysik

Edited by

R. Weber, W. Schlüter, U. Schreiber, O. Titov

ISSN 1811-8380

Schriftenreihe der Studienrichtung VERMESSUNG UND GEOINFORMATION
TECHNISCHE UNIVERSITÄT WIEN

2004
Published by the Institutes
of the Course on „Geodesy and Geoinformation“
of the Vienna University of Technology
Gußhausstr. 27-29
A-1040 Vienna

Responsible for this Issue: R. Weber
Printed by: Grafisches Zentrum HTU GmbH

Die Kosten für den Druck wurden vom Institut für Geodäsie und Geophysik übernommen.

Auflage: 80 Stück

ISSN 1811-8380

Table of content

Preface

At the XXVII General Assembly of the European Geophysical Society (EGS), Nice, France, April 2002, session G9 *Evolving Space Geodesy Techniques (SLR, GPS, DORIS, Altimetry, VLBI)* was one of the largest sessions of the Geodesy section. Techniques such as VLBI (Very Long Baseline Interferometry), SLR/LLR (Satellite and Lunar Laser Ranging) and microwave techniques GPS, GLONASS, and DORIS constitute the basis for space geodesy. Each of these techniques contributes in a different and unique way to the major tasks in geodesy, in particular the realization of reference frames, the determination of site coordinates and velocities, Earth rotation and gravity field. Session G9 highlighted the state-of-the-art of each individual technique and demonstrated the potential of the combination of all techniques.

At the end of the session it was decided to publish papers of the oral presentations in a special issue of the ELSEVIER journal *Physics and Chemistry of the Earth*. Several papers were submitted and were subject to a reviewing process according to the standards of the above mentioned journal. Unfortunately, due to organisational and technical problems this special issue never got published.

The main task of this issue of the *Geowissenschaftliche Mitteilungen* is to provide a platform for publishing all those papers which were - after the reviewing process - finally accepted by the guest-editors and which have not been published somewhere else. In total these are papers (three for SLR, four for GPS/Galileo, two for VLBI, and one paper on atmospheric excitation of polar motion which was also presented at EGS2002).

The variety of research topics which are treated within this issue indicates how closely geodesy is related to its neighbouring disciplines such as geophysics, meteorology, space science, and computer science. Joint efforts in different fields are needed to reach the goals which are common in modern society, such as precise navigation on Earth or in space, the realisation of precise reference frames, or a thorough description of the various interactions in 'System Earth'.

The main-editor wants to thank Wolfgang Schlüter (Wettzell), main-convenor of the EGS session, the guest-editors and the authors of the various papers making this volume a very interesting one.

Robert Weber

Evolving IVS Products and Related Observing Programs

Wolfgang Schlüter (Chair)[1], Harald Schuh (Chair of WG2)[2], Nancy Vandenberg (Director IVS Coordinating Center)[3]

[1] Bundesamt fuer Kartographie und Geodäsie, Fundamentalstation Wettzell, D-93444 Koetzting, Tel.: 49-9941-603 107, Fax: 49-9941-603 222, E-Mail: schlueter@wettzell.ifag.de
[2] Institute of Geodesy and Geophysics, Vienna University of Technology, Gusshausstrasse 27-29, A-1040 Wien, Austria, Tel.: 43-1-58801 12860, Fax: 43-1-58801 12896, E-Mail: hschuh@mars.hg.tuwien.ac.at
[3] NVI, Inc./GSFC, Code 920.1, Greenbelt MD,20771, USA, Tel.: 1-301-614-5939, Fax: 1-301-614-5970, E-Mail: nrv@gemini.gsfc.nasa.gov

Abstract

The International VLBI Service for Geodesy and Astrometry (IVS) has designed an observing program to meet its product goals, which are fundamental for the maintenance of global reference frames, in particular for observing the Earth orientation parameters (EOP's), which are essential for the transformation between the International Celestial (ICRF) and the International Terrestrial Reference Frame (ITRF). Moreover goals were set for improvements and suggestions were made as how the improvements may possibly be achieved in the future. The new IVS observing program for 2002 was established, with the overall observing time increased by 30%. Significant improvements in accuracy and timeliness can be expected. This paper describes the scientific rationale and the new observing program and discuss the resources and operational commitments that will be necessary to realize the program over the next few years.

Keywords:

Celestial reference frame, terrestrial reference frame, Earth rotation, plate tectonics, Very Long Baseline Interferometry.

1. General Remarks

The International VLBI Service for Geodesy and Astrometry (IVS) is a Service of the International Association of Geodesy (IAG), International Astronomical Union (IAU) and of the Federation of Astronomical and Geophysical Data Analysis Services (FAGS). The charter and the basis for international collaboration is given by the Terms of Reference (ToR) accepted by IAG and IAU and by the proposals provided by individual agencies in response to the call for participation.

IVS is an international collaboration of organizations that operate or support Very Long Baseline Interferometry (VLBI) components. The goals are

- to provide a service to support geodetic, geophysical and astrometric research and operational activities,
- to promote research and development activities in all aspects of the geodetic and astrometric VLBI technique,
- to interact with the community of users of VLBI products and to integrate VLBI into a global Earth observing system.

As IVS has no funds of its own, but is tasked by IAG and IAU for the provision of timely, highly accurate products (Earth Orientation Parameters (EOPs), Terrestrial Reference Frame (TRF), Celestial Reference Frame (CRF), etc.), IVS is dependent on the support of individual agencies.

In order to maintain the strong requirement for consistency, which is the basis for realizing and maintaining global reference frames such as the CRF and TRF, IVS initially employed and accepted existing infrastructure, observing programs such as the National Earth Orientation Service (NEOS), coordinated by the US Naval Observatory, or the Continuous Observations of the Rotation of the Earth

(CORE), initiated by NASA. During its first two years of existence, the efforts of IVS were concentrated on the installation of new components and adoption of new IVS tasks. Coordination of activities within the service took effort, resources and time to mature.

All the activities of the first years are documented in the Annual Reports of the IVS for the years 1999, 2000 and 2001 [1], [2], [3]. The first General Meeting was held in Kötzting/Germany in February 2000, the second General Meeting was held in Tsukuba/Japan in February 2002 and several technical meetings concerning analysis and technology aspects were conducted. Proceedings of the General Meetings are available [4],[5].

Emphasis was placed on data analysis, coordinated by the Analysis Coordinator. Today six analysis centers provide a timely, reliable, continuous solution for the entire set of five Earth Orientation Parameters (EOPs) - two polar motion coordinates, Universal Time 1 determined by the rotation of the Earth minus Coordinated Universal Time (UT1-UTC), two celestial pole coordinates. The IVS Analysis Coordinator makes a combined solution – the official IVS product - as timely input for the IERS and its combination with the GPS-, SLR/LLR- and DORIS solutions. It turns out that the IVS combined solution gains 20% in accuracy over the single VLBI solutions.

After the initiating phase of IVS as service the question “are the products appropriate to meet the service requirements” came up and a WG was initiated at the 5th Directing Board Meeting in February 2001.

2. Scientific Rationale and Motivation

For research and applications in the fields of geodesy, geokinematics, geodynamics and astronomy, as well as in space research and space application programs, highly reliable reference frames are a strong requirement. Both the CRF and the TRF are demanded, and the EOPs that are the connecting elements between the systems must be derived from observations. In order to make full use of all the results obtained in related fields and to compare results from the past with results to be obtained in the future, the consistency of the reference frames is not only of great importance, it is the strongest requirement. Descriptions of “global change” as, for example, the result of mass transport or circulation in the atmosphere, oceans and lithosphere, or as the interaction of the masses of the planets, presume that the reference systems must be realized to the state of the art. Existing space missions such as CHAMP, and upcoming missions such as GRACE and GOCE, will provide results that describe variations in the gravity field with extremely high time resolution. The high precision of new altimeter missions will result in very precise information on profiles of the Earth. Not only is the consistency of the reference frames over decades of time a demand but also the ability to describe geometric and geophysical phenomena in one common reference frame will be necessary to generate comparable results. The accuracy of information will be on the level of 10^{-8} to 10^{-9}, which at least requires a uniform reference frame precise to 10^{-9}.

A reference frame at the level of 10^{-9} cannot be achieved by only one technique. The limitation comes from observing errors, modeling errors and unknown systematic effects. A demand by IAG is the combination of results provided by various techniques so as to benefit from the different sensitivities. While satellite techniques must include the orbit integration, and employ a gravity field, VLBI directly connects the inertial reference frame, EOPs and TRF, thus eliminating one major error source. It has to be emphasized that VLBI play the fundamental role in maintaining global reference frames in particular the CRF (e.g. IAU resolutions, http://www.iau.org/IAU/Activities/publications/bulletin/, 2000).

Combination means that all techniques provide independent comparable time series, which can be combined using SINEX or, preferably, on the observation level. Combination does not mean to derive the required products by one single technique (e.g. GPS) and, if required, along with a few selected determinations of corrections from a superior technique (VLBI). This will not help to eliminate and understand systematic errors and will not support the science driven by the best time series available.

IAG has promoted the establishment of the services in order to obtain such products as time series, which finally are combinable by IERS. In the sense of IAG, the services (IVS, ILRS and IGS) must generate timely products so that a joint automatic procedure can be established to generate the final results. Investigations are required to understand discrepancies and to improve analysis procedures. Such a bootstrap technique, successfully used in the past, will help obtain a better understanding of the “changing Earth” and improve models for describing the phenomena. There is no doubt that time series obtained during the past 100 years, at the time generated on the level of state of the art, have been, and still are, of fundamental interest for research and for proving the models in related fields. As such the services are the basis for research and will drive most of the research by themselves. In its

new structure IAG acknowledges the services as the basis for all its research activities by giving the services a high rank, on the same level as the Commissions. IGGOS (Integrated Global Geodetic Observing System), a candidate IAG project, points out the strong requirement for the services and the demand for the reference frame on the level of 10^{-9}.

IVS is recognized as a service of IAU, as the VLBI technique is the only technique that uniquely realizes the inertial reference frame, the EOPs, and the TRF, which are urgently required for astronomical research and for all missions in space.

It has to be emphasized that IVS is working hard towards developing the procedures to provide their products in the required form. Further steps in organization and development are needed.

3. Review of products and observing programs

At the 4th IVS Directing Board meeting held in September 2000 in Paris, the requirement for reviewing the products and the related observing programs was discussed with the view that IVS must meet its service requirements and improve its products. Because such a review requires overall expertise, a broad discussion and acceptance within the entire community, a Working Group (WG2) for Product Specification and Observing Programs was established at the 5th Directing Board Meeting in February 2001. (The Minutes of all meetings are published and made available on the IVS web site.) The assignment of WG2 was to

- review the usefulness and appropriateness of the current definition of IVS products and suggest modifications,
- recommend guidelines for accuracy, timeliness, and redundancy of products,
- review the quality and appropriateness of existing observing programs with respect to the desired products,
- suggest a realistic set of observing programs which should result in achieving the desired products, taking into account existing agency programs,
- set goals for improvements in IVS products and suggest how these may possibly be achieved in the future,
- present a written report to the IVS Directing Board at its next meeting.

To establish a broad basis for discussion and to secure acceptance in the community, the members were chosen from among experts in the field of geodetic/astrometric VLBI. Led by Professor Harald Schuh from Technical University of Vienna as chair, the following experts are the members of the Working Group:

- Patrick Charlot, Observatoire Bordeaux/France
- Hayo Hase , Bundesamt für Kartographie und Geodäsie, Concepcion/Chile
- Ed Himwich, NVI Inc./Goddard Space Flight Center, Greenbelt/USA
- Kerry Kingham, US Naval Observatory, Washington D.C./USA
- Calvin Klatt, Geodetic Survey Division of Natural Resources Canada, Ottawa/Canda
- Chopo Ma, Goddard Space Flight Center, Greenbelt/USA
- Zinovy Malkin, Institut of Applied Astronomy, St. Petersburg/Russia
- Arthur Niell, MIT Haystack Observatory, Westford-Haystack/USA
- Axel Nothnagel, Geodätisches Institut, Universität Bonn /Germany
- Wolfgang Schlüter, Bundesamt für Kartographie und Geodäsie, Wettzell/Germany
- Kazuhiro Takashima, Geographical Survey Institute, Tsukuba/Japan
- Nancy Vandenberg , NVI Inc./Goddard Space Flight Center, Greenbelt/USA

A report of the WG2 was presented in November 2001. The IVS Directing Board reviewed the final version and accepted it for publication ,which is available under http://ivscc.gsfc.nasa.gov/WG/wg2 or in the Annual Report 2001 [6]. The report is the basis for continuous improvements and for related research within IVS over the next few years. The results of the report will help IVS meet the objectives

and future requirements set up by the IAG and IAU for research in the geosciences and astronomy. The following sections are based on the WG2 report..

4. Products and prospective improvements in the next few years

IVS is required to deliver products according to its ToR. Some products are uniquely provided by VLBI: UT1, CRF, and celestial pole; other products are available from more than one technique: Polar Motion, EOP, TRF, and certain geodynamical and physical parameters. The IVS products can be defined in terms of their accuracy, reliability, frequency of observing sessions, temporal resolution of the estimated parameters, time delay from observing to final product, and frequency of solutions. The current situation with IVS products is described in detailed tables in the WG2 report. The products, their current accuracies and the goals are summarized in table 1.

Products	Specification	Status	Goal (2002-2005)
Polar Motion x_p, y_p	accuracy	x_p ~ 100μs, y_p ~ 200μs	x_p , y_p: 50 μs ..... 25 μs
	latency	1 – 4 weeks ..... 4 months	4 – 3 days 1day
	resolution	1 day	1 day ..... 1 h ..... 10 min
	frequency of solution	+3 days/week	..... 7 days/week
UT1	accuracy	5μs .... 20 μs	3μs 2μs
	latency	1 week	4 – 3 days ..... 1 day
	resolution	1 day	1 day ..... 10 min
$\Delta\varepsilon$, $\Delta\psi$	accuracy	100 μas .... 400 μas	50 μas ..... 25 μas
	latency	1 – 4 weeks ..... 4 months	4 – 3 days ..... 1 day
	resolution	1 day	1 day
	frequency of solution	~ 3 days/week	..... 7 days/week
TRF (x, y, z)	accuracy	5 mm – 20 mm	5mm ..... 2 mm
CRF	accuracy	0.25 mas – 3 mas	0.25mas (improved distribution)
	frequency of solution	1 year	1 year
	latency	3 – 6 months	3 months .... 1 month

Table 1: Summary of IVS main products, status and goal specifications

As of late 2001, IVS products are generated from ~3 days/week observing with 6-station networks. The time delay ranges from several days up to 4 months, with an overall average value of 60 days. Over the next four years, the goals of IVS with respect to its products are the following (specific goals for each product are listed in the WG2 report tables):

- improve the accuracies of all EOP and TRF products by a factor of 2 to 4 and improve the sky distribution of the CRF,
- decrease the average time delay from 60 to 30 days, and designate 2 days per week as rapid turnaround sessions with a maximum delay of 3-4 days, starting 2002,
- increase the frequency of observing sessions from 3 to ~7 days per week,
- deliver all products on a regular, timely schedule.

It is certainly feasible to achieve these challenging goals for IVS products, if the proposed observing programs are carried out and if required improvements are realized.

The VLBI technique will allow to provide side-products and IVS intents to set up the products summarized in table 2.

Earth Orientation Parameter additions	• dUT1/dt (length of day) • dx_p /dt; dy_p /dt
Terrestrial Reference frame (TRF)	• x- , y- , z – time series • Episodic events • Annual solutions • Non linear changes
Celestial Reference Frame (CRF)	• Source structure • Flux density
Geodynamical Parameter	• Solid Earth tides (Love numbers h, l) • Ocean loading (amplitudes and phases A_i, $\varphi_{\square}$ • Atmospheric loading (site-dependent coefficients)
Physical Parameter	• Tropospheric parameters (e.g.1st IVS Pilot Project) • Ionospheric mapping • Light deflection parameter γ

Table 2: Extended products derived by VLBI and intented to be provided by IVS

5. Evolving observing programs

To meet its product goals IVS has designed an observing program which was coordinated with the international community beginning with the 2002 observing year. The observing program includes the following sessions:

- EOP: Two rapid turnaround sessions each week, initially with 6 stations, increasing to 8 when station and recording media resources are available in future years. These networks will be designed to have comparable x_p and y_p results. One-baseline 1-hr INTENSIVE sessions four times per week, with at least one parallel session.
- TRF: Monthly TRF sessions with 8 stations including a core network of 4 to 5 stations and using all other stations three to four times per year. The number of stations may be increased if the correlator can support the increase data load.
- CRF: Bi-monthly RDV sessions using the Very Long Baseline Array (VLBA) and 10 geodetic stations, plus quarterly astrometric sessions to observe mostly southern sky sources.
- Monthly R&D sessions to investigate instrumental effects, research the network offset problem, and study ways for technique and product improvement.
- Annual, or semi-annual if resources are available, 14-day continuous sessions to demonstrate the best results that VLBI can offer, aiming for the highest sustained accuracy.

Although certain sessions have primary goals, such as CRF, all sessions are scheduled so that they contribute to all geodetic and astrometric products. Sessions in the observing program that are recorded and correlated using S2 or K4 technology will have the same accuracy and timeliness goals as those using Mk4 or Mk5.

To support the IVS Coordinating Center in the coordination of the observing program with the international community and to realize the new program a Observing Program Committee has been established. The new observing program already started in January 2002.

The observing programs and product delivery can only be accomplished by making some changes and improvements in IVS observing program resources (station days, correlator time, and magnetic media), by improving and strengthening analysis procedures, and by pursuing a vigorous technology development program.

6. Requirements to IVS components

The WG2 report contains many recommendations for different aspects of IVS, its products, and its programs. What follows is a summary of the most important ideas.

Program resources: The number of required station observing days increases by about 30% over the next two years and by 2005 the top dozen geodetic stations will need to be observing up to 4 days per week. Increased station reliability and unattended operations can improve temporal coverage by VLBI and also allow substantial savings in operating costs. Higher data rate sessions can yield more accurate results, and therefore all geodetic stations must be upgraded to Mk4 or Mk5 capability as soon as possible. More stations need to be equipped with S2 and K4 systems so that global geodetic networks can be designed using these systems. The present level of support at the three Mk4 correlators must be sustained to meet the IVS product goals, and support is needed from the S2 and K4 correlators. The efficiency of the correlators needs to approach a processing factor of unity, i.e. one day processing for one day observing. All correlators must commit to handling the IVS data with priority processing for meeting timely product delivery requirements. Additional recording media capacity, equivalent to ~100 Mk4 tapes, will be needed to support the higher data rate observing that is necessary for increased accuracy. Alternatively, additional media capacity can be realized by using rapid shipping modes to shorten the tape cycle time.

Analysis: More analysis centers and those using different software packages should participate in the analysis that is required for robust IVS products. The increased amount of VLBI data to be produced under the new observing program will require analysis centers to handle a larger load. Partially automated analysis procedures will help improve the timeliness of product delivery. New IVS products such as EOP rates, a combined TRF solution, tropospheric parameters and geodynamical parameters should be developed because they can contribute to scientific investigations.

Technology upgrades and improvements: The Mk5 system under development should be deployed as soon as feasible because not only will it enable higher data rate recording but it will also improve station and correlator reliability and efficiency. In addition, new methods for data transmission, including electronic media, should be strongly pursued because higher data rates, automated observing and processing methods will lead to increased accuracy, reliability, timeliness, and efficient use of resources.

At the 2nd IVS General Meeting held in Tsukuba/Japan in February 2002 the following resolution has been released:

Tsukuba, February 6, 2002

The International VLBI Service for Geodesy and Astrometry

recognizing

1) that geodetic and astrometric VLBI is fundamental for the establishment and maintenance of the ICRF and contributes extensively to the generation of the ITRF, and
2) that geodetic VLBI plays an essential role in geodesy and astrometry due to its uniqueness in observing the complete set of Earth orientation parameters (EOPs) which describes the transformation between the ICRF and ITRF stable over a time span longer than a few days, and
3) that providing the reference frames and EOPs consistent over decades on the highest accuracy level will be a challenging role for IVS,

noting

the final report of the IVS Working Group 2 for Product Specifications and Observing Programs,

recommends

that all IVS components should concentrate their effort and resources to accomplish the following objectives:

- signifcant improvements of the accuracy of VLBI products
- shorter time delay from observation to availability of results
- continuous temporal coverage by VLBI sessions.

7. Conclusions

IVS has the capacity to meet the requirements set up by IAG and IAU in the realization of the reference frames and related products. In general, precise time series of the products, with sufficient accuracy (bias free), density, and timeliness must be generated. IVS as a Technique Center of IERS must guarantee the realization of precise celestial and terrestrial reference frames that are consistent over decades.

To meet this guarantee, improvements are required in the availability and reliability of the network stations. Automation for unattended observing will help to overcome the weekend gaps. More capacity is required in data transmission media, which will be solved by the development of a modern disk based recording system (Mk5) and by the ability to transfer data via the Internet (e-VLBI). These new systems will reduce the time delay and dramatically reduce expenses currently needed for tapes and tape drives. The global network configuration has to be improved, especially in the southern hemisphere, and more observing time is required. Encouraging additional related institutions and including the S2 and K4 technologies will also improve the situation. High priority has to be placed on rapid turnaround sessions at the correlator. To avoid backlogs the throughput at the correlators has to be improved. More analysis centers with different software are required to improve the analysis and to increase the robustness of the products.

IVS's primary duty is to provide the best possible results through optimized and efficient coordination of all the resources available. The new product specifications and the new related observing programs should give the basis for cooperation and for contributions by collaborating institutions. Nevertheless, the current IVS situation is highly dependent on only a few institutions and requires the strong, continued support and contributions of those key players.

8. References

[1] Vandenberg, N.R. (editor): Annual Report 1999, NASA/TP-1999-209243, Greenbelt, MD, August 1999

[2] Vandenberg, N. R., Baver K.D.(editors): Annual Report 2000, NASA/TP-2001-209979, Greenbelt, MD; February 2001

[3] Vandenberg, N. R., Baver K.D.(editors): Annual Report 2001, NASA/TP-2002-210001, Greenbelt, MD; February 2002

[4] Vandenberg, N. R., Baver K.D.(editors): 2000 General Meeting Proceedings, NASA/CP-2000-209893, Greenbelt, MD; June 2000

[5] Vandenberg, N. R., Baver K.D.(editors): 2002 General Meeting Proceedings, NASA/CP-2002-210002, Greenbelt, MD; June 2002

[6] Schuh, H. et al.; IVS Working Group 2 for Product Specification and Observing programs, Final Report, Annual Report 2001, page 13 – 45, NASA/TP-2002-210001, Greenbelt, MD; February 2002

all references can be downloaded from the IVS homepage (http://ivscc.gsfc.nasa.gov)

Comparison and combination of tropospheric parameters determined by several VLBI Analysis Centers

Eva Messerer[1], Johannes Boehm[1], Harald Schuh[1]

[1] Institute of Geodesy and Geophysics IGG, University of Technology, Vienna, Gusshausstr. 27-29, 1040 Wien, Austria, Email: hschuh@luna.tuwien.ac.at

Abstract

In February 2001 it was agreed that one part of the 2nd IVS (International VLBI Service for Geodesy and Astrometry) Analysis Pilot Project should deal with a comparison of tropospheric parameters to be submitted by the IVS Analysis Centers (ACs). Nine ACs provided ten series of tropospheric parameters, derived from all NEOS-A sessions in the years 1999 and 2000. For each 24h session hourly values of the total zenith path delays and of the horizontal gradients in north-south and east-west direction were submitted except from those ACs which applied the Kalman filter technique and provided only one value for the 24 hours. Most of the ACs also submitted their results for the hydrostatic and the wet part of the total zenith path delays. The comparison presented here was done for these six VLI stations which provided the highest number of observables. Generally a good agreement between the individual submissions was found. A procedure for combining the submitted time series to a single VLBI series with a resolution of one hour was developed and daily (24h) mean values were derived, too. For most of the VLBI stations the mean standard deviations of the combined hourly total zenith path delays are about ±4mm, those of the daily (24h) values are about ±2mm. External comparisons to results provided by the International GPS Service (IGS) show that the VLBI and GPS total zenith path delays are of comparable accuracy with a mean standard deviation of better than ±3mm for all stations except Fortaleza (Brazil). However, there are systematic biases between the VLBI and GPS time series of the individual sites.

Keywords:

VLBI, tropospheric zenith path delays (total, hydrostatic, wet), GPS

1. Introduction

In February 2001 the 2nd IVS (International VLBI Service for Geodesy and Astrometry) Analysis Pilot Project (PP) was initiated and the IVS Analysis Centers (ACs) were requested to submit Earth orientation parameters and tropospheric parameters derived from all 104 NEOS-A sessions in 1999 and 2000. The Institute of Geodesy and Geophysics (IGG) at the Vienna University of Technology, Austria, being in charge of the tropospheric part of the 2nd PP received ten different solutions from nine ACs with the Onsala Space Observatory (OSO) submitting two solutions (Table 1). Four ACs used the Occam VLBI software package, another four Calc/Solve and the AC at Jet Propulsion Laboratory (JPL) applied the Modest software package. Apart from two ACs (AUS, IAA) which used the Kalman Filter technique, all other ACs applied the 'classical' least-squares fit with the Gauss-Markoff model. In all analyses the tropospheric zenith delays were mapped to the elevation of observation by the Niell mapping functions (Niell, 1996). The cutoff elevation angles were always below 8°, mostly set to five 5° elevation. As requested for the 2nd Pilot Project, all station coordinates and velocities were fixed to the ITRF2000 (International Terrestial Reference Frame 2000).

The goal of the 2nd PP was to examine the quality of the submissions of the individual ACs, to identify problems and to give feedback to the ACs. Furthermore, combined time series of tropospheric parameters should be generated representing the performance of VLBI. In particular a comparison of the combined series obtained by VLBI with those published by the IGS (International GPS Service) should help to investigate whether future VLBI results will be of sufficient quality to be released as official IVS products. Mainly the two latter aspects will be dealt with in this publication.

For each session the two ACs (AUS, IAA) using the Kalman filter technique provided one value for the 24 hours and all the other ACs submitted hourly values of the following tropospheric parameters:

- total zenith path delays (ZPD_{total});
- hydrostatic and/or wet zenith path delays ($ZPD_{hydrost.}$, ZPD_{wet});
- horizontal gradients in north-south (GR_{north}) and east-west (GR_{east}) direction (submitted by all ACs, except IAA).

In total eleven stations participated in the VLBI sessions treated in this project. Table 2 gives an overview of the six stations which provided the largest number of observables over the two years and therefore were used for our comparisons.

If one of the zenith path delays (ZPD_{total}, $ZPD_{hydrost.}$, ZPD_{wet}) was missing, it was calculated by IGG from the two other parts. If two zenith path delay parameters ($ZPD_{hydrost.}$ + ZPD_{wet} or $ZPD_{hydrost.}$ + ZPD_{total}) were missing, the $ZPD_{hydrost.}$ was calculated using meteorological data recorded at the stations and then the remaining unknown part was determined from the other two values.

Abbrev.	Institute	VLBI Software
AUS	Australian Surveying and Land Information Group, Australia	Occam
BKG	Federal Agency for Cartography and Geodesy, Germany	Calc/Solve
CAN	NRCanada Geodetic Survey Division, Canada	Calc/Solve
DGF	Deutsches Geodätisches Forschungsinstitut, Germany	Occam
GSF	Goddard Space Flight Center, U.S.A.	Calc/Solve
IAA	Institute of Applied Astronomy, Russia	Occam
IGG	Institute of Geodesy and Geophysics, Austria	Occam
JPL	Jet Propulsion Laboratory, U.S.A.	Modest
OSO	Onsala Space Observatory, Sweden	Calc/Solve
OS2	Onsala Space Observatory, Sweden	Calc/Solve

Table 1: Overview of the participating Analysis Centers (AC). Ten solutions were submitted by nine ACs.

Abbrev.	Station, Country	Latitude [° min sec]	Longitude [° min sec]	Ellipsodial Height [m]
ALGO	Algonquin Radio Observatory, Canada	45 57 19.80	-78 04 21.81	224.0
FORT	Fortaleza, Radio Observatorio Espacial do Nordes, Brazil	-3 52 40.29	-38 25 33.09	23.1
GILC	Gilmore Creek Geophysical Observatory, U.S.A.	64 58 42.28	32 30 08.95	332.1
KOKE	Kokee Park Geophysical Observatory, U.S.A.	22 07 35.90	20 20 05.65	1176.6
NYAL	Ny-Ålesund Geodetic Observatory, Norway	78 55 44.80	11 52 10.89	87.3
WETT	Fundamentalstation Wettzell, Germany	49 08 42.03	12 52 38.82	669.1

Table 2: Overview of the participating VLBI stations which provided the largest number of observations over the two years.

2. Combination procedure

2.1 Editing

Before combining and comparing the various solutions from the different ACs it was necessary to edit the submitted data. Obvious outliers were removed, gaps due to missing data were closed by interpolation and - if necessary - the submitted data had to be referred to the integer hours (18.00 UTC, 19.00 UTC,...). A typical example of the resulting time series in hourly resolution is shown in Figure 1.

2.2 Combination

The procedure that was applied to generate combined parameters for a particular session and a particular station is shown in the diagram of Figure 3. In a first step biases between the solutions of the individual ACs had to be determined. This was done by calculating the unweighted arithmetic mean of the 24 hourly values for every session (per AC and station). With those results an arithmetic mean from all the ACs for the particular station and particular session was calculated, with a 2-sigma outlier test (5% probability of type I error) included. With this mean value a bias was obtained for every AC and the hourly values were shifted by those biases. The mean biases for all 104 VLBI sessions at Wettzell for the ZPD_{total} are given in Table 3. Most of the biases between the individual submission and the combined series are below ±3mm except one solution (CAN) that was shifted by more than 25mm. Finally, an unweighted combined VLBI solution was calculated by simply determining the arithmetic mean of the de-biased time series of all ACs for the hourly epochs (also plotted in Figure 2). Data were removed as outliers if the difference to the combined time series was larger than 2.5 times the standard deviation (2.5-sigma limit which yields a 1% probability of type I error) at a certain epoch. This procedure was performed for all stations, all sessions and all parameters. It should be noted that using L1-norm for the estimation of the combined solution yielded almost identical results.

The results presented here are always based on an unweighted combination. Detailed analyses to determine optimum weights by an iterative procedure for the combination of EOP time series within IVS are described by Nothnagel and Steinforth (2002). As their weighting factors found for the individual IVS ACs do not differ very much (usually between 0.9 and 1.1) the unweighted approach is appropriate to determine the general quality of the results.

A very similar procedure can be applied for the determination of combined VLBI daily (24h) mean values: for a particular station the 104 session means of each AC are entered as input data, a mean for the two years is computed and a common bi-annual mean of all ACs. Again this allows to de-bias the individual series and finally to determine one combined VLBI value per session. The outlier tests applied, were similar to those described above.

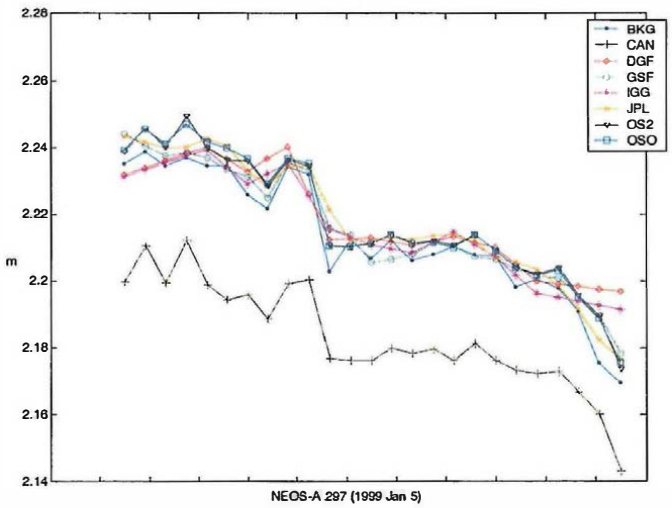

Figure 1: Hourly total zenith path delays (ZPD_{total}) [m] at Wettzell, Germany, for session NEOS-A 297. Data from IAA and AUS are not plotted because those two ACs submitted only one value per 24h session.

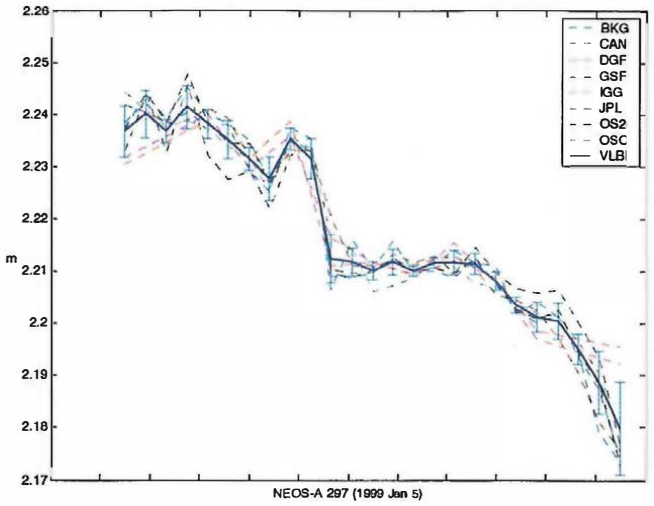

Figure 2: De-biased individual submissions and the combined VLBI solution (solid line, with one-sigma error bars, average standard deviation σ_{ZPD} = ±3.9mm) of hourly total zenith path delays (ZPD_{total}) [m] at Wettzell for NEOS-A 297. Data from IAA and AUS are not plotted because those two ACs submitted only one value per 24h session.

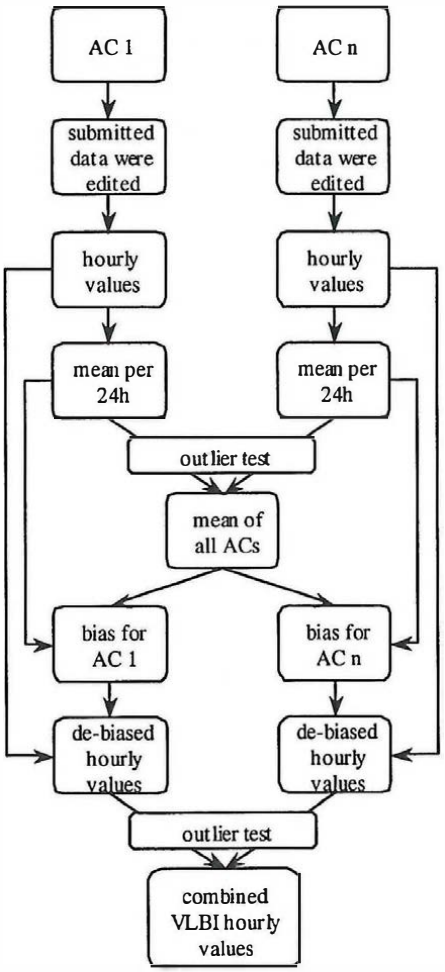

Figure 3: Procedure for the determination of combined VLBI hourly values derived from the time series submitted by the individual ACs. (Remark: a similar procedure can be applied for the determination of combined VLBI daily (24h) mean values as described in the text.)

AC	BKG	CAN	DGF	GSF	IGG	JPL	OS2	OSO
ΔZPD_{total}	-2,12	25,26	0,57	-2,84	2,73	-0,06	0,65	0,65

Table 3: Mean biases [mm] for the total zenith path delay between the combined values and the individual solutions for all 104 VLBI sessions at Wettzell.

3. Comparison of tropospheric parameters submitted by the ACs

3.1 Hourly values

The eight time series of hourly values were treated as described in section 2.2 and combined hourly values were derived for every session and every station. The mean standard deviations of the combined hourly total zenith path delays per station for January 1999 till December 2000 are given in Table 4. For most of the VLBI stations they are about ±4mm what gives an idea about the precision (or 'internal accuracy') of future corresponding IVS products. Figure 4 provides the mean standard deviations and biases w.r.t. the common mean per session per AC for the station Wettzell. It is interesting to note that in the summer months (week 20 – 40 and 70 – 90 in the plot) the standard deviations are slightly higher than in the other time periods, probably because of the higher humidity during the summer, increasing the wet part of the tropospheric path delay.

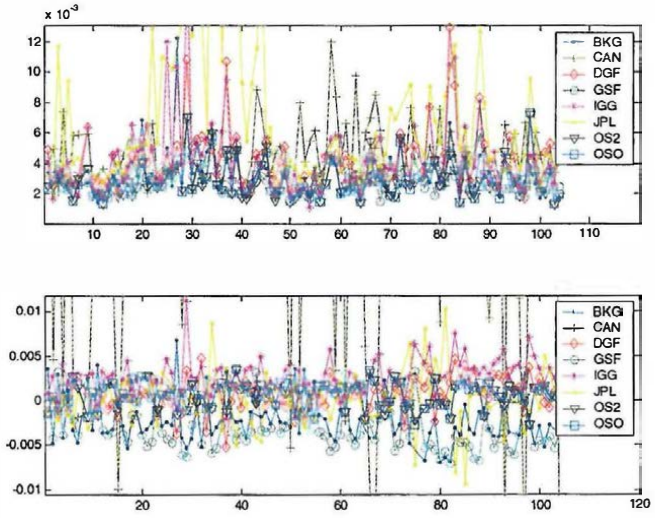

Figure 4: Mean standard deviations of the hourly total zenith path delays (upper panel) and biases w.r.t. the common mean from January 1999 till December 2000 (lower panel) at Wettzell for all ACs. The units of the x-axis are weeks from January 1^{5th}, 1999.

Station St.dev.	ALGO	FORT	GILC	KOKE	NYAL	WETT
σ_{ZPD} (1h)	±4.1	±5.6	±3.4	±4.1	±3.8	±3.9
σ_{ZPD} (24h)	±1.8	±2.7	±1.9	±2.0	±1.9	±2.4

Table 4: Mean standard deviations σ_{ZPD} [mm] of the combined hourly (1h) and of the daily (24h) total zenith path delays per station for 1999 and 2000.

3.2 Daily (24h) mean values

As described in section 2.2 the combined solution is the arithmetic mean per session of all time series (Figure 5) after referring them to a common mean per station for the total time span (from January 1999 to December 2000) (Figure 6). The mean standard deviations of the combined daily (24h) total

zenith path delays are also given in Table 4. They are about ±2mm for most of the stations and only slightly bigger for Wettzell (±2.4 mm) and Fortaleza (±2.7mm).

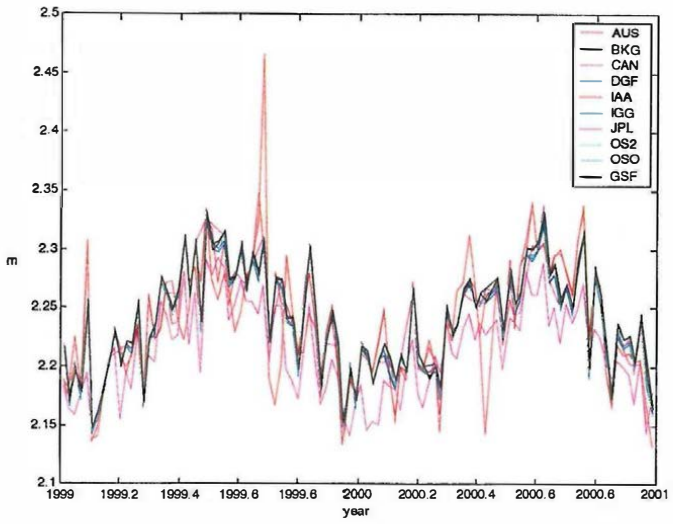

Figure 5: Daily (24h) mean values of the total zenith path delays [m] as submitted by the nine ACs for station Wettzell.

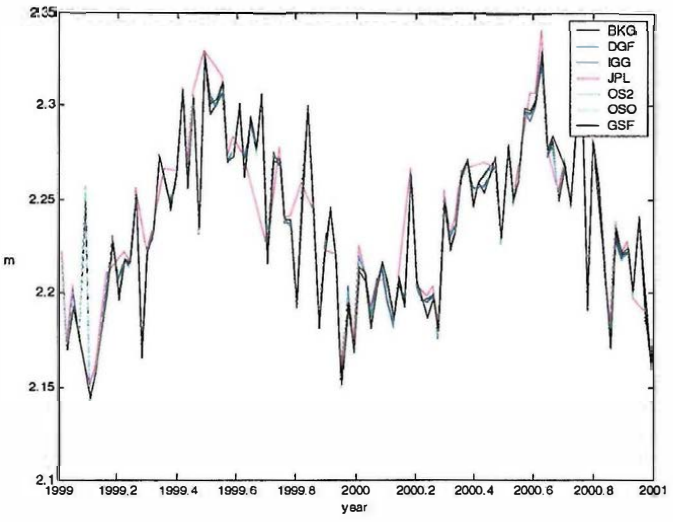

Figure 6: Daily (24h) mean values of the total zenith path delays [m] for Wettzell after shifting them to a common mean for the total time span (1999 and 2000). Only those seven solutions are plotted here, that were used for calculating the daily (24h) mean combined VLBI series. The scatter around the mean daily (24h) value is ±2.4mm.

4. Comparison with IGS time series

The total zenith path delays of the combined VLBI solutions were compared to GPS total zenith path delays released as official IGS (International GPS Service) products (Gendt, 1996) (http://igscb.jpl.nasa.gov/).

4.1 Hourly values

The combined VLBI solutions for the 104 sessions were compared to the corresponding IGS time series. Figure 7 shows the two series for session NEOS-A 297. Generally, trend and short time variations agree quite well, but in all of the sessions there is an offset between the VLBI and GPS results.

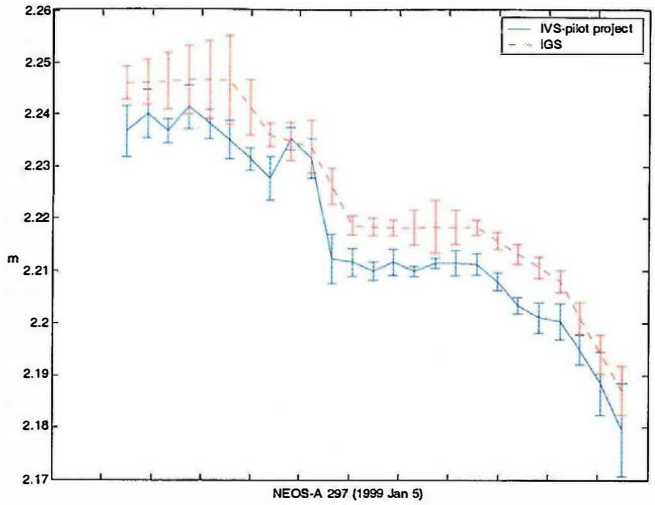

Figure 7: Combined VLBI solution of hourly total zenith path delays [m] at Wettzell for NEOS-A 297 (solid line) compared to the IGS time series (dashed line). The latter are published in 2h time intervals and are interpolated to hourly values.

4.2 Daily (24h) mean values

The combined bi-annual VLBI solution of total zenith path delays was compared to the corresponding IGS time series. Both are of comparable accuracy but for all stations there remain offsets between the two series (Figure 8) which are almost constant over the two years. The standard deviations of the offsets given in column 2 of Table 5 correspond to the mean standard deviation between VLBI and GPS and thus can be understood as an 'external accuracy' of the VLBI results. It is interesting to note that the agreement for almost all of the stations is better than ±3mm for the total zenith path delays and thus about factors 1.5 bigger than the 'internal accuracy' of the daily (24h) values given in section 3.2, except for Fortaleza (Brazil) with differences in the range of ±6.9mm. It has to be investigated whether this is due to the Fortaleza VLBI system, due to the Fortaleza GPS data or due to irregular weather conditions at Fortaleza. Of course, the additional hydrostatic and wet zenith path delays that are due to the height differences between the VLBI radiotelescopes and the GPS antennas have to be accounted for (see Table 5 for a detailed description). The remaining offsets might be caused by different estimation strategies (cutoff angles, mapping functions, ..), GPS phase center variations and multipath effects, VLBI subreflector bending, different ITRFs, and geophysical models used for data analysis.

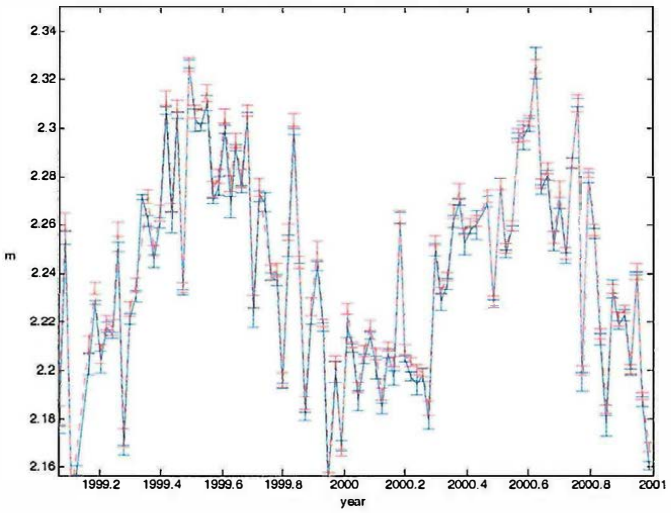

Figure 8: Combined VLBI solution of mean daily (24h) values per session of the total zenith path delays [m] at Wettzell compared to the IGS daily (24h) mean time series.

Station	ΔZPD_{obs} [mm]	ΔH [m]	ΔZPD_{h+w} [mm]	ΔZPD_{res} [mm]
ALGO	-13.9 ± 2.1	23.1	7.1 + 2.1	-4.7
FORT	-14.6 ± 6.9	3.6	1.1 + 0.8	-12.7
GILC	-5.0 ± 2.0	13.1	3.9 + 0.5	-0.6
KOKE	-13.6 ± 2.9	9.2	2.5 + 1.5	-9.6
NYAL	-3.4 ± 2.2	8.8	2.7 + 0.3	-0.4
WETT	-3.6 ± 2.4	3.1	0.9 + 0.3	-2.4

Table 5: Mean offsets ΔZPD_{obs} and standard deviations between the combined VLBI solution of daily (24h) mean total zenith path delays and the corresponding parameters from IGS at the same station. The second column shows the offsets and standard deviations resulting from a first comparison. The third column provides the height differences ΔH between the VLBI radiotelescope and the GPS antennas and the fourth column the corresponding hydrostatic and wet zenith path delays ΔZPD_{h+w} calculated for the mean temperatures, atmospheric pressures and relative humidities at each station. After applying these corrections there still remain residual offsets ΔZPD_{res} between the VLBI and GPS time series (fifth column) that are always negative. The biggest offsets were obtained for the stations FORT (Fortaleza, Brazil) and KOKE (Kokee Park, Hawaii, U.S.A.) where generally the humidity of the air is very high and correspondingly the wet component of the tropospheric zenith path delay is very large. All offsets are given in the sense VLBI-GPS.

5. Conclusions and future outlook

The comparisons show a good agreement between the tropospheric parameters submitted by most IVS ACs. Weaknesses of individual AC solutions were detected in terms of biases or outliers and useful feedback to the ACs could be given. There are various possible reasons for the differences of the tropospheric results submitted by the ACs. The ACs applied different VLBI analysis software packages and different analysis strategies (outlier detection, weighting procedure, elevation cutoff angle, ...). Combined VLBI series yield standard deviations of about ±4mm for the 1h total zenith path delays. This value will probably decrease if more rigorous outlier tests (e.g. with a 2-sigma limit) and an appropriate weighting procedure are applied. External comparison between the combined 24h series determined by VLBI and GPS yield a standard deviation of better than ±3mm for five of six station. The large standard deviation observed for station Fortaleza (±6.9mm) needs further investigation. More results including the comparison of horizontal gradients describing the azimuthal asymmetry of the refractivity at a site cannot be shwon here due to the limited space but are provided in a final report accessible via the IVS homepage (http://ivscc.gsfc.nasa.gov/). There the combination procedure is also explained in more detail. Based on these results a new Pilot Project was approved at the 7th IVS Directing Board Meeting in February 2002 in preparation of official IVS tropospheric products.

References

Gendt, G., Comparisons of IGS tropospheric estimates, Proceedings IGS Analysis Center Workshop, 19-21 March 1996 Silver Spring, Maryland USA, Eds. R. E. Neilan, P. A. Van Scoy, J. F. Zumberge, pp. 151-164, 1996.

Niell, A.E., Global Mapping Functions for the Atmospheric Delay at Radio Wavelengths, J. Geophys. Res., 101 (B2), pp. 3227-3246, 1996.

Nothnagel, A., Steinforth, Ch., IVS Analysis Coordination, CSTG Bulletin, Eds. H. Drewes, W. Bosch, H. Hornik, No. 18, 2002.

Applications of the real-time Swiss permanent GPS network 'AGNES'

E. Brockmann[1], S. Grünig[1], D. Schneider[1], A. Wiget[1] and U. Wild[1]

[1] *swisstopo* (Swiss Federal Office of Topography); Geodesy Division, Seftigenstrasse 264, CH-3084 Wabern, Switzerland, Phone: ++41 31 963 22 56, Fax: ++41 31 963 24 59, e-mail: elmar.brockmann@swisstopo.ch, Web-Site: http://www.swisstopo.ch

Abstract

The Swiss Federal Office of Topography (*swisstopo*) has been building up and operating an automated GPS network for Switzerland (AGNES) since 1998. The final expansion of 29 permanently operating GPS tracking stations was reached at the end of 2001. AGNES is a multipurpose network for surveying applications (reference frame maintenance, densification of the reference frame) as well as for scientific applications (geodynamics and atmospheric research). In addition, a positioning service is offered on a commercial basis under the product name *swipos*-GIS/GEO® (Swiss Positioning Service for GIS and Geodetic Applications).

The paper focuses on the different applications and the results achieved so far.

In the field of geodynamics, results of a kinematic model of the tectonic movements in the Swiss Alps derived from GPS time series will be shown. Since the end of 2001, *swisstopo* contributes hourly zenith path delay estimates with a time delay of 1:15 hours to the European project COST-716 and to MeteoSwiss as additional information for numerical weather prediction.

Furthermore, results of the high-precision real-time positioning service *swipos*-GIS/GEO (accuracy 0.01-0.1m) using the GSM technique for broadcasting differential corrections are presented with the focus on improving the performance (ambiguity initialization, coordinate repeatability) by using the virtual reference station concept.

Introduction

The Swiss national GPS reference network, consisting of 104 well monumented main stations, was installed in the years 1989 to 1992. These sites were used to define the new reference frame for Switzerland, called CHTRF95 / LV95. The site coordinates, observed in several campaigns, are assumed to have a precision (1 sigma) of below 1 cm horizontally and 3 cm vertically. At that time only the GPS receiver in Zimmerwald (ZIMM) was operating permanently. The assumed precision was verified with a re-observation of all sites in summer 1998. The end of this campaign was the beginning of the permanent AGNES network, which started with 7 permanent sites *[Wild et al., 1996].*

At the end of 2001, *swisstopo* completed the installation of AGNES, which now consists of 29 permanently operating GPS tracking stations (see Fig. 1).

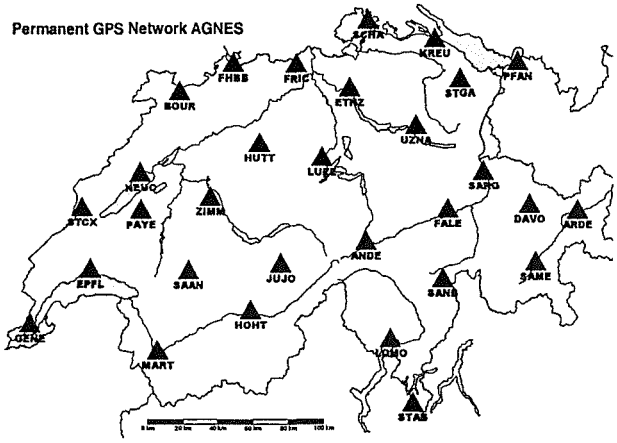

Fig. 1: Permanent GPS Network AGNES 2002

Concept and installation of AGNES

AGNES was designed as a multipurpose network serving different applications *[Brockmann et al., 2001a].* One third of the stations are installed on masts, well founded on bedrock (Tab. 1; Fig. 2), which is important for geotectonic studies. For surveying applications a homogeneous station distribution is required. The distance from any site to the nearest station is below 25 to 30 km. All stations (except Pfänder) are connected to the real-time data network of the Swiss federal administration, which makes surface-covering RTK applications available. The high density of the stations is also important for meteorological applications.

The AGNES stations are equipped with different GPS receivers and antennas. The GPS receivers are Trimble 4000SSI (7), Trimble 4700 (21) and Leica SR520 (1). The following GPS antennas are used for AGNES: The "microcentered" antenna TRM33429.20+GP (20), the "zephyr" antenna TRM41249.00 (1), and the "choke ring" antennas

TRM29659.00 (7) and LEIAT504 (1). The different antenna types in the network require an antenna calibration for highest accuracies (constant and elevation-dependent antenna phase center variations relative to the choke ring antenna type). Results of the individual antenna calibrations are shown later.

Class	Stability / ground	Number of stations
A	stable / on stable bedrock	9
B	stable / installed on concrete underground pillar or on stable building	3
C	uncertain / temporary installation on buildings	17
all	Total	29

Tab. 1: AGNES permanent GPS network. Classification of stations

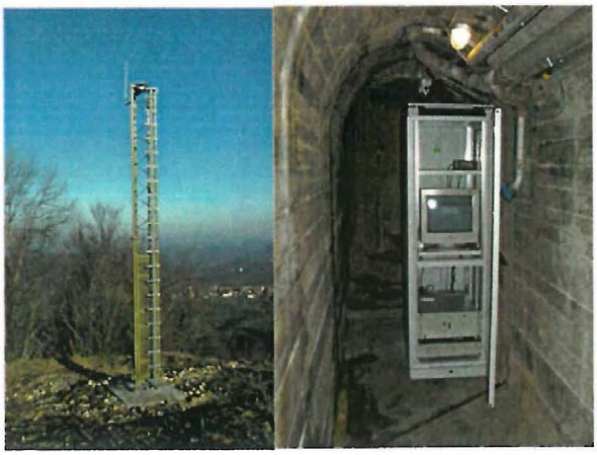

Fig. 2: Example of AGNES permanent GPS station (antenna installed on mast founded in bedrock; computer rack)

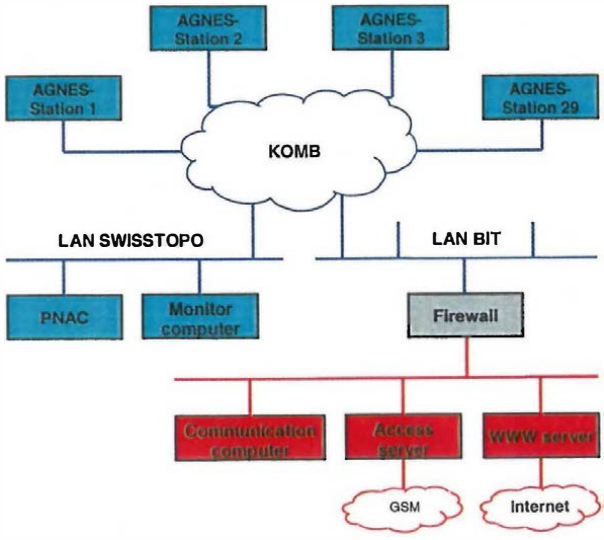

Fig. 3: Data flow within the AGNES network

The data flow in AGNES, shown in Fig. 3, is based on a centralized concept. The GPS data flow every second from the station computer at the AGNES sites (program GPSBase) via the federal network KOMBV ("named pipe" connection) to the monitor computer located at *swisstopo* in Berne (program GPSMonitor). From there a winsock connection is established via the firewall to the communication computer (program GPSNet).

The GPSNet software computes the network solution (including ionosphere, troposphere and ambiguity resolution) and prepares RTCM 2.2 corrections depending on the position of the user. The position is transmitted from the GPS receiver using GSM via the NMEA message (GGA string) to the communication computer.

The actual status of the network solution is displayed graphically for the "AGNES operator" on the communication computer. For computing a virtual reference station, the ambiguities must be solved (indicated by green baselines). If the ambiguities are not solved (red lines), or if only 4 ambiguities are solved (yellow lines), RTCM corrections of the next reference site are transmitted (RAW mode).

The access server (type Cisco AS5300) is able to handle 240 modems or 8 ISDN primary connections respectively. For the *swipos-GIS/GEO* service which has been in operation since January 2002, the single primary ISDN number handles 30 different users simultaneously.

The time delays between the GPS stations and the communication computer (all within the federal KOMBV network) are of the order of 30-100 msec. The total time delay from the reference receiver to the rover receiver is usually below 1 second.

For post-processing applications hourly files (1-, 5- and 30-second data) and daily files (30-second data) are available via the Internet.

The data are analyzed at *swisstopo* for different applications (monitoring, surveying, geotectonics, meteorology) using the computer of the PNAC group (Permanent Networks and Analysis Center).

With the described infrastructure *swisstopo* actively enables the users to access the Swiss reference frame CHTRF95 / LV95 in real-time and also for post-processing applications as an alternative to accessing the frame by means of classical reference network (point monuments).

Surveying applications using AGNES

The data of the AGNES network are extensively used for national surveying and for further densifications of CHTRF95 / LV95. Thanks to the high precision of the Swiss national GPS reference network, the "principle of neighbourhood" is not as important as in classical surveying, where a new site must always be integrated in the network de-

fined by the neighbouring 2-3 sites in order to minimize possible biases. Therefore, numerous occupations of neighbouring sites can be avoided when using AGNES. Presently only 1 neighbouring site is measured for validation reasons. Due to the precise monitoring of the AGNES network (see next section), densifications can be realized with a higher reliability and accuracy compared to densifications using classical GPS campaigns.

Station monitoring using AGNES

The data of the AGNES sites are being monitored since the end of 1998 on a daily basis and since Dec. 2001 on an hourly basis (see section "GPS Meteorology"). In addition to the 29 AGNES sites, 40 EUREF sites are processed using the Bernese GPS Software Version 4.2 [*Hugentobler et al., 2001*]. This monitoring allows the detection of possible site movements. An updated multi-year solution where the site coordinates and velocities are solved for is automatically generated if an additional week of data is processed. The results (estimated velocity, repeatability plots, etc.) are available under http://www.swisstopo.ch/ (survey section).

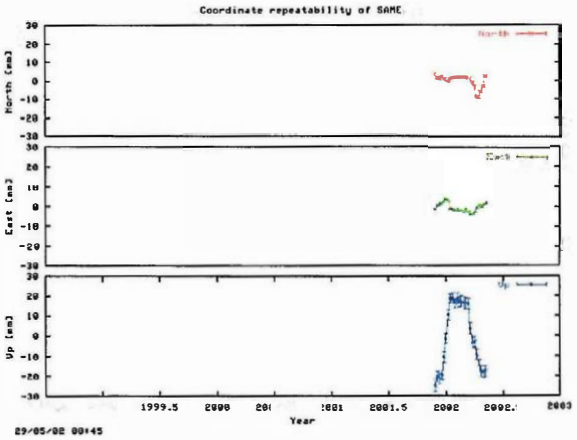

Fig. 4: Time series (north, east, up) of the AGNES station SAME (Samedan)

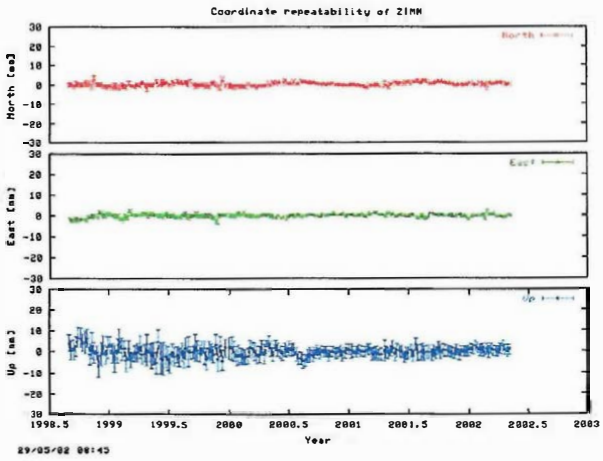

Fig. 5: Time series (north, east, up) of the AGNES station ZIMM (Zimmerwald)

An example of an "unstable" site (we assume that ground water is responsible for the movement in the station height of SAME) is given in Fig. 4.

Fig. 5 shows an example of a stable station. The weekly repeatability is below 1 mm horizontally and 3 mm vertically. It is also clearly visible that the quality of the solutions has improved since mid-2000 (denser network, more reliable ambiguity resolution).

Site velocities (see Fig. 6) are estimated for sites with a time series longer than 0.5 years using the full variance-covariance information of the weekly solutions. All estimated site movements are smaller than 2 mm/yr. It seems that the sites of the Swiss Plateau (stations along a straight line from Geneva in the southwestern part to Pfänder in northeastern part such as Huttwil (HUTT) and Luzern (LUZE)) are moving slightly northwest. Movements of the Alps in the southeastern part can not be detected reliably (time series too short). Nevertheless, the sites Davos (DAVO) and Locarno (LOMO), sites with almost 4 years of observations, do not show significant movements.

The uncertainties of possible vertical movements are worse by approximately a factor of 3 compared to the horizontal velocities. From levelling observations covering a time span of more than 100 years the Alpine uplift could be verified very precisely for a dense network of stably monumented markers (southwestern part of the Alps is rising with approximately up to 1.5 mm/yr ± 0.3 mm/yr) [*Gubler et al, 1981*]. It is therefore important to combine the horizontal movements detected by GPS with the vertical movements detected by levelling.

Velocities were also derived from coordinate differences stemming from the various GPS campaigns between 1988 and 2002. Despite the long time span of maximally 14 years and the high density of more than 100 sites, no significant movements of particular regions are detectable.

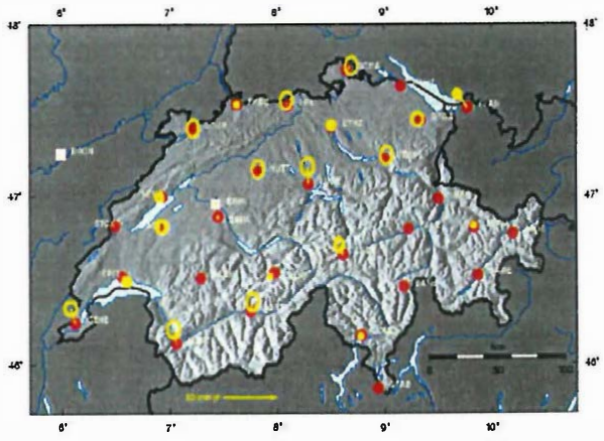

Fig. 6: Site velocities in ITRF00 (relative to Zimmerwald) for sites with a "history" of more than 0.5 years.

We assume that the early "relatively weak" GPS solutions are responsible for that due to the sparse GPS constellations in the years 1988 – 1990. It is planned to re-observe the complete network in the year 2004.

To derive a kinematic model of the entire Alpine area, the Alpine countries share the results of the weekly coordinate estimates (SINEX format) in order to integrate them into the permanent network of the EUREF stations [*Brockmann et al., 2001b* and *Brockmann et al., 2002*].

Calibrations of AGNES antennas

All GPS antennas are individually calibrated on a test field before they are used for the AGNES network. The choke ring antenna TRM29659.00 is used as reference, and at least one additional, previously calibrated antenna (e.g. the "geodetic" antenna TRM14532.00) is used for validation.

Due to the fact that most of the AGNES antennas are of the type TRM33429.20+GP, we will focus on the results of this antenna type. Fig. 7 shows an "individual-to-individual" antenna agreement of better than 1 mm for the "North L2" antenna offsets. Compared to the IGS calibration which is widely used within the GPS community, we have a systematic difference of 1.2 mm for the "North L2" component (see Tab. 2). For all other components the differences are smaller. The differences of the vertical offsets which are determined using weighted observations (weighted with the cosine of the zenith angle) and an elevation cut-off of 10 degrees, are larger. The L1 phase center is higher than L2 for the *swisstopo* calibration, and vice versa for the IGS values.

The corresponding elevation-dependent corrections for the L1 phase center are given in Fig. 8. All individual antennas agree on a level of 1-2 mm. The differences to the IGS values are clearly visible.

The influence of the different antenna values (*swisstopo* versus IGS) on a daily coordinate estimation depends on the solution type (L1, L2 or the ionosphere-free L3 linear combination). For the mentioned antenna TRM33429.20+GP we found a difference of approximately 14 mm for the estimated heights (L3 solution). This value differs slightly from day to day due to the elevation-dependence of the corrections.

For the "zephyr" antenna we have an impact of the antenna calibration of 8 mm (L3 solution).

Comparisons of other antenna types ("geodetic" antenna TRM14532.00 and "choke ring" antenna TRM29659.00) with the IGS/NGS antenna model and also comparisons with previous *swisstopo* calibrations show only minor differences.

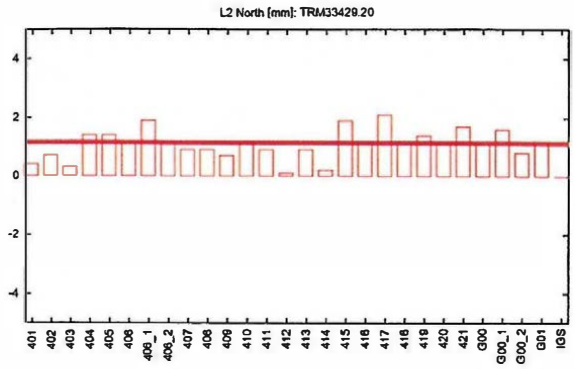

Fig. 7: Offsets "North L2" [mm] for different "microcentered" antennas TRM33429.20+GP (sorted by serial numbers) compared to averaged values (label "G*") and IGS values (label "IGS"; used as reference for the comparison)

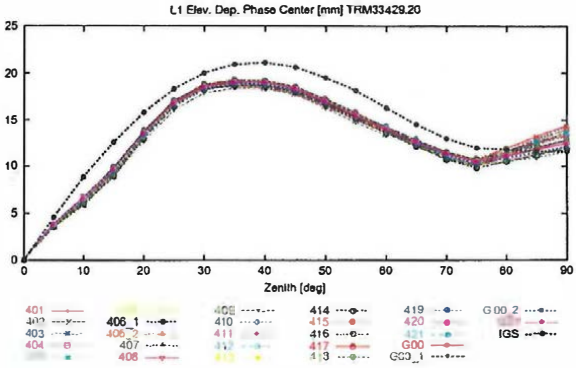

Fig. 8: Elevation-dependent phase center corrections L1 [mm] for different "microcentered" antennas TRM33429.20+GP compared to averaged values (label "G*") and IGS values (dotted line)

Freq.	Comp.	IGS antenna model NGS(3) 01/08/29	*swisstopo* antenna model LPT(21) 02/03/18
L1	North	-0.4	0.4
	East	-1.0	0.1
	Up	72.9	77.0
L2	North	-0.4	1.2
	East	-1.3	-0.1
	Up	75.0	72.8

Tab. 2: Comparison of two different antenna models (IGS and an averaged value from 21 individual calibrations from *swisstopo*; the given values are in [mm]) for the constant antenna offsets of the "microcentered" antenna TRM33429.20+GP

The precise positioning service *swipos*-GIS/GEO using AGNES

After a pilot phase in 2001, the precise real-time positioning service has been available on a commercial basis since January 2002 under the brand name *swipos*-GIS/GEO. An overview of the concept was already given at the beginning of this paper. Further details and some performance numbers of the RTK positioning service can be found in *[Wild et al., 2000* and *Brockmann et al., 2001a].* Here we would like to focus on results of a special test which was performed on the roof of the *swisstopo* building in order to demonstrate the potential of the virtual reference station concept.

The test configuration was the following:

- 4 hours RTK positioning on the *swisstopo* roof using 2 Trimble 5700 receivers (with 2 GSM) and a single "zephyr" antenna (+ antenna splitter).
- One receiver was receiving the corrections generated according to the virtual reference station concept ("net" mode) – the second receiver (same antenna) received corrections from the data of the nearest reference station located in Zimmerwald, 5.8 km away ("raw" mode).
- RTK positions (float and ambiguity fixed solutions) were stored every second; a new initialization was forced every 15 minutes.

The results are shown in Fig. 9 (horizontal components) and Fig. 10 (vertical component). The biases are negligible in all cases. Also the standard deviations (1 sigma) of the coordinate estimates in all 3 components are comparable (see Tab. 3). The substantial improvement is the increased number of ambiguity-fixed RTK positions (see also the x-axes in Fig. 10). Only 5% of the initialization attempts failed for the "net" mode, whereas 45% attempts were unsuccessful for the "raw" mode.

	"raw" corrections	"net" corrections
Horizontal rms [cm]	0.7	0.8
Vertical rms [cm]	3.6	2.5
# float solutions [%]	45	5

Tab. 3: Performance of RTK positioning using the data of the nearest reference station ("raw") and using the virtual reference station concept ("net")

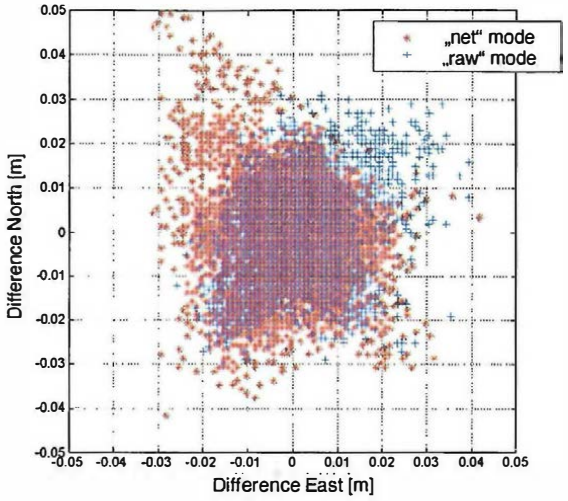

Fig. 9: Scatter of the RTK horizontal positions ("raw" and "net" mode; only ambiguity-fixed solutions)

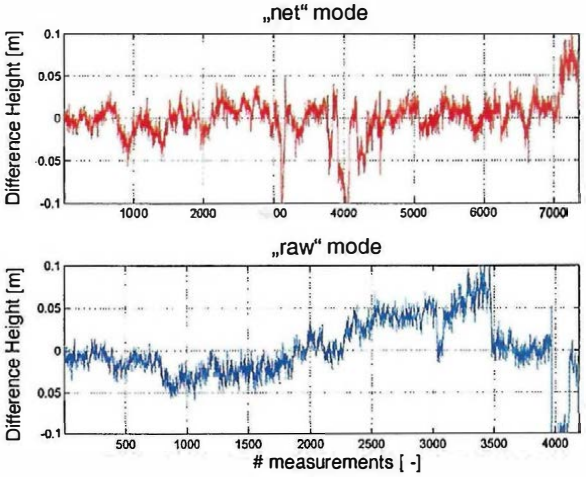

Fig. 10: Scatter of the RTK vertical positions ("net" mode in the upper plot and "raw" mode in the lower plot; only ambiguity-fixed solutions)

GPS meteorology using AGNES

Since 1999 the Swiss Federal Office of Topography has been active in the European project COST 716 (exploitation of ground-based GPS for climate and numerical weather prediction application). After a successful benchmarking *[van der Marel et al., 2001], swisstopo* has been contributing zenith total delay estimates in near real-time (NRT-ZTD) since Dec. 2001. Fig. 11 shows the stations used. In addition to the 29 AGNES sites, 20 EUREF sites are processed. Furthermore, about 12 sites from other networks (mainly France) are being used in order to improve the station distribution in the western part of Europe. This area is important because the dominating weather conditions from the Atlantic Ocean usually pass over France before they reach Switzer-

land. 95% of the solutions arrive at the data archive of the UK met office within 1 hour and 45 minutes (usually within 1:15).

MeteoSwiss used the NRT-ZTD estimates in a test study for numerical weather prediction. The numerical forecast models (aLMo) were computed for the test period of September 2001 in two different ways: A run with assimilated GPS-derived ZTD estimates and a run without assimilated ZTDs. A comparison of the results showed a positive impact of GPS *[Guerova et al., 2002]*. The difference of the integrated water vapor field is given in Fig. 12.

A by-product of the hourly processing is coordinate monitoring. Problems such as the station height change in Samedan (Fig. 4) were detected very early. Cumulative solutions averaging 12-24 hourly solutions already allow the estimation of coordinate changes of the order of below 2 cm.

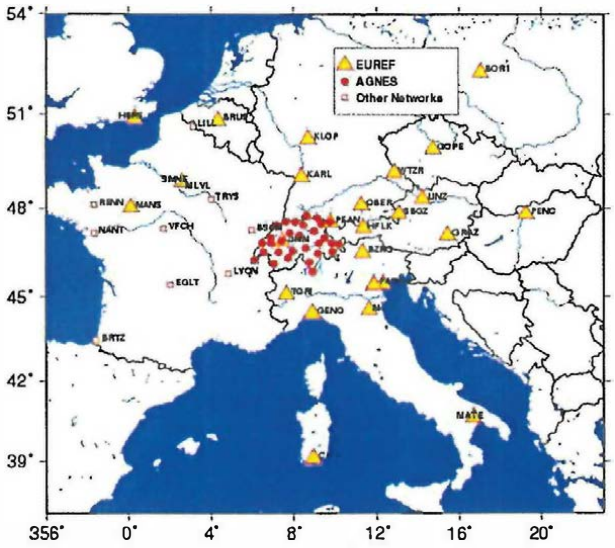

Fig. 11: European permanent GPS stations processed by *swisstopo* in the COST 716 Project

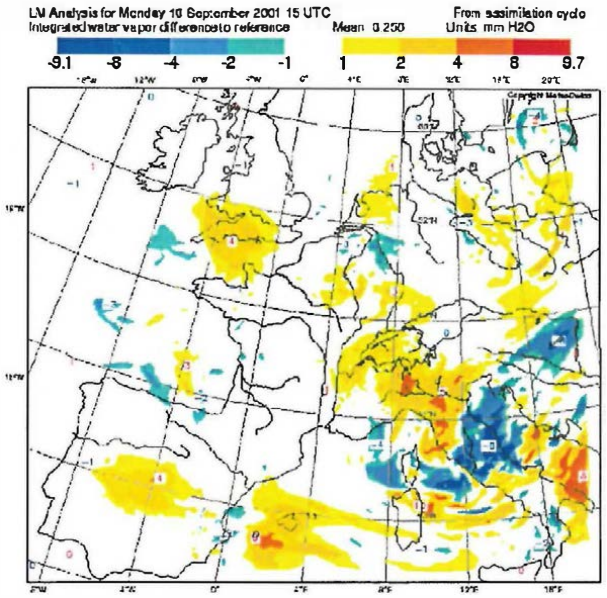

Fig. 12: Difference of the integrated water vapor field (Sep. 10, 2001; 15:00 UTC) with and without assimilated GPS zenith total delay estimates

Conclusions

Since 1998 *swisstopo* has been developing a multi-purpose permanent GPS network called AGNES. At the end of 2001, the planned 29 sites were in operation. AGNES is supposed to serve different applications such as surveying, positioning and scientific applications (geotectonics, meteorology). As described in the paper, promising results are already achieved in all of these applications. Making these applications operational and reliable and developing further applications of AGNES will therefore be a main task of *swisstopo* for the next 2-3 years.

References

Brockmann E., S. Grünig, R. Hug, D. Schneider, A. Wiget and U. Wild (2001a): *Introduction and first applications of a Real-Time Precise Positioning Service using the Swiss Permanent Network 'AGNES'*. In: Torres J.A. and H. Hornik (Eds): Subcommission for the European Reference Frame (EUREF). National Report of Switzerland, EUREF Publication No. 10, Mitteilungen des Bundesamtes für Kartographie und Geodäsie, Vol. 23, Frankfurt am Main 2002, pp. 272 – 276.

Brockmann E., E. Calais, J.-M. Nocquet, A. Caporali, F. Vespe, G. Weber, R. Weber and G. Stangl (2001b): *Alpine Network.* EUREF Permanent Networks 3rd Local Analysis Center Workshop 31 May - 1 June 2001, Reports on Geodesy, No. 3 (58), 2001.

Brockmann E., R. Hug and Th. Signer (2002*)*: *Geotectonics in the Swiss Alps using GPS.* In: Torres J.A. and H. Hornik (Eds): Subcommission for the European Reference Frame (EUREF). EUREF Publication No. 11 (in prep.).

Gubler E., H.-G. Kahle, E. Klingelé, St. Müller and R. Olivier (1981): "Recent Crustal Movements in Switzerland and their Geophysical Interpretation". Tectonophysics, Volume 71, pp.125-152.

Guerova G., J.-M. Bettems, E. Brockmann and Ch. Matzler (2002): *Assimilation of GPS in the Alpine Model: sensitivity experiment*. Proceedings of the COST-716 workshop Potsdam, Jan. 28-29 2002.

Hugentobler U., S.Schaer and P. Fridez (Eds.) (2001*)*: *Bernese GPS Software Version 4.2 documentation.* Astronomical Institute of the University of Berne, 2001.

Marel H., E. Brockmann, E. Calais, J. Dousa, G. Gendt, M. Ge, S. de Haan, M. Higgins, J. Johansson, D. Offiler, R. Pacione, A. Rius and F. Vespe (2001): *The COST-716 Benchmark GPS Campaign for Numerical Weather Prediction Applications*. EGS General Assembly, Nice, 29 March 2001. Geodesy and Meteorology. Publication in prep.

Schneider D., E. Brockmann, U. Marti, A. Schlatter and U. Wild (2000*)*: *Introduction of a Precise Swiss Positioning Service "swipos" and Progress in the Swiss National Height Network "LHN95"*. In: Torres J.A. and H. Hornik (Eds): Subcommission for the European Reference Frame (EUREF). National Report of Switzerland. EUREF Publication Nr. 9, pp. 315-322, München 2000.

Wild U., A. Wiget and H. Keller (1996): *The Automated GPS network in Switzerland (AGNES) for Navigation and Geodesy: Concept and First Test Results*. Proceedings of Differential Satellite Navigation Systems (DSNS'96), Volume 2, St. Petersburg 1996.

Wild U., E. Brockmann, R. Hug, Ch. Just, P. Kummer, Th. Signer and A. Wiget (2000): *Automatisches GPS-Netz Schweiz (AGNES), ein Multifunktionales Referenznetz für Navigation und Vermessung*. Vermessung, Photogrammetrie, Kulturtechnik, 5/2000.

The permanent GPS network in the Iberian Peninsula: application for geodynamics

R.M.S. Fernandes[1*°], B.A.C. Ambrosius[1], R. Noomen[1], L. Bastos[2], E. Buforn[3], R.E.M. Riva[1]

[1] Delft Institute for Earth-Oriented Space Research, TU Delft, The Netherlands.
[2] Observat´orio Astron´omico da Universidade do Porto, V.N. Gaia, Portugal.
[3] Departement of Geophysiscs, Universidad Complutense, Madrid, Spain.
*DEOS - Delft Institute for Earth-Oriented Space Research, Faculty of Aerospace Engineering, TU Delft, Kluyverweg 1, 2629 HS Delft, The Netherlands.
° also at DI, UBI, Portugal

Abstract

In recent years, the number of permanent GPS sites in the Iberian Peninsula has increased significantly: in the beginning of 1996 there were just 2 sites with publicly available data. This number had risen to 15 by the end of 1999, and recently (at the end of 2001), it has reached 18. For many sites, the observation time-span is already sufficiently long to derive a reliable estimate of their individual motion. In combination with the relatively good geographical distribution of the sites, this velocity field contains unique information to study the tectonics of the Iberian Peninsula, both internally and with respect to the rest of Europe. In the framework of a combined DEOS-AOUP research project called GPS Iberian Network (GIN), the observations of all available GPS sites in the region (including some in North Africa, the Azores archipelago and France) are processed on a daily basis since the middle of 2000 (with backward processing extending to January 1996). As a consequence of this project, DEOS became an official Local Analysis Centre (LAC) of the European Reference Frame (EUREF) in the beginning of 2001. The DEOS weekly solutions *Preprint submitted to Physics and Chemistry of the Earth 27 June 2002* are included in the official EUREF Permanent Network (EPN) analysis chain, which results in weekly coordinate solutions for the entire EPN network. DEOS computes these two different solutions (GIN and EPN) using the same software but applying different strategies. In this paper, a general overview of the characteristics of the two solutions is given. Also, the differences in the solutions are analyzed in order to pinpoint data problems and processing errors. Furthermore, the GIN velocity field is compared with the one derived from the official EPN solution. Special attention is paid to the diffrent procedures to project the solutions into a unified reference frame. Finally, this paper presents a preliminary interpretation of the contemporary tectonics of the Iberian Peninsula based on the derived velocity fields. There is evidence of significant intra-plate deformation in the Iberia region and there are indications that parts of the Iberian Peninsula exhibit a differential motion with respect to stable Eurasia.

Keywords:

GPS, Iberian Peninsula, Geodynamics, Permanent Processing

1 Introduction

During the last decade, a number of (semi) real-time processing systems for the observations of GPS networks have been implemented worldwide by different organizations. Some of them aim at a global network of stations, whereas others are edicated to support and/or carry out regional geodynamic studies in different parts of the Earth, like Japan (Miyazaki et al., 1998) and California (Bock et al., 1997).

As an alternative to completely carrying out their own GPS processing, researchers also have the option to use GPS solutions for individual station positions and/or velocities which are publicly available; examples are those of the Jet Propulsion Laboratory (JPL) and the Scripps Orbit and Permanent Array Center (SOPAC). In addition, public combination solutions are derived on an operational basis from

redundant individual contributions of different organizations. EPN (Bruyninx, 2000) and the International GPS Service (IGS) (Davies and Blewitt, 2000) are good examples of such combined GPS network analyses. However, these sets have one major handicap: normally, they concentrate on a subset of "core" stations and they do not provide time-series for all GPS stations present and active in a certain region. Consequently, dedicated processing is unavoidable when detailed geodynamics studies are performed.

In 2000, the DEOS and AOUP groups implemented the daily processing of a permanent GPS network, called GPS Iberian Network (GIN), using JPL's GIPSY software package (Webb and Zumberge, 1995) with the Precise Point Positioning (PPP) strategy. The GIN network was designed with the goal of providing geodetic evidence for geodynamic studies on the western segment of the Eurasia-Africa plate boundary (Fernandes et al., 2000).

In the Iberian Peninsula region, the plate boundary is very complex and diffuse. During the last years, several models have been proposed suggesting different locations and mechanisms responsible for the behavior of the African and Eurasian plates (Buforn et al., 1995; Jim´enez-Munt et al., 2001). Basically (see Figure 1), it changes from a narrow W-E oriented transform system westward of the Gorringe Bank (36±N, 12±W) to a compression stress regime in the eastern region. From the Gorringe Bank to 3.5±E, including the Betics and Rif Cordilleras and the Alboran Sea, the boundary is more diffuse, extending through a wide area with a general stress regime of N-S to NNW-SSE compression, with horizontal E-W extension at the Alboran Sea. For many authors, the plate boundary in this region is formed by a wider area of deformation (Buforn et al., 1988; Hayward et al., 1999). In the Pyrenees, located north of the Iberian block, the stress pattern obtained from focal mechanisms is in agreement with the general stress regime of N-S compression, better defined at the western part.

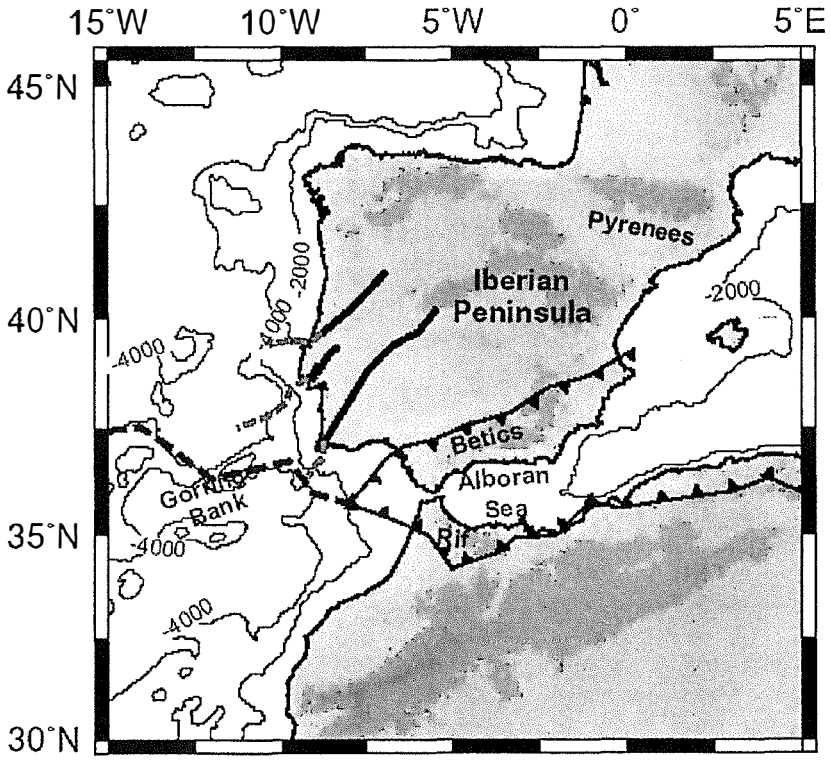

Fig. 1: An overview of the major geodynamic features of the Iberian Peninsula.

After the presentation of the preliminary results of GIN (Fernandes et al., 2000), DEOS was appointed as the thirteen LAC of EPN, with the obligation to provide weekly solutions for a network similar to GIN, as shown in Figure 2. DEOS-EPN is only a sub-network of EPN, which currently counts more than 100 stations concentrated in the European region. Since the others LACs use different software packages

and/or approaches, the time-series for common stations allow a comparison between the GIN and the (combined) EPN methodologies, which will be extensively discussed in this paper.

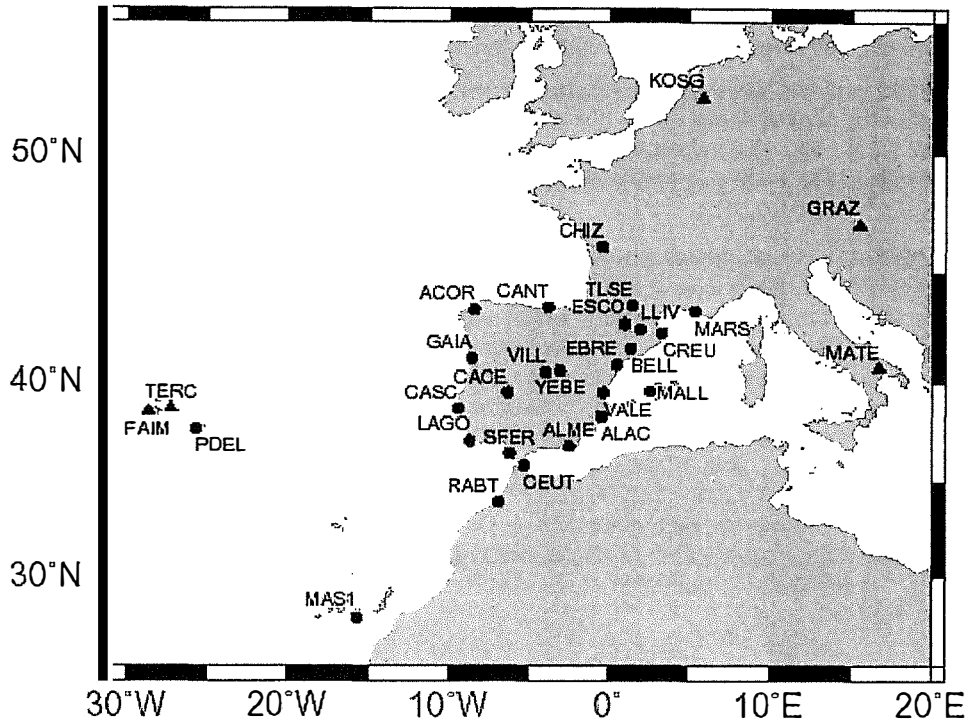

Fig. 2: The GPS stations included in the GIN and EPN networks as processed at DEOS. Triangles represent stations only processed in the GIN project (managed by DEOS/AOUP or for comparison studies).

In addition, the time-series of solutions coming out of the two activities are converted into independent velocity fields. The results will be the subject of a discussion on the geodynamics of the Iberian Peninsula. The observed relative motions will be analyzed both internally and with respect to the surrounding major plates.

2 GPS Data Processing Approaches

The software package used at DEOS for this analysis, GIPSY, processes the GPS measurements as undifferentiated observations by estimating the unknown parameters with a very stable Kalman filter algorithm. The strategy which is used for the GIN network, PPP, implies that precise and internally consistent orbits and corrections to the satellite clocks are available and kept fixed (they are provided by JPL on a daily basis) (Zumberge et al., 1997). When no ambiguity fixing is performed, this approach allows to estimate each station position independently, which has significant advantages in terms of computational efficiency. However, a requirement for EPN is the use of IGS orbit solutions: in this case, another strategy, called Free Network solution (FN) is applied. Here, all stations are processed simultaneously, solving for clock corrections to receivers and satellites. In both approaches, no constraints are imposed on the a-priori receiver positions. Because the orbits, although fixed in the daily processing, are only loosely constrained to a reference frame, the orientation of the network, as a whole, can slightly vary from day to day.

Using the above strategies, DEOS obtains solutions for each network (GIN and EPN) on a daily basis. In the DEOS-EPN processing, there is a possibility that bad data from one or more stations degrade the position solutions of the entire network (or even prevent to obtain any). By virtue of its site-by-site

approach, such bad stations are easily identified in the GIN processing. Therefore, GIN also acts as a supporting tool for the EUREF activities of DEOS.

The daily solutions of each network are separately combined into weekly solutions, applying outlier rejection. Again, no constraints are applied, so these solutions are not yet mapped into a known reference frame. The DEOS-EPN weekly solution is the product submitted to EUREF, where the mapping to the adopted reference system is carried out.

DEOS is the only LAC out of 15 using GIPSY, whereas all other LACs are using the BERNESE software package (Rothacher and Mervart, 1996), with the exception of ASI that is using MicroCosm (Van Martin, 1998). BERNESE is based on the double difference formulation, in which satellite and receiver clock errors are eliminated. This implies that it is not possible to process each station individually, in a way similar to the GIPSY-FN approach.

3 Data sets

The EPN combined solutions are available since GPS week 834 (January 1, 1996), currently accounting for more than 300 weekly solutions. In this paper, the analysis covers the period between week 860 (June 1, 1996) and week 1155 (February 24, 2002). The reason for starting at week 860 is that, from thatmoment, the phase center corrections were introduced, leading to jumps in the time-series. GIN was reprocessed starting from the beginning of 1996, what already provides a long time-series for the existing sites (only two at that time in Iberia, one of which, MADR, has been later dismantled). Table 1 lists the amount of weekly solutions for all stations discussed in this paper (the sites with a history longer than two years in the GIN network). The number of available solutions in the GIN data set is larger than the EPN set because: (1) GIN has been processed up to week 1162 (April 20, 2002), and (2) all available observations have been used (including the data observed before those stations became part of EPN).

Site	Starting	# Weekly Solutions	
	Month	GIN	EPN
GRAZ	Jan 96	330	293
KOSG	Jan 96	329	293
MATE	Jan 96	328	293
VILL	Jan 96	320	280
MAS1	Jan 96	300	267
SFER	May 96	286	273
EBRE	Jan 97	305	281
CASC	May 97	257	172
BELL	Jan 99	175	158
CREU	Jan 99	170	155
ESCO	Mar 99	110	102
LLIV	Jun 99	151	131
ALAC	Aug 99	143	130
ACOR	Sep 99	137	126
LAGO	Nov 99	108	55
GAIA	Nov 99	82	55

Table 1: GPS sites in the region of interest with a tracking history longer than two years.The table shows the month when the first observations became available and the number of weekly solutions estimated (for the two approaches separately).

4 Mapping into the Reference Frame

The weekly solutions must be mapped into a unique reference system in order to derive a velocity field and perform any comparative analysis or solution combination. Currently, the global reference system adopted by the scientific community is the International Terrestrial Reference System (ITRS) (Mc- Carthy, 1996). It is realized through the publication of epoch positions and velocities for a polyhedron of stations covering the entire globe, estimated from space geodetic techniques (Boucher et al., 1999). During the last decade, several realizations, called the International Terrestrial Reference Frame (ITRF), have been produced with a continuous increase in the number of stations and the quality of the solutions. The current realization, ITRF2000, contains more than 500 stations (Altamini et al., 2001).

The usual approach to project the weekly solutions into a known reference frame is composed of a number of steps: (1) the selection of a subset of so-called reference stations with reliable estimations of their position/velocities in the ITRF solution (known for their high and consistent data quality and quantity), and reasonably distributed over the network or the Earth (for regional or global mapping, respectively); typically, IGS stations are used for this purpose; (2) the processing of these stations together with the network of interest; (3) the propagation of the ITRF coordinates of the reference sites to the week of interest; (4) the estimation of the Helmert parameters required to project the weekly network solution onto ITRF; (5) the application of these Helmert parameters to the entire weekly solution.

Due to the small number of high quality ITRF stations included in the GIN network, no reliable Helmert parameters can be computed. To avoid the inclusion of more reference stations, a faster approach has been adopted. JPL already provides, together with the orbit products, the seven Helmert parameters to project the daily solutions onto ITRF2000 (step 4). These parameters are computed by JPL by using a global network of stations with a long tracking history. However, this approach may not be optimal when the objective is to analyze a regional network, as will be discussed later.

For the EPN solution, a completely different approach has to be followed to have the entire data set in the ITRF2000. The weekly solutions provided by EUREF are already mapped into an ITRF by tightly constraining some stations to their predicted positions for each epoch. However, throughout the years, those solutions have been mapped into different realizations of ITRF (see Table 2). The constraints imposed in the original mapping have to be first removed. This has been carried out by applying the procedures described in Davies and Blewitt (2000). These resulting solutions are in an undefined reference frame. They are then projected onto ITRF2000 by applying seven Helmert parameters, computed using the predicted positions at each week for the last set of reference stations listed in Table 2. This set has been favored for all weeks since, within EPN, it presently provides the most stable link to ITRF2000. In this way, the consistency of the geometry of the reference network is also retained.

GPS Weeks	Reference Frame	Reference Stations
0860-0946	ITRF94	BRUS GRAZ KOSG MATE METS ONSA WTZR ZIMM
0947-0981	ITRF96	BOR1 GRAZ KOSG MATE ONSA POTS REYK WTZR ZIMM ZWEN VILL
0982-1020	ITRF96	BOR1 GRAZ KOSG MATE ONSA POTS REYK WTZR ZIMM ZWEN VILL GRAS
1021-1056	ITRF97	BOR1 GRAZ KOSG MATE ONSA POTS REYK WTZR ZEWN VILL GRAS NYA1 TRO1 THU1
1057-1142	ITRF97	BOR1 GRAZ KOSG MATE ONSA POTS REYK WTZR VILL GRAS NYA1 TRO1 THU1
1143-	ITRF2000	BOR1 GRAZ KOSG MATE ONSA POTS REYK WTZR VILL GRAS NYA1 TRO1 THU1

Table 2: Overview of the reference stations originally used to tie the EPN combined solution to the successive ITRS realizations. Each line indicates a switch from one ITRS realization to another or a change in the selected sites.

5 Time-series Discussion

Once all solutions have been mapped into ITRF2000, a best trend-line is fitted through the three position components of each station. This results in a 3-dimensional velocity field. This procedure has been applied to both networks (GIN and EPN).

Table 3 lists the estimated motions. The associated formal uncertainties are not provided due to reasons of clarity and meaningfulness. In fact, the statistical estimates of the precision are too optimistic due to the large amount of data. A more reasonable value is the r.m.s. of the coordinates fitting (the difference between the weekly position solution and the trend-line). This has been computed and the results show a good agreement for all stations: with respect to the GIN estimates the r.m.s. is on the level of 3 mm, 3-4 mm and 6-10 mm for North, East and Up components, respectively. EPN shows slightly better values: 1-4 mm, 1-4 mm and 3-9 mm. This difference is amplified by the sum of two effects: (1) For GIN, the use of the generic JPL parameters, not optimized for Europe, might increase the dispersion of the weekly solutions. Simons et al. (2002) shows that a dedicated mapping, including two sets of regional and global reference stations, reduces the misfit between the weekly solutions and the trend-line. (2) For EPN, the combined solution has generally less scattering with respect to the trend than the individual submitted solutions (at least three LACs per station). Figure 3 shows an example of the higher dispersion that is observed in the time-series of most stations in the GIN network. Note that the formal uncertainty of the trend is larger for EPN due to the outsized formal errors of the weekly solutions in some periods, which are already present in the original SINEX files.

For most of the stations, both solutions agree within 1 mm/yr, 2 mm/yr and 3 mm/yr for the North, East and Up components, respectively. This confirms that the approach used by DEOS (GIPSY PPP strategy) provides reliable results, considering that they are comparable with the EPN combined solutions. In particular, the EPN reference stations (GRAZ, KOSG, MATE and VILL) have a very good agreement. Within the group of long time-span stations, only MAS1 and SFER show some disagreement in both horizontal components. MAS1 has the worst repeatabilities in the analyzed EPN stations (4 mm in both North and East). This fact is not observed in GIN, thus might be related to its location in the edge of EPN. With respect to SFER, this station suffered known problems until the receiver replacement in the middleof 1998.

Five other stations, namely CREU, ACOR, CASC, LAGO and GAIA, show some disagreement. CREU performs poorly in the horizontal components and, in addition, its estimated motion in both solutions differs significantly from all surrounding sites. The same occurs in the East component of ACOR. Therefore, both stations have been removed from the final velocity field. For the other three stations, the available data cover a much longer time-span in GIN (cf. Table 1). This is especially true for GAIA and LAGO that only entered in EPN in June of 2000. Since PPP has proved to perform well, the GIN motionsare expected to be more reliable than the EPN estimates for these stations (for LAGO, the EPN solution is completely unreliable).

Site	North (mm/yr)	East (mm/yr)	Up (mm/yr)
GRAZ	14.5	21.5	-0.6
	14.6	21.4	-1.2
KOSG	15.9	18.2	-1.5
	15.5	17.8	-2.1
MATE	17.4	24.9	0.4
	17.4	24.1	-0.8
VILL	15.6	18.6	-1.4
	15.4	19.1	-1.0
MAS1	17.2	15.7	0.4
	16.5	16.1	1.6
SFER	16.2	16.1	0.2
	17.1	16.8	-2.9
EBRE	15.5	19.1	-1.6
	14.5	20.2	-0.8
CASC	16.7	16.5	1.7
	15.2	18.7	-2.2
BELL	15.1	18.2	0.8
	15.1	19.3	-0.4
CREU	20.2	23.1	1.3
	18.1	18.7	-0.5
ESCO	16.4	18.9	1.8
	14.8	19.2	-2.9
LLIV	15.4	19.7	0.5
	15.4	19.5	-2.3
ALAC	15.4	19.5	0.9
	15.6	20.0	-5.4
ACOR	17.0	22.2	-2.9
	16.9	24.2	-5.6
LAGO	14.5	17.5	-0.9
	13.8	32.4	-3.7
GAIA	14.3	17.2	0.8
	14.8	19.2	-3.7

Table 3: Estimated motions (GIN in the first row and EPN in the second row) for the stations with a history longer than 2 years, computed within the ITRF2000 reference frame.

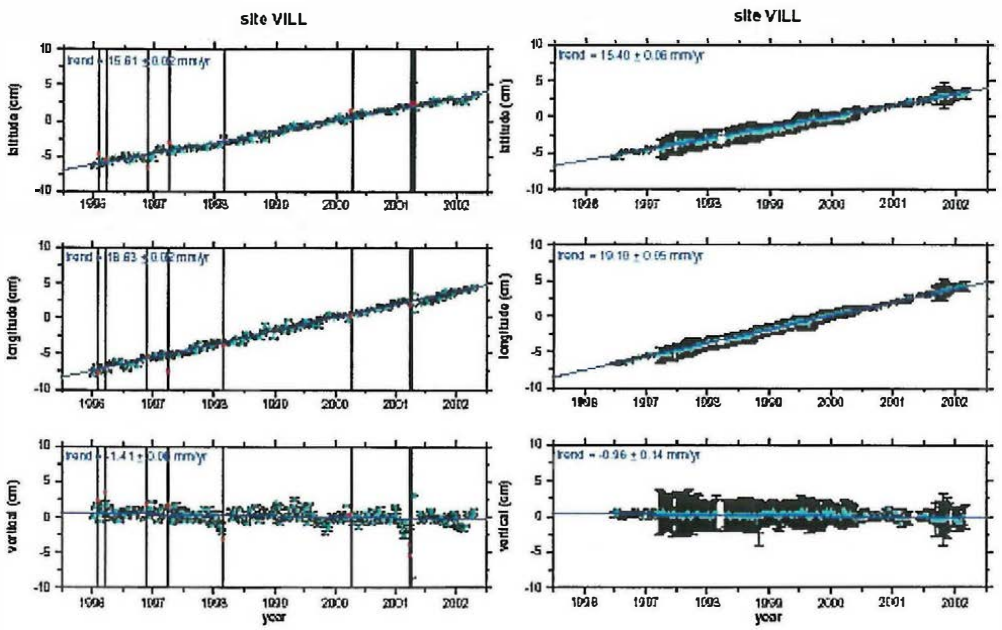

Fig. 3: VILL trend derived from GIN (left) and EPN (right). Outsized sigmas show detected and removed outliers.

6 Velocity Field Discussion

Figure 4 shows the relative horizontal motions for the reliable stations in both GIN and EPN. The plotted velocities are residuals with respect to the predicted DEOS2k motions of stable Eurasia. DEOS2k is a model for the motions of the major tectonic plates based on the ITRF2000 data set (Fernandes et al.,2002). It describes the contemporary observed geodetic motions better than other models, such as NUVEL-1A.

The stations located in Central Europe (KOSG and GRAZ) agree remarkably well with the predicted motions. MATE is showing the expected NE relative motion of Southern Italy with respect to stable Eurasia. The last station outside Iberia, MAS1, in spite of the observed noise in the weekly solutions,has estimated motions similar to the velocity predicted by DEOS2k.

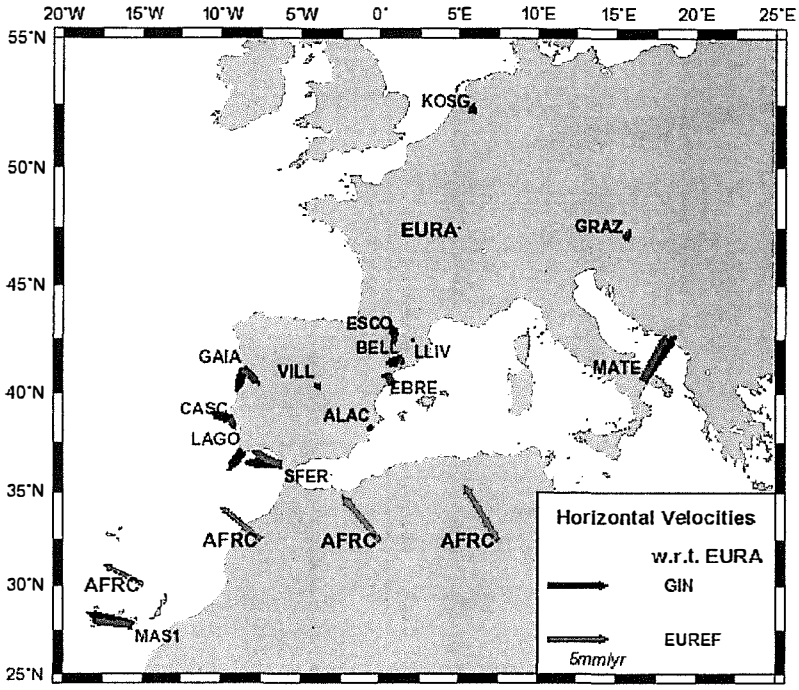

Fig. 4: Horizontal relative motions for the significant stations derived from the GIN and EPN solutions, with respect to the Eurasian plate. AFRC denotes the relativemotion of Africa (in that point) as predicted by DEOS2k. The overoptimistic formal error ellipses are not shown.

Analyzing the observed motions in the Iberian Peninsula, the stations located in the Central and Eastern parts do not show any significant differential motion with respect to stable Eurasia (in both networks).

Differently, relative motions are observed in the Western and South-Western stations. SFER and CASC (in GIN network) show a significant westward component of the relative horizontal velocities. This implies internal deformation, which is confirmed by the high seismic activity observed in this region. In general terms, this westward motion can be an effect of the pushing force exerted by the African plate at its margin with Eurasia. The small differences observed between these stations, although comparable to the noise level, can be due to a real signal coming from the complex faulting of the region (cf. Figure 1). This consideration applies also to GAIA and LAGO, even if it is not possibleto exclude artefacts derived from the still relative short time-series.

7 Conclusions

PPP proves to be an efficient technique to analyze data on a station-by-station basis: the quality of the PPP results is comparable to the EPN combined network solution. A main reason for the discrepancies observed in the weekly solutions is due to the different mapping approaches applied by DEOS and EUREF. This is an issue that requires further studies to fully understand its implications.

From the analysis of the stations with significant difference in the time-span of observations (between GIN and EPN), it can be stated that, in general, time-series shorter than 2 years do not guarantee reliable velocity estimates.

In the specific case of ACOR and CREU, the anomalous motion is still not understood. Detailed studies have to be performed to distinguish between possible reasons: station settings (equipment, surrounding environment, etc.) or local geological effects.

In general, the number of stations with a good observation time-span is still too small to draw definitive conclusions about the tectonics of the Iberian region. However, some trends can already be observed. The Central and Eastern parts of Iberian Peninsula appear to be part of stable Eurasia. The GIN solution, inparticular, indicates a significant westward motion of the western stations with respect to the rest of Iberia, suggesting that this region is in the deformation zone between the African and Eurasian plates.

References

Altamini, Z., D. Angermann, D. Argus, G. Blewitt, C. Boucher, B. Chao, H. Drewes, R. Eanes, The Terrestrial Reference Frame and the Dynamic Earth, Eos Trans. AGU, 82, 273-279, 2001.

Boucher, C., Z. Altamimi, P. Sillard, The ITRF97 International Terrestrial Reference Frame (ITRF97), IERS Technical Note 27, Observatoire de Paris, Paris, 1999.

Bock, Y., S. Wdowinski, P. Fang, J. Zhang, S. Williams, H. Johnson, J. Behr, J. Genrich, J. Dean, M. van Domselaar, D. Agnew, F. Wyatt, K. Stark, B. Oral, K. Hudnut, R. King, T. Herring, S. Dinardo, W. Young, D. Jackson, W. Gurtner, Southern California permanent GPS geodetic array: Continuous measurements of crustal deformation between the 1992 Landers and 1994 Northridge earthquakes, J. Geophys. Res., 102, 18013-18033, 1997.

Bruyninx, C., Status and prospects of the permanent EUREF network, Proc. of Symposium of the IAG Subcomission for Europe held in June 1999, Prague, Eds. E. Gubler, J.-A. Torres, H. Hornik, EUREF publication, n. 8, 42-46, 2000.

Buforn, E., A. Ud´ýas, M. Colomb´as, Seismicity source mechanisms and tectonics of the Azores-Gibraltar plate boundary, Tectonophysics, 152, 89–118, 1988.

Buforn, E., C. Sanz de Galdeano, A. Ud´ýas, Seimotectonics of the Ibero- Maghrebian region, Tectonophysics, 248, 247-261, 1995.

Davies, P., G. Blewitt, Methodology for global geodetic time series estimation: A new tool for geodynamics, J. Geophys. Res., 105, B5, 11083-11100, 2000.

Fernandes, R.M.S., B.A.C. Ambrosius, R. Noomen, L. Bastos, J. D´avila, Analysis of a permanent GPS Iberian Network (GIN), Book of Extended Abstracts of Tenth General Assembly of the Wegener Project, S. Fernando, Spain, September, 2000.

Fernandes, R.M.S., B.A.C. Ambrosius, R. Noomen, L. Bastos, M.J.R. Wortel, W. Spakman, R. Govers, Predicted motions on the Africa-Eurasia plate boundary from a space-geodetic global tectonic model (DEOS2k), *submitted for publication*, 2002.

Hayward, N., A. Watts, G. Westbrook, J. Collier, A seismic reflection and GLORIA study of compressional deformation in the Gorringe Bank region, eastern North Atlantic, Geophys. J. Int., 138, 831-850 1999.

Jim´enez-Munt, I., P. Bird, M. Fern`andez, Thin-shell modeling of neotectonics in the Azores-Gibraltar region, Geophys. Res. Lett., 28, 6, 1083-1086, 2001.

McCarthy, D. (edt.), IERS Conventions (1996), IERS Technical Note, 21, Observatoire de Paris, 1996.

Miyazaki, S., Y. Hatanaka, T. Tada, T. Sagiya, The nationwide GPS array as an Earth observation system, Bulletin of the Geographycal Survey Institute of Japan, 44, 1998.

Rothacher, M., L. Mervart, The Bernese GPS software version 4.0, Astronomical Institute, University of Berne, 1996.

Simons, W.J.F., B.A.C. Ambrosius, S. Haji Abu, M.A. Kadir, Analysis of 1999-2000 data from the Permanent Malaysian (MASS) GPS network: Results and Outlook, DEOS Report, March, 2002.

Van Martin, T., MicroCosm System Description, Vol. 1, MicroCosm software manuals, 1998.

Webb, F., J. Zumberge, An Introduction to GIPSY/OASIS-II, CALTECH, JPL D-11088, 1995.

Zumberge, J., M. Heflin, D. Je®erson, M. Watkins, F. Webb, Precise Point Positioning for the e±cient and robust analysis of GPS data from large networks, J. Geophys. Res., 102, 5005–5017, 1997.

OVERVIEW OF GALILEO AND ITS APPLICATIONS FOR GEODESY

Juan R. Martin Piedelobo[1], Alvaro Mozo García[1], Miguel M. Romay Merino[1]

[1] GMV S.A., Isaac Newton 11, PTM-Tres Cantos, 28760 Madrid, SPAIN
Phone: + 34-91-807 21 00, Fax: + 34-91-807 21 99, e-mail: jrmartin@gmv.es

ABSTRACT:

Global Positioning Systems, like GPS and GLONASS, have paved the way for a new age in the field of Satellite Geodesy. In the future, new satellite systems like GALILEO will complement these constellations, improving the accuracy and reliability of geodetic parameters that are the object of estimation. This paper provides and overview to the GALILEO architecture and the most relevant functions of the system. Special attention is paid to a few important system aspects from the geodetic perspective: the constellation design, expected performance, and the techniques that have been proposed for precise orbit determination and time synchronisation. Integrity issues are also explored, since they represent a point of added value of GALILEO with respect to current systems. Finally, the paper presents the results of some simulations that have been performed to assess the benefits that GALILEO could bring to the geodetic community. The simulations address the combination of GALILEO with current GNSS systems. In particular they show the benefits that could be achieved in the estimation of station co-ordinates, plate motion and Earth rotation parameters.

1. INTRODUCTION

GALILEO, the European radio navigation satellite system, will be an independent, global European-controlled satellite-based navigation system [1.] [3.] [4.]. It will have a constellation of satellites complemented with a Ground Control Segment providing system and satellite monitoring and control, and an Integrity Determination Segment that broadcasts real-time warnings of satellite or system malfunctions.

Each satellite will broadcast precise time ranging signals, together with clock synchronisation, orbit ephemeris and other data. Any user equipped with a suitable receiver will be able to determine his/her position to within a few metres when receiving signals from just four GALILEO satellites.

The ground segment includes all the assets necessary to control the space segment and the system mission. It will provide the necessary raw data to be broadcast for the Positioning and Timing Services and will manage and control the whole GALILEO constellation, monitoring satellite health and up-loading data for subsequent broadcast to users. The key elements of this data, clock synchronisation and orbit ephemeris, will be calculated from measurements made by a worldwide network of sensor stations.

The GALILEO Integrity Segment will provide integrity services by monitoring the quality of the signals of all the GALILEO satellites and broadcasting integrity messages to users via GALILEO satellites. GALILEO will also incorporate Local Components, which will be able to provide various services with a view to improve accuracy, integrity and robustness on a local basis. GALILEO satellites may incorporate a Search & Rescue Payload that may receive and forward distress signals from beacons operating in the COSPAS-SARSAT system. Moreover, GALILEO satellites will be able to relay responses to these distress messages back to the user and to rescue personnel. GALILEO will provide a range of guaranteed services to users equipped with receivers meeting GALILEO specifications. The GALILEO User receivers are part of the system. GALILEO Service Centres, not part of GALILEO, will provide users with a point-of-contact to the GALILEO system and will also be able to provide value-added services. In addition, GALILEO will provide raw data information to the scientific user communities in the area of time and geodesy.

The GALILEO programme is currently broken down into two "Overall Phases":

1. The Definition, Design, Development and In-Orbit-Validation (IOV) Phase (spanning 2002 - 2006): The Definition Phase is aimed to achieve a precise definition of the mission architecture and to prepare requirement specifications in order to select suppliers and to support the decision to start the subsequent phase. Then, the detailed design down to equipment level will be completed during the Design Phase. Finally, the IOV Phase will address the development, production, integration, validation and launch of a "mini-constellation" of satellites for in-orbit testing purposes. Then an IOV test campaign phase will follow with the aim to validate the system functions and the relevant main performances including the space segment, the SIS and the system interfaces.
2. The Full Operation Capabilities –FOC- Deployment Phase (spanning 2006 - 2008): It is aimed to complete the development of the complete final system (space and ground segments), taking into account the results of the IOV phase. More particularly, the manufacture, launch and in-orbit tests of the full constellation of satellites will be completed during this phase. As a result, full navigation, integrity and other complementary services will be provided to users. The FOC also includes a Replenishment phase aimed to provide the means to replace failed satellites while minimising any impact on system performance.

Currently, at mid 2002, the system is facing its Preliminary System Design Review (PSDR), the Definition Phase final milestone.

2. OVERVIEW OF THE GALILEO SYSTEM ARCHITECTURE

GALILEO will provide the users with a series of services on a global, regional and local basis. The GALILEO Global component will be composed of a Space Segment and a Ground Segment, whilst the Regional and the Local components will be ground-based.

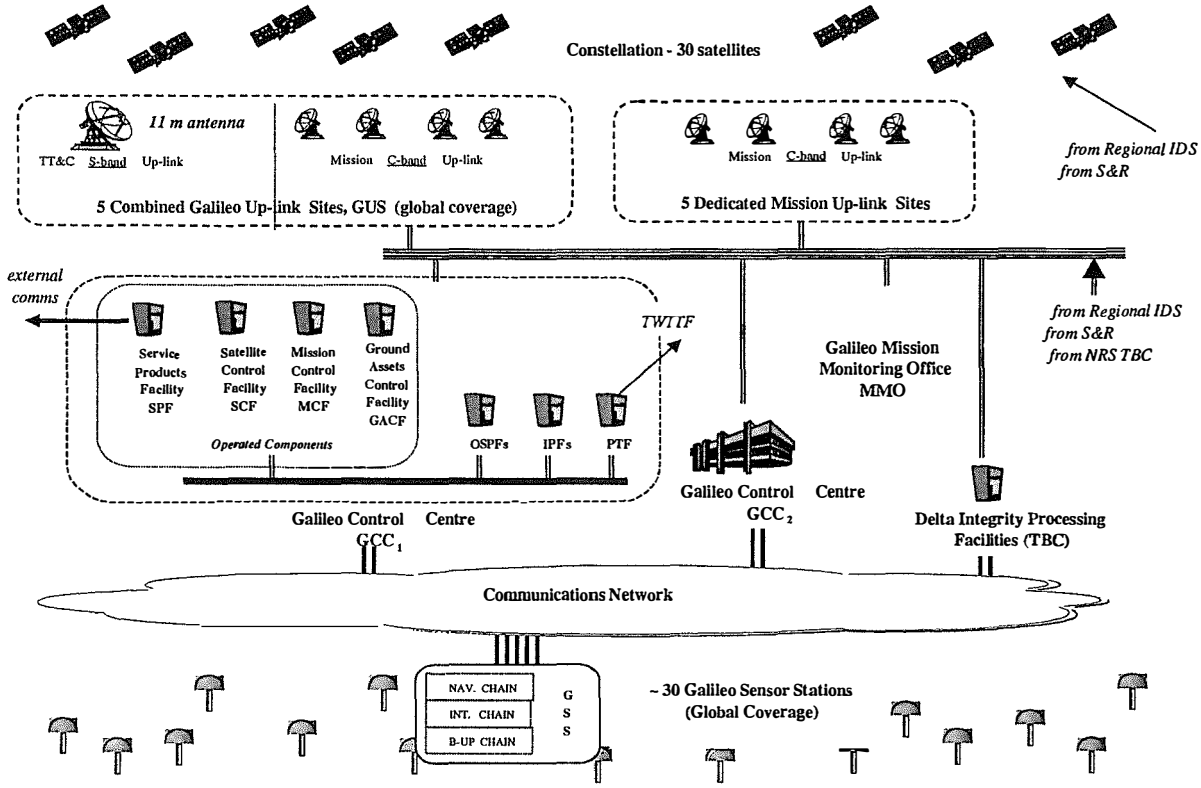

Figure 1: Overview of the GALILEO system architecture.

The GALILEO Space Segment, in the Global Component, will comprise a constellation of 27 plus 3 spare satellites in medium-Earth orbit at 23616 km altitude, so that its geometrical properties provide the required positioning and integrity performance. The satellites will be deployed in three orbital

planes, inclined 56 degrees. The spare satellites will be also active, and transmit the navigation message in the same way the nominal satellites do. The satellite replacement strategy allows a failed satellite to be replaced by a spare within 7 days. New launches will be then needed to put a new spare in orbit. The satellites are designed for a 15 years maximum lifetime (the whole system lifetime is 20 years). After roughly 13 years from the initial constellation deployment a constellation renewal phase would occur. Most of the constellation would be re-deployed by that time.

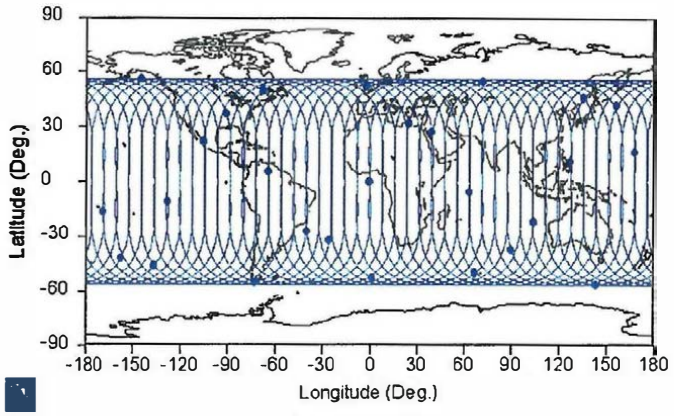

Figure 2: Ground tracks of the baseline GALILEO constellation.

The ground segment includes all the assets necessary to control the space segment and the system mission. Two main control facilities are currently addressed in the ground segment:

- The so-called **Satellite Control Facility (SCF)**, in charge of monitoring and commanding the satellites so as to maintain the constellation in the required configuration. The SCF lets also the rest of the system be aware of the status of the satellites.
- The so-called **Mission Control Facility (MCF)**, in charge of managing the navigation and integrity missions of the system; this management includes ensuring correct on-ground collection and processing of navigation and integrity data, correct on-ground generation of navigation and integrity messages, and correct and timely unlinking of updated information to the satellites.

In addition to the SCF and the MCF, the ground segment includes a facility controlling all the assets of the ground segment (GACF) and a service product facility (SPF) in charge of interfacing the service providers external to GALILEO.

The system interfaces non-European integrity determination systems (NEIDS), COSPAS-SARSAT for Search & Rescue (SAR), and navigation-related service providers (NRS) to allow broadcasting of their information through the GALILEO Satellites.

The system integrity mission includes a worldwide (global) integrity determination (on-ground processing) and dissemination (broadcasting) system. To this purpose, the navigation signals are monitored by a worldwide network of some 30 GALILEO Sensor Stations (GSS).

The GSS measurements will be collected and processed at two different facilities within the GALILEO Control Centres (GCC):

- The Orbit and Synchronisation Processing Facility (OSPF) for the generation of the navigation messages. The OSPF is the number crunching centre of the GALILEO system. It is in charge of calculating satellites orbit data (ephemeris and almanacs), clocks synchronisation data, and Signal In Space Accuracy indicators (SISA) for all satellites of the constellation. The OSPF will implement a number of real time processing functions such as:
    1. GSS data acquisition and pre-processing
    2. GALILEO satellites orbit determination, providing almanacs and precise ephemeris
    3. Satellites clocks correction data determination

4. Signal-In-Space Accuracy (SISA) determination for each satellite
5. Navigation data elaboration and transmission for uplink to the satellites

- The Integrity Processing Facility (IPF) for the generation of the integrity messages within the most demanding time-to-alarm requirements.

Besides the IPF and the OSPF, the ground segment also includes the so-called Precision Timing Facility (PTF) in charge of generating the GALILEO System Time (GST). For this purpose, the PTF includes several high-stability Cs and H-Maser clocks, and also a dedicated interface to an UTC/k laboratory for steering the GST to the UTC.

Finally, the ground segment also includes all of the assets necessary to uplink the satellites, basically:

- 5 telemetry, tracking, and command stations (TTCS) in the S-band for satellite control purposes, and
- 10 mission uplink stations, 5 of which are collocated with the TTCS, to deal with navigation and integrity missions related uplink.

3. OVERVIEW OF SERVICES

The panoply of GALILEO services includes a number of precise positioning and timing, integrity, and search&rescue (SAR) services.

The different positioning and timing services have been classified into Open, Commercial, Safety-of-Life (SoL) and Public Regulated (PRS) [4.]. The Open services will be provided via open signals in two different carriers, without payment of any fee. The SoL service addresses the dissemination of integrity data incorporated into the navigation data that is provided via the open signals. The access to this SoL service shall be controllable. The Commercial service address the dissemination by GALILEO satellites of ranging and data signals with negotiable performance, including integrity, to which access shall be controllable in order to allow fees to be levied. Finally, GALILEO will provide a Public Regulated navigation & timing service by means of independent, restricted-access navigation signals.

A user equipped with a GALILEO Dual-Carrier Satellite-Only Receiver will be able to determine its position with a horizontal accuracy of 4 metres and a vertical accuracy of 8 metres with 95% confidence. A user equipped with a GALILEO Single-Carrier Satellite-Only Receiver will be able to determine its position with a horizontal accuracy of 15 metres and a vertical accuracy of 35 metres with 95% confidence [5.].

GALILEO will also enable the dissemination by selected GALILEO satellites of integrity data generated by independent regional integrity services, with negotiable performance. GALILEO will provide data up-linking services for these independent regional integrity services, or could enable them to have a direct access to the GALILEO satellites for integrity dissemination purposes.

GALILEO will receive Distress Signals from SAR Beacons and transmit them to MEO Local User Terminals (MEOLUT) of the COSPAS-SARSAT Search and Rescue (SAR) Service. GALILEO will also receive return messages from the COSPAS-SARSAT Search and Rescue (SAR) System, and will incorporate them into navigation data messages of selected GALILEO satellites for re-transmission to 3rd Generation SAR Beacons endowed with GALILEO receiving capability.

4. CONSTELLATION DESIGN

The GALILEO Space Segment will comprise a constellation of 27 plus 3 spare satellites in, near circular, medium-Earth orbit (MEO) at a 23616 km altitude[1], so that its geometrical properties provide the required positioning and integrity performance. The nominal 27 satellites constellation will be deployed in three orbital planes, inclined 56 degrees according to a 27/3/1 Walker pattern. The three spare satellites, deployed one per plane, will be also active and transmit the navigation message in the same way the nominal satellites do.

Orbital perturbations will cause the orbits to deviate from the nominal ones, thus leading to degradation in the performances of the constellation. When performances do not fulfil an acceptance

[1] Corresponding to a nominal semi-major axis of 29994 km.

level, corrective manoeuvres must be performed in order to restore the constellation to its nominal state. An in-orbit control strategy has been defined to reduce insofar as possible the number of corrective manoeuvres, since they increase considerably the cost of the system and reduce the availability level of the constellation.

In order to do this, the orbital elements of the nominal constellation were propagated over 15 years using a precise orbit propagator. Then the evolution of the constellation performance over this period was analysed. The following maps depict the evolution of the worst case of vertical accuracy (95%) during the simulation period at each location in the Globe. The scale goes from 3 metres, plotted in white, to 8 metres, in black. The darker the colour the worse the vertical accuracy. A black area indicates a vertical accuracy worse or equal to 8 metres. A white are indicates a vertical accuracy better or equal to 3 metres.

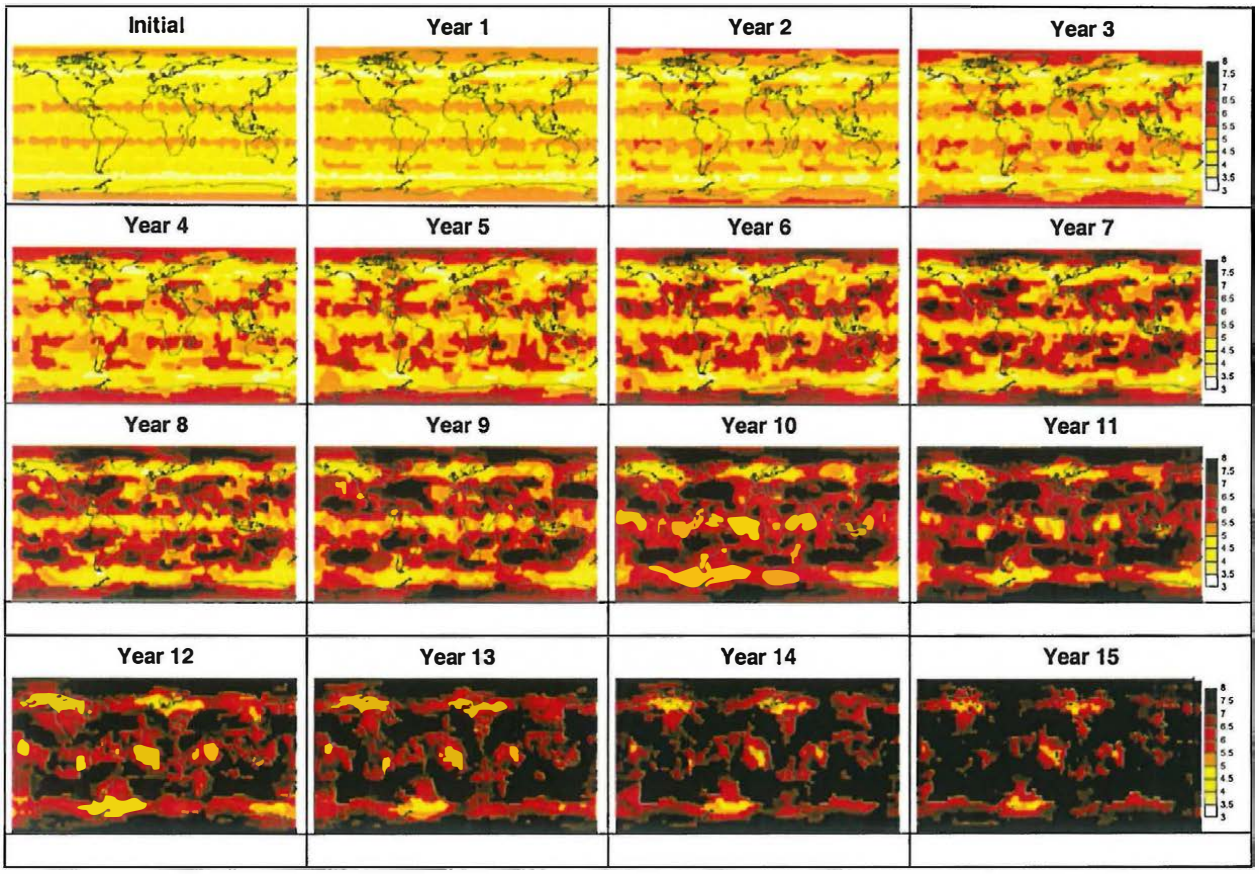

Figure 3: Evolution of the vertical accuracy (metres) over 15 years before orbit stabilisation.

The plots show that the vertical accuracy have degraded significantly after 5 years of propagation. Corrective housekeeping manoeuvres shall be therefore performed in order to maintain the performance within acceptable limits.

A detailed analysis of the phenomena behind this degradation indicates that it is due to certain orbital perturbations which are changing the relative phase angle between satellites, the inclination (roughly 3 degrees over 15 years), and the Right Ascension of the Ascending Node – RAAN - (a few degrees over 15 years). It was found that the relative phase between satellites was drifting in a quasi-linear manner and therefore, can be compensated by a slight (< 1 Km) correction in the semi-major axis. On the other hand, the inclination and RAAN drifts can be tuned so that the average over the constellation lifetime keeps closer to the nominal values. The orbit optimisation process is explained in more detail in [6.].

These modifications would be performed in the nominal orbital elements beforehand, the satellites being deployed in these optimised orbits at the beginning of their operational life. As a result the

constellation would become much more stable over the 15-year period, as it can be noticed in the following plots depicting the evolution of the worst case of vertical accuracy (95%) over this period.

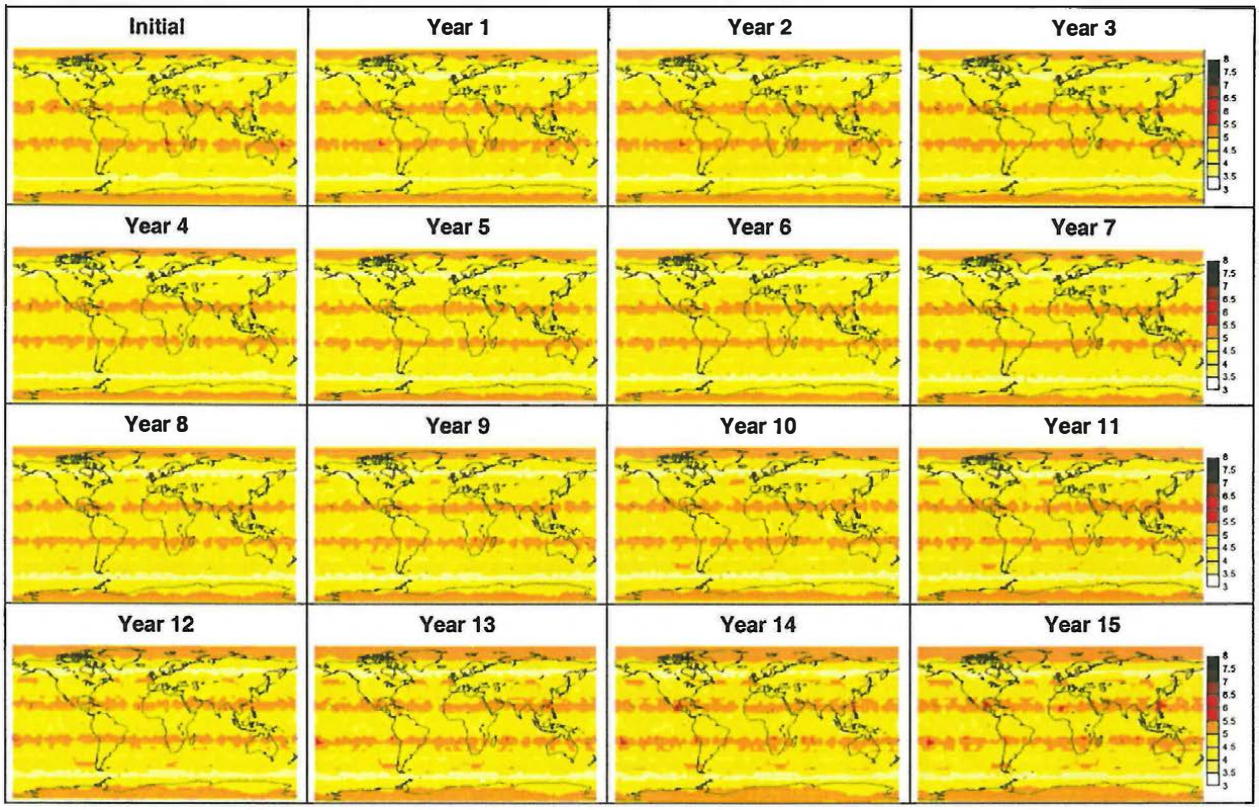

Figure 4: Evolution of the vertical accuracy (metres) over 15 years after orbit stabilisation.

Although small accuracy degradation can be still observed, as a result of the orbit stabilisation the performance remain very stable over the 15-year period. Therefore, no housekeeping manoeuvres are foreseen necessary.

5. OVERVIEW OF OD&TS TECHIQUES IN GALILEO

The Orbit Determination and Time Synchronisation (OD&TS) is a key function within GALILEO, since it is the basis for providing the navigation data to the users. The main job of the OD part in the algorithm is the determination and the prediction of the satellite orbits. To this purpose a large set of data (days) acquired from several monitoring stations (e.g. 15 minimum) are processed in batches. As of today, the OD predictions are estimated to be accurate to within few tens of cm (e.g. 20 cm, 1 σ).

One of the products of the OD&TS process is the "instantaneous" clock estimation (snapshots) that serves as the basis for time synchronisation. The "instantaneous" clock estimations are the biases of each of the clocks in the system with respect to the GALILEO System Time (GST). A model is then fitted to these snapshots in order to predict the clock bias evolution. Current estimations report snapshot accuracy in the order of 0.2 ns (1 σ).

The overall OD&TS process can be described in four steps:

1. First, a Pre-Processing module receives raw tracking data from the GSS network, performs a data validation and corrects the various observables for a number of errors such as propagation delays.
2. The pre-processed observables are then passed along to the Orbit Determination & Clock Extraction module, which calculates the orbits and clock snapshots for all of the satellites during the observation period, and generates precise satellite orbit predictions.

3. The predicted orbits are then used to compute the Ephemeris Messages and almanacs to be broadcast to users in the navigation message.
4. The clock snapshots are then used to build the clock prediction models to be broadcast to the users in the navigation message.

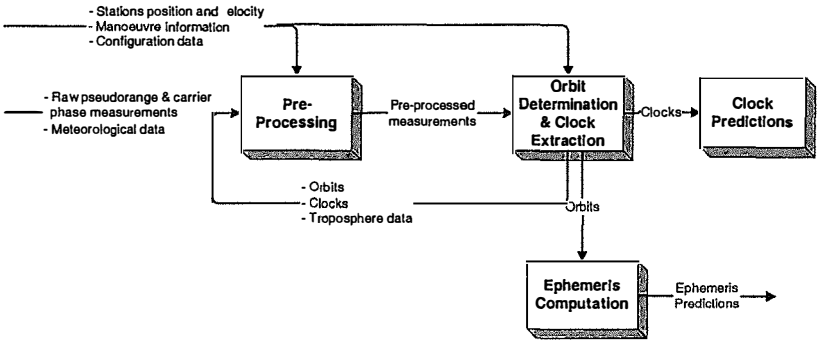

Figure 5: Overall OD&TS process overview.

The basic structure of the OD&TS will be that of an off-line batch process. A batch process produces, for each included satellite, a continuous orbit arc that runs from a certain starting epoch in the past up to a certain end epoch in the future (relative to the moment at which the batch process starts). The prediction part (future part) of the orbit provides the other OSPF processes with real-time orbit information during the period that starts as soon as the batch process has finished.

Because the reliability of such prediction degrades with time, a new solution process will have to be executed fairly soon after the previous process. This results in a series of consecutive batch processes, executed at regular intervals. This interval will normally be short in comparison to the length of the solution arc itself so that successive solution arcs have a substantial overlap in time.

6. OVERVIEW OF THE GALILEO INTEGRITY SERVICE

Besides hosting the OD&TS process, the OSPF will also estimate the so-called Signal-In-Space Accuracy (SISA) for each satellite. The SISA is a statistical bound of the clock and ephemeris errors affecting the Signal-In-Space, which will be broadcast to users in the navigation message. This will allow GALILEO users to estimate the positioning and timing errors, which are usually referred to as Protection Levels (PLs). The comparison of these protection levels against certain predefined thresholds, usually called Alert Limits (ALs), will allow the users to determine whether the positioning and timing services provided by GALILEO are suitable or not for the intended use.

SISA and protection levels thus constitute a powerful mechanism to warn users when they should not use the positioning and timing services. This capability is usually referred to as integrity, and can be defined as a measure of the trust that can be placed in the correctness of the information supplied by the system, including the ability to provide users with timely and valid warnings (alerts).

However, it should be noted that an integrity service that is built only upon SISA has an important limitation, which the time required to notify to users a warning, this is the associated time to alert. As a matter of fact, in this concept, a degradation of the service that is provided by any individual satellite must be accompanied by a subsequent change of its associated SISA indicator. Since this parameter is transmitted in the navigation message, its update can only be done on the occasion of navigation messages updates. In current design, this update is carried out every 100 minutes, which is a too long time for an integrity service to be effective enough for certain applications.

In order to overcome this limitation, GALILEO will be endowed with a dedicated subsystem to determine and report the service integrity. The core of this subsystem is the Integrity Processing Facility (IPF). The IPF is in charge of the calculation of a so-called integrity flag (IF), which contains information about the correctness of the SISA indicator. Unlike for SISA, the integrity subsystem does

have the capability to broadcast to users this information in near-real time, thus allowing meeting the most demanding Time-To-Alarm requirements.

The integrity flag will provide users with information about which satellites are being monitored at a given instant. For monitored satellites, the IF will warn the users about situations in which the SISA indicator is not correct and therefore the resulting protection levels could be misleading.

7. INTERFACE WITH THE GEODETIC COMMUNITY

The exploitation of the GALILEO Services is expected to need the provision of a number of geodetic and geophysical services such as:

- The definition of a geocentric Cartesian Reference System, whose implementation is named GALILEO Terrestrial Reference Frame (GTRF), including:
    1. The GTRF co-ordinates of the GALILEO Sensor Stations (GSS), which enable their master(s) facility (OSPF) to determine the orbits, as well as the Signal-In-Space Accuracy (SISA) of each satellite
    2. A geometrical model of the Earth, to perform the transformation of the GTRF geocentric Cartesian co-ordinates into ellipsoidal co-ordinates (typical process in the GALILEO receiver), and vice versa
    3. A physical model of the Earth: angular velocity, mass (primary parameters) and possibly a detailed gravity field model (secondary parameters), to be used in the orbit determination process, both at OSPF and user level
- The transformation matrices and procedures between GTRF co-ordinates and the other existing reference frame (global, regional, national, local) co-ordinates of interest to the GALILEO users
- SLR data, to be used for the first calibration of the OD&TS algorithms in the IOV phase, and the possible following performance evaluations and re-calibrations

This mission will be entrusted to a Geodetic Reference Service Provider (GRSP). The exchange of geodetic products will be performed via a so-called Service Product Facility (SPF), and controlled via a dedicated Interface Control Document (ICD). This ICD is currently under definition.

8. ENVISAGED BENEFITS

In spite GALILEO will represent a true alternative to GPS, the major benefits that are currently envisaged result from the combination of GALILEO with GPS. A number of activities, including Pilot Projects, have been sponsored by the European Commission and ESA in the latest years to demonstrate the benefits GALILEO would bring in a number of sectors.

Some simulation results showing the benefits that GALILEO could bring to the geodetic community are presented hereinafter. The simulations address the combination of GALILEO and GPS and show:

- First, the general benefit from the mere geometrical perspective in terms of number of satellites in view and PDOP (Figure 6) and, more particularly
- How this could improve two typical tasks performed by the geodetic community such as the estimation of station co-ordinates and Earth rotation parameters. 1 depicts some results showing the expected improvement in the estimation of Earth Rotation Parameters (ERPs), station co-ordinates and plate motion. This improvement has been estimated as the improvement in the covariance matrices associated to the estimation of these parameters. It is assumed in the simulation that the ground stations are endowed with dual GPS/Galileo receivers connected to a common time reference. In both cases, it can be observed that the combination of GPS and GALILEO has the potential to provide a 30% accuracy increase with respect to what is currently obtained with GPS alone. This benefit can be explained due to the improved geometry and increased observability of the parameters that are the object of estimation thanks to the use of the two systems. Moreover, the use of two independent systems has as an additional advantage the capability to compensate for systematic errors in each individual system, which could not be detected otherwise (e.g. using GPS alone). These

results have been obtained by simulating GPS & GALILEO pseudorange data over 3 days for some 20 stations, which were then processed with a state-of-the-art OD&TS SW Package in order to assess the benefits of adding GALILEO data to the standalone GPS solution.

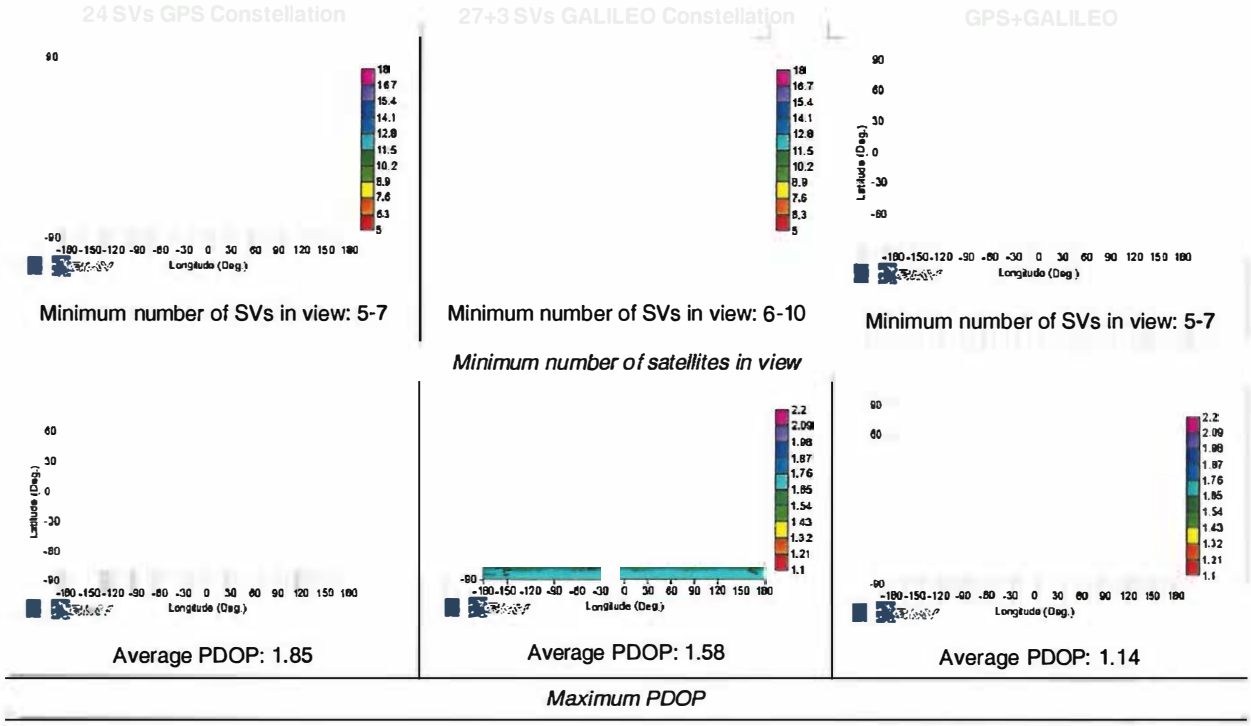

Figure 6: Expected geometrical improvements resulting from the combination of GPS and GALILEO.

Estimation of Station co-ordinates	Estimated Improvement		
	Lon	Lat	Height
Example 1: Kiruna	34.22%	33.68%	30.25%
Example 2: Newnorcia	34.22%	39.64%	34.69%
Example 3: Kourou	34.22%	32.87%	39.18%
Example 4: Papeete	34.22%	36.78%	37.62%
Example 5: Hartebeestoek	34.22%	38.43%	36.12%

Estimation of ERPs	Estimated Improvement		
	xp	yp	LOD
Day 1	31.80%	32.21%	26.35%
Day 2	31.82%	31.67%	6.67%
Day 3	31.51%	31.05%	25.71%

Table 1: Expected improvement in the estimation of station-co-ordinates and ERPs resulting from the combination of GPS and GALILEO.

9. CONCLUSIONS

GALILEO, the European radio navigation satellite system, will be an independent, global European-controlled satellite-based navigation system [1.] [3.] [4.]. It will provide an accurate, independent; GNSS open service to all users.

The GALILEO services will be available in early 2008, with an initial In-Orbit Validation phase starting in 2006. The Programme is now concluding the Preliminary Design Phase with Preliminary System Design Review expected in mid July.

Precise Orbit Determination & Time Synchronisation techniques are the core of the provision of positioning and timing services, since they provide the basis for the determination of the satellite ephemeris and clock models to be included in the navigation message to users.

In spite GALILEO represents an alternative to GPS, major benefits result from the combination of GALILEO with GPS. This paper has shown some examples in which the combination of GPS and GALILEO could improve two typical tasks performed by the geodetic community such as the estimation of station co-ordinates, plate motion and Earth rotation parameters. In both cases, a 30% enhancement can be expected when both systems are combined.

10. REFERENCES

[1.] Communication of the European Commission to the European Parliament and the Council on GALILEO. Brussels, 22 November 2000.

[2.] Council Resolution on the involvement of Europe in a new generation of satellite navigation services. Brussels, 19 July 1999.

[3.] European Commission Communication on GALILEO. Brussels, 10 February 1999.

[4.] GALILEO Mission High Level Definition Document. European Commission. Issue 2, April 3, 2001.

[5.] GALILEO System Requirements Document (GSRD, ESA-APPNS-REQ-00011). Issue 2, 11 March 2002.

[6.] A.B. Martín-Peiro et. al.: "*In-Orbit Control Strategy (for Galileo)*". Proceedings of the IAIN World Congress in association with the U.S. ION 56th Annual Meeting. San Diego, California USA. June 26-28 2000.

IMPACT OF GALILEO AND MODERNIZED GPS ON HEIGHT DETERMINATION

Hans van der Marel[1]

[1] Mathematical Geodesy and Positioning, Delft University of Technology
Thijsseweg 11, 2629 JA Delft, The Netherlands
Email: H.vanderMarel@geo.tudelft.nl

ABSTRACT

The height has always been the more difficult parameter to estimate in high precision GPS positioning applications. In this paper we investigate the impact of GALILEO, the proposed European satellite navigation system, and modernized GPS on the height and other parameters. The GALILEO and modernized GPS system will provide more and better signals on both existing and new frequencies, resulting in improved observations, in particular for the so-called ionosphere free linear combination. First, as an introduction, the new GPS and GALILEO signals are discussed. Secondly, the effect of the new signals on the ionosphere free linear combination is given. The new signals on L5 result in a 24% improvement in the precision (in terms of variance) of the ionosphere free linear combination, if used instead of L2, or 30% if all three frequencies are used, under the restrictive assumption that the carrier phase observations have the same accuracy as GPS. This means that possible improvements in tracking-performance of the new signals have not been taken into account yet. Thirdly, the effect of additional satellites is discussed. If the receiver tracks both GPS and GALILEO, the precision in height for a mid-latitude station is improved by about 63-75% if only the effect of additional satellites is taken into account. This is beyond what can be expected from just doubling the number of satellites. These numbers are derived for quite a conservative situation, in which the station position, satellite clock errors, independent GPS and GALILEO receiver clock errors, tropospheric delays and the initial phase ambiguities for every satellite are estimated. The improved redundancy in case of a dual GNSS constellation will also make it possible to introduce additional parameters to reduce (systematic) errors, and the improved accuracy will make new applications possible. For instance, the precision of troposphere parameters is improved considerably with the use of GPS and GALILEO, especially for moving receivers, thus making it possible to collect water vapor information for meteorologists from ships and buoys on the oceans where observations of water vapor have always been sparse.

Keywords:

GPS, GALILEO, Geodesy, Precise Positioning, Height, Water Vapour

1. INTRODUCTION

On 26 March 2002 the European Union gave the go-ahead for the GALILEO project, the European satellite navigation system. The system will consist of about 30 global navigation satellites at 23,616 km altitude and is expected to become operational in 2008 [2]. The launch of a first experimental satellite is foreseen for 2004 and operational launches should commence in 2005-2006. Although very similar to GPS in concept, the actual signals and orbits for the GALILEO system will be different from GPS. However, interoperability with GPS is one of the design considerations of GALILEO, so more or less the same frequency bands and similar ranging codes are used in order to facilitate combined GPS&GALILEO receivers for high precision applications. Signal integrity will be provided by GALILEO as an integral service. The EGNOS system, the European GPS/GLONASS Integrity Service, which will be operational in 2002, will be integrated with GALILEO starting in 2006/2008, although EGNOS will be available from geostationary satellites until 2015. GALILEO will be operated completely independently from the GPS system, and should either system fail the other will be able to take over for critical applications.

The GALILEO system will consist of 30 satellites, of which 3 are active spares, in circular orbits at 23,616 km altitude in three different orbital planes at 56° inclination [5]. For comparison, the GPS system consists nominally of 24 satellites (although 28 satellites are operational now) in circular orbits at 20,200 km altitude in six orbital planes at 55° inclination. For the GALILEO the altitude of the satellites has been raised in order to have an orbital period of 14^h22^m (1+2/3 rev/day) instead of the 11^h58^m (2 rev/day) for GPS, which is close to the semi-diurnal resonance frequency. It is expected therefore that the GALILEO satellites require much less orbital manoeuvres than the GPS satellites, which will ease the precise orbit determination. Furthermore, the GALILEO system will use 10 ranging codes on four different carrier frequencies. At first sight this may seem a big step forward compared to the one civil signal and two military signals on GPS, but one should take into account that only 6 GALILEO ranging codes on three frequencies will be un-encrypted and that the GPS system will be modernized as well. The present day GPS system will also see some major changes. Starting in 2003, with the launch of the remaining, albeit refurbished, block IIR satellites, new military signals will be transmitted on L1 and L2 and a new civil - CA code like - signal will be transmitted on L2. Secondly, starting with the new block IIF satellites in 2005, P-code like signals will transmitted on a third frequency, the so-called L5 at 1176.45 MHz [6]. There is a downside to all these new signals as well, as it becomes in a relative measurement set-up all too easy for receivers not to track the same signals, and thereby effectively reducing the number of possible single difference observations.

In this paper the impact of the future GALILEO system and modernized GPS system on the precision of the position and zenith delay parameters is investigated. Two scenarios are considered: a constellation of only GPS satellites and a combined GPS plus GALILEO constellation. A GALILEO only scenario is not considered in this paper, since the main benefit comes from roughly doubling the number of satellites in view. Our computations are not based on real data: they are design studies based on simple assumptions on the standard deviations of the observations and assumed GPS and GALILEO constellations. We focus on applications with long baselines and long observation time spans, involving the ionosphere free linear combination of observations. For results on short baselines and real-time kinematic applications, whereby ambiguity resolution is a key ingredient, we refer to [1].

2. GPS AND GALILEO SIGNAL STRUCTURE

The signals for the modernized GPS system are given in Table 1. The signals in bold are the signals that are available on the present day GPS system. This is the encrypted P code (Y-code) on the L1 and L2 carrier frequencies, and the C/A code on L1. The P and C/A codes on L1 are modulated in phase quadrature, using the I-channel (cosine) and Q-channel respectively. From 2003 onwards, the remaining – albeit refurbished - block IIR satellites will have a second civil signal as well: the CS code on L2. This is a C/A code like signal that is modulated on the Q-channel of L2. At the same time new military signals will be provided in the two side-lobes of the L1 and L2 carriers using a modulation techniques know as "Binary Offset Carrier" (BOC) or split frequency. The next generation of GPS satellites, the block IIF, will be transmitting additional signals on a third carrier frequency, the so-called L5 at 1176.45 MHz [6]. These will be P-code like signals; using the same "Binary Phase Shift Keying" (BPSK) modulation technique as the P- and C/A codes [4]. The Q-channel of L5 will contain a ranging code without data message: a so-called pilot signal. This will greatly enhance the tracking performance under difficult situations.

	Carrier	**Code**	**Channel**	**Chip-rate**	**Data**	**Remarks**
L1	1575.42 MHz	**P(Y)**	**I(cos)**	**10.23 Mcps**	yes	
		CA	**Q(sin)**	**1.023 Mcps**	yes	
		M	Binary Offset Carrier			2003 onwards
L2	1227.60 MHz	**P(Y)**	**I(cos)**	**10.23 Mcps**	No	
		CS	Q(sin)	1.023 Mcps	TDMA	2003 onwards with remaining block IIR
		M	Binary Offset Carrier			
L5	1176.45 MHz	BPSK	I(cos)	10.23 Mcps	yes	2005 onwards Block IIF
		BPSK	Q(cos)	10.23 Mcps	pilot	

Table 1: Signals for the modernized GPS system. The signals of the present block II satellites are given in bold.

The proposed signals for GALILEO are given in Table 2, using [3] as the main source of information. The reader should be aware that the signals for GALILEO are not yet finalized and that the information given in table 2 can still change. A total of 10 ranging codes are proposed for GALILEO. However, the ranging codes and data messages of 4 of the signals will be encrypted for Commercial Services (CS) and Public Regulated Services (PRS) for governmental institutes, and will be unavailable to the public. This leaves 6 ranging codes for the Open Service (OS) and the Safety-of-Life Service (SAS). The gray boxes in Table 2 denote the open signals. Basically GALILEO will provide P-code like ranging codes on the E5a carrier (which is the same as the L5 carrier of GPS) and the E5b carrier, using the BPSK modulation technique, and a BOC[2,2] signal on L1 (BOC[x,y]: x is the offset of the sub-carriers, y is the bandwidth). The Q-channel will contain a data free pilot signal. Furthermore, the data message on E5b will be encrypted for Commercial Services (CS). Additionally, for the CS and PRS services BPSK and BOC ranging codes will be provided on the E1/2 sub-carriers and E6 carrier.

	Carrier	Code	Chan.	Chip-rate	Data	Service
E2-L1-E1	1575.42 MHz	BOC[2,2]	I(cos)	2.026 Mcps	200sps	OS/SAS
			Q(sin)	2.026 Mcps	Pilot	
		BOC[14,2]	E2 and E1 subcarriers			PRS
E5a = L5	1176.45 MHz	BPSK (P-like)	I(cos)	10.23 Mcps	50sps	OS/SAS
			Q(cos)	10.23 Mcps	Pilot	
E5b	1202.025 MHz	BPSK (P-like)	I(cos)	10.23 Mcps	500sps	OS/SAS/CS
			Q(cos)	10.23 Mcps	Pilot	
E6	1278.75 MHz	BPSK (CA-like)	I(cos)	5.115 Mcps	1000sps	CS
			Q(sin)	5.115 Mcps	Pilot	
		BOC[10,5]		5.115 Mcps	1000sps	PRS

Table 2: Provisional signal structure for GALILEO (subject to change). The gray boxes indicate un-encrypted ranging codes and data messages form the Open Service (OS). Three other services are provided: a Commercial Service (CS) using the OS signals with additional ranging codes on E6 and encrypted data messages on E6 and E5b, a Public Regulated Service (PRS) for governmental institutes with encrypted ranging codes and navigation messages on E1-L1-E2 and E6 carriers and a Safety-of-Life Service (SAS) using the OS ranging codes and navigation data messages with additional integrity messages.

What can we expect from these new signals in terms of tracking performance? Firstly, not much will change for the GPS tracking performance on L1, unless encryption on the P-code is switched off so that one may use the P-code instead of the C/A code on L1. GALILEO will use a different modulation technique on L1, BOC[2,2], which has a bandwidth and chipping rate that is larger than the GPS C/A code. It is therefore expected that the GALILEO code and carrier phase on L1 have a lower noise than GPS [1,4]. Secondly, tracking the GPS L2 will be improved considerably with the new CS ranging code, resulting in improved Signal-to-Noise ratios and more observations at lower elevation angles compared to cross-correlating the GPS L2 and L1 P-code signals. We may expect a similar noise level for L2-CS as for L1-C/A. Thirdly, the proposed signals on L5, E5a and E5b hold the greatest promise. This is because these are P-code like signals on both the Q- and I-channels, with higher bandwidth and chipping rate than the C/A-code signals, and with one of them a data free pilot signal. So, we can expect smaller standard deviations for the code and carrier phase observations and more observations at lower elevations (a factor 3 is reported in [1] and [3]). The downside of all these new signals is that a situation may occur where, for instance, two receivers each track two signals, but it so happens that neither tracks the same signals as the other and hence no single differences can be formed in which the satellite clocks and biases are eliminated. This situation may easily occur if one receiver is tracking L1&L5 and the other L1&L2, or both are tracking L1&L2, but one is using the new CS code and the other is using cross-correlation. Whether this will be a real problem, or can be solved by the receiver hardware, is not clear at present (at least not to the author).

3. PRECISION OF THE IONOSPHERE FREE LINEAR COMBINATION

The ionosphere free linear combination ($\phi_{if.}$), the ionosphere delay observation ($\phi_{i1.}$) and their standard deviations are given in Table 3 for various combinations of frequencies, with f_{L1}=1575.42 MHz, f_{L2}=1227.60 MHz, f_{L5}=1176.45 MHz, $f_{E2\text{-}L1\text{-}E1}$= f_{L1}=1575.42 MHz, f_{E5a}=f_{L5}=1176.45 MHz and f_{E5b}=1202.025 MHz. The GALILEO frequencies are still tentative, in particular for E5b. We assumed that the standard deviation for all observations is the same, which is not very realistic. It may be hoped that the precision of the L1 and E2-L1-E1 observations will be better than the other observations since these observations have the largest amplification factor in the ionosphere free linear combination, and thus they tend to dominate the precision of the ionosphere free observation. Also, the amplification factors in the three-frequency case will change when the actual precision of the observations is taken into account. This is because the ionosphere free and ionosphere delay observations in the three-frequency cases result from a simple least-squares adjustment using the following model for GPS

$$E\{\underbrace{\begin{bmatrix}\phi_{L1}\\ \phi_{L2}\\ \phi_{L5}\end{bmatrix}}_{y}\} = \underbrace{\begin{bmatrix}1 & 1\\ 1 & f_1^2/f_2^2\\ 1 & f_1^2/f_5^2\end{bmatrix}}_{A}\underbrace{\begin{bmatrix}\phi_{if}\\ \phi_{i1}\end{bmatrix}}_{x} \quad ; \quad D\{\begin{bmatrix}\phi_{L1}\\ \phi_{L2}\\ \phi_{L5}\end{bmatrix}\} = \underbrace{\begin{bmatrix}\sigma_0^2 & 0 & 0\\ 0 & \sigma_0^2 & 0\\ 0 & 0 & \sigma_0^2\end{bmatrix}}_{Q_y} \quad \text{with} \quad \hat{x} = (A^T Q_y^{-1} A)^{-1} A^T Q_y^{-1} y \ ,$$

with a similar model for GALILEO. The results are given in Table 3. To summarize, from this provisional analysis it can be concluded that the variance of the ionosphere free observation is improved by 24% if the new L5 is used instead of L2, and by about 30% in case of three-frequency GALILEO and GPS compared to two-frequency GPS. The resulting positions, height and other parameters will improve by the same amount.

Two frequency GPS: L1 & L2	$\phi_{if} = 2.5457\ \phi_{L1} - 1.5457\ \phi_{L2}$ $\phi_{I1} = -1.5457\ \phi_{L1} + 1.5457\ \phi_{L2}$	$\sigma_{if} = 2.98\ \sigma_0$ $\sigma_{I1} = 2.19\ \sigma_0$
Two frequency GPS: L1 & L5	$\phi_{if} = 2.2606\ \phi_{L1} - 1.2606\ \phi_{L5}$ $\phi_{I1} = -1.2606\ \phi_{L1} + 1.2606\ \phi_{L5}$	$\sigma_{if} = 2.59\ \sigma_0$ $\sigma_{I1} = 1.78\ \sigma_0$
Three frequency GPS: L1, L2 & L5	$\phi_{if} = 2.3269\ \phi_{L1} - 0.3596\ \phi_{L2} - 0.9673\ \phi_{L5}$ $\phi_{i1} = -1.3470\ \phi_{L1} + 0.4682\ \phi_{L2} + 0.8788\ \phi_{L5}$	$\sigma_{if} = 2.55\ \sigma_0$ $\sigma_{i1} = 1.68\ \sigma_0$
Two frequency GALILEO: E2-L1-E1 & E5b	$\phi_{if} = 2.3932\ \phi_{L1} - 1.3932\ \phi_{E5b}$ $\phi_{i1} = -1.3932\ \phi_{L1} + 1.3932\ \phi_{E5b}$	$\sigma_{if} = 2.77\ \sigma_0$ $\sigma_{i1} = 1.97\ \sigma_0$
Two frequency GALILEO: E2-L1-E1 & E5a	$\phi_{if} = 2.2606\ \phi_{L1} - 1.2606\ \phi_{E5a}$ $\phi_{i1} = -1.2606\ \phi_{L1} + 1.2606\ \phi_{E5a}$	$\sigma_{if} = 2.59\ \sigma_0$ $\sigma_{i1} = 1.78\ \sigma_0$
Three frequency GALILEO: E2-L1-E1, E5b & E5a	$\phi_{if} = 2.3088\ \phi_{L1} - 0.5063\ \phi_{E5b} - 0.8024\ \phi_{E5a}$ $\phi_{i1} = -1.3138\ \phi_{L1} + 0.5584\ \phi_{E5b} + 0.7553\ \phi_{E5a}$	$\sigma_{if} = 2.50\ \sigma_0$ $\sigma_{i1} = 1.62\ \sigma_0$

Table 3: Ionosphere free linear combination $\phi_{if.}$, ionosphere delay observation ϕ_{I1} and their standard deviation, with σ_0 the standard deviation of the original observations. The phase observations ϕ are expressed in meters (not in cycles). The ionosphere delay observation is related to the geometry free linear combination in GPS (ϕ_{L2} - ϕ_{L1}), but it has been scaled by a factor 1.5457 in order to give the ionospheric delay on L1.

4. IMPACT OF A COMBINED GPS AND GALILEO CONSTELLATION

The impact of the future GALILEO system on the precision of the position and zenith delays is investigated. Two scenarios are considered: a constellation of only GPS satellites and a combined GPS plus GALILEO constellation. A GALILEO only scenario is not considered in this paper, since the main benefit comes from roughly doubling the number of satellites in view. The computations are not based on real data: they are design studies based on simple assumptions on the standard deviations of the observations and assumed GPS and GALILEO constellations.

In this study a nominal GPS constellation of exactly 24 satellites is used. The positions of the GPS satellites have been derived from a recent almanac, whereby we removed a few well-chosen satellites in order to get the nominal 24-satellite constellation. The GPS satellites are in near-circular orbits at 20,200 km altitude with an orbital period of 11^h58^m, divided over 6 orbital planes with inclination of 55^o. For the GALILEO system we assumed a constellation of 30 satellites in near-circular orbits at 23,616 km altitude in 3 orbital planes with an inclination of 56^o, resulting in an orbital period of 14^h22^m [5]. The distribution of the GALILEO and GPS satellites over the sky is very similar, with the same a-symmetric N-S distribution of satellites at mid-latitudes.

For the observations we assumed a standard deviation of 3 mm for the carrier phase and 30 cm for the code measurements on all frequencies. We also assumed that the ionosphere free linear combination of the observations is used. In the case of two frequency GPS the standard deviation of the ionosphere free linear combination is three times the standard deviation of the original observations, resulting in standard deviations of 9 mm for carrier phase and 90 cm for code observations. The same standard deviation is used for both GPS and GALILEO. This is on purpose, because we like to separate between the effects of additional satellites on the one hand and the precision of the observations on the other hand. In reality, modernized GPS and GALILEO have a slightly better performance with respect to the ionosphere free linear combination as explained in the previous section.

The following parameters were modelled: station position, phase ambiguities, receiver clocks and zenith total delays (ZTD). Satellite clock errors were eliminated by using single differences with respect to a base station, or by using satellite clock corrections estimated from a global network (Precise Point Positioning). In both cases we assumed a scenario involving precise orbits in which we can neglect the effects of orbital errors, but the effect of using single differences was taken into account in the standard deviations of the observations, which we multiplied by $\sqrt{2}$. The remaining parameters were solved in a least-squares adjustment. Independent sets of ambiguities and receiver clock errors were estimated for GPS and GALILEO. The GPS receiver clock error, GALILEO receiver clock error and the troposphere zenith delay were estimated for every epoch. For the position both static and kinematic applications are considered. In the latter case three coordinates are estimated for every epoch, whereas for the static case only three coordinates are estimated over the full period of observation. For the phase ambiguities both float and fixed solutions have been evaluated. In the float solutions one ambiguity parameter is estimated for each satellite pass. In the fixed solutions the double difference ambiguities were constrained to integer values. A very simple mapping function – 1/sin(elevation) – is used in the zenith delay estimation since no real data is involved.

In Fig.1 the number of GPS and GALILEO satellites is shown for a 24-hour period. The station is located at ESTEC in Noordwijk, The Netherlands (52.217^o N, 4.420^o E, MSL). The measurement interval is 180 seconds, resulting in 481 epochs. An elevation cut-off angle of 10^o was used. The average number of satellites in view is then 6.85 for GPS, 8.9 for GALILEO and 15.75 for both. The number of observations (ionosphere free l.c.) is 3291 for GPS and 4285 for GALILEO, with 46 unknown carrier phase ambiguities for GPS and 51 for GALILEO. In total twelve different solutions were analysed using three main scenarios: I) static receiver with ZTD parameters estimated, II) moving receiver without estimating ZTD and III) moving receiver with ZTD parameters estimated. For each scenario four solutions were evaluated: GPS only with float ambiguities (GPS/float), GPS only with ambiguities fixed (GPS/fixed), combined GPS&GALILEO with float ambiguities (G&G/float) and GPS&GALILEO with fixed ambiguities (G&G/fixed). The number of observations, unknowns and the redundancy for each of the solutions is given in Table 4. The redundancy is equal to the number of observations minus the number of unknowns, plus the rank-defect. The rank-defect is 1 for the GPS/float and 2 for the G&G/float solutions, the rank-defect is zero for the fixed solutions.

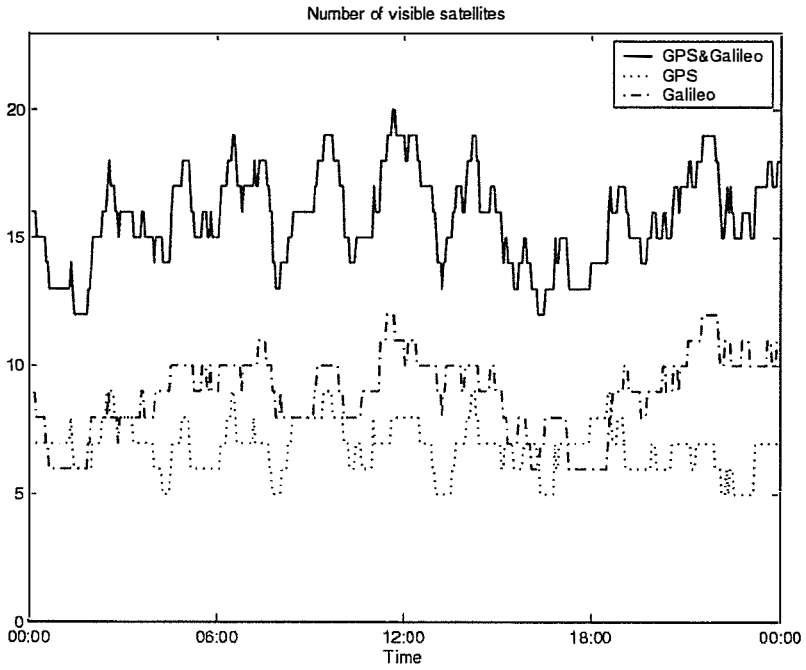

Fig. 1: Number of GPS and GALILEO satellites visible from the Netherlands (52.217° N, 4.420° E) on a typical day. The elevation cut-off angle is 10°.

			#Observ.	*#Unkowns*	*#Degrees of Freedom*		*Ratio*
GPS	Static	Float	3291	481*2+3+46	2281	$N^*(m_{GPS},-2)-N_{amb}-3+1$	
		Fixed	3291	481*2+3	2326	$N^*(m_{GPS},-2)-3$	
	Kinematic w/o ZTD	Float	3291	481*4+46	1322	$N^*(m_{GPS},-4)-N_{amb}+1$	
		Fixed	3291	481*4	1367	$N^*(m_{GPS},-4)$	
	Kinematic w/ ZTD	Float	3291	481*5+46	841	$N^*(m_{GPS},-5)-N_{amb}+1$	
		Fixed	3291	481*5	886	$N^*(m_{GPS},-5)$	
GPS& GALILEO	Static	Float	7576	481*3+3+97	6038	$N^*(m_{G\&G}-3)-N_{amb}-3+2$	0.615
		Fixed	7576	481*3+3	6130	$N^*(m_{G\&G}-3)-3$	0.616
	Kinematic w/o ZTD	Float	7576	481*5+97	5076	$N^*(m_{G\&G}-5)-N_{amb}+2$	0.510
		Fixed	7576	481*5	5162	$N^*(m_{G\&G}-5)$	0.515
	Kinematic w/ ZTD	Float	7576	481*6+97	4595	$N^*(m_{G\&G}-6)-N_{amb}+2$	0.428
		Fixed	7576	481*6	4690	$N^*(m_{G\&G}-6)$	0.435

Table 4: Number of Observations, Unknowns and Degrees of Freedom (Number of observations minus unknowns, plus rank-defect), with N the number of epochs and m_{GPS}, and $m_{G\&G}$ the average number of GPS and GALILEO satellites in view. In the last column the square root of the ratio of the degrees of freedom of the GPS and GPS&GALILEO solution is given.

5. DISCUSSION OF THE RESULTS

In Table 5 the standard deviation for the North, East and Up component of the position is given for each of the solutions. In Table 6 the median, mean, minimum and maximum of the standard deviation of the ZTD parameter is given for each of the eight solutions, which involved ZTD parameters. Clearly, some of the parameters are not solved very well, which is indicated in the Tables by the grey boxes: these are all the parameters from the kinematic GPS solution with ZTD's solved and the height of the kinematic GPS&GALILEO solution with ZTD's. The horizontal position components and the ZTD itself from the latter solution are actually quite acceptable. The standard deviation of the position in North, East, Up and ZTD, are plotted as function of time in Fig. 2. The plots on the left in Fig. 2 show the results for the GPS only solution, the plots on the right show the results for the combined GPS&GALILEO solutions. The top row shows the standard deviation for the static solution, the middle row for the kinematic solution without ZTD parameters,

and the bottom row for the kinematic solution with ZTD parameters. In Fig. 2 only the standard deviation for the ambiguity float solutions is given. The solutions with ambiguities fixed give only a marginal improvement because of the long observation period (one day), as can be seen from Table 5 and 6, and in particular Table 7. The main improvement of ambiguity fixing is in the horizontal coordinates, in particular the East component for the static solution, and not so much in the kinematic position parameters and almost no improvement for the ZTD parameters. The standard deviations for the other parameters that are estimated, such as the GPS and GALILEO receiver clock errors (two unknowns per epoch in case of GPS&GALILEO) and the float ambiguities (one per satellite pass), are not shown in this paper.

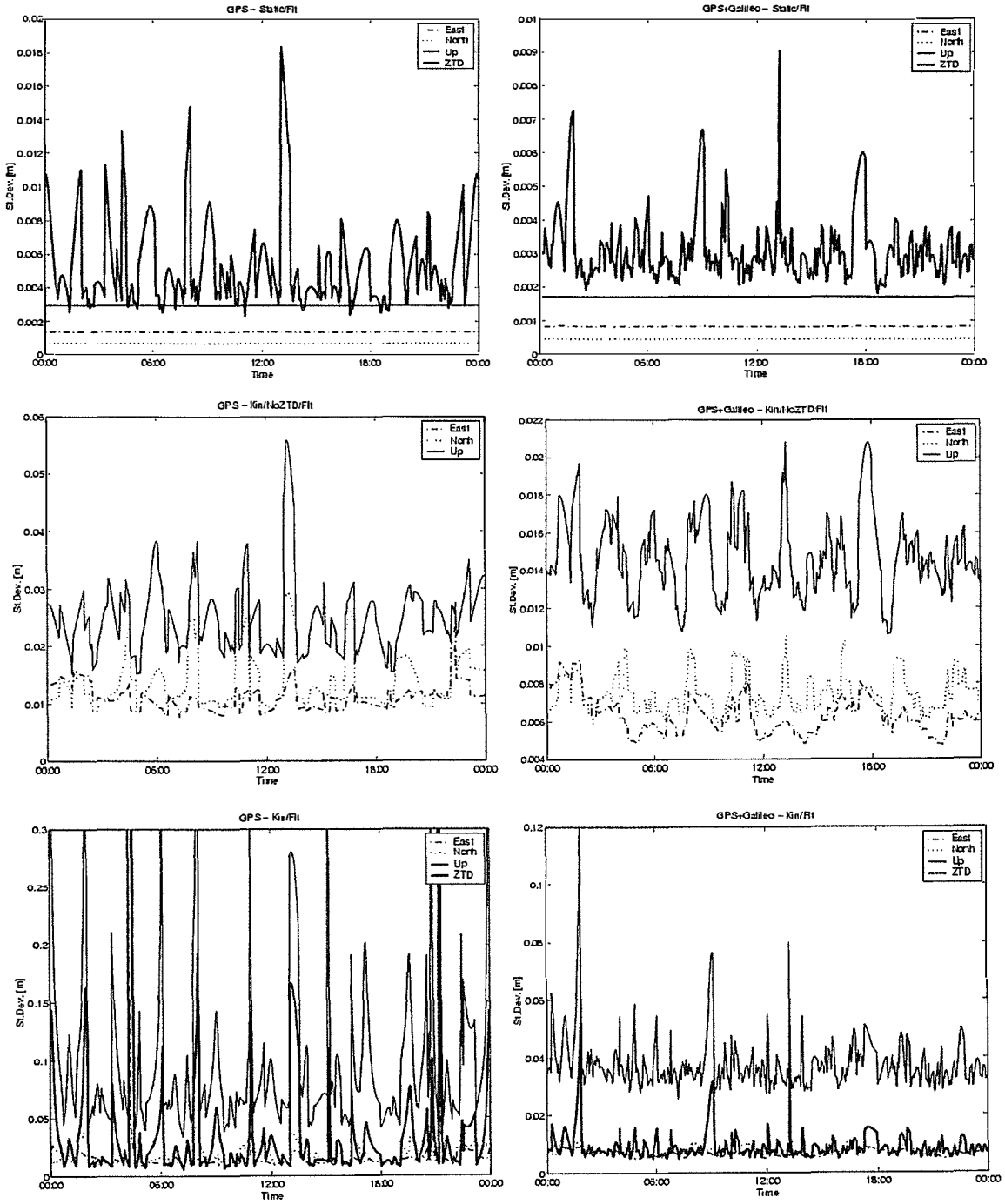

Fig. 2: Standard deviation of East, North, Height and ZTD for six different scenarios: static position (top row), kinematic position without ZTD estimation (middle row) and kinematic position with ZTD estimation (bottom

row), for GPS only (left column) and GPS&GALILEO (right column), with independent receiver clocks and float ambiguities for GPS and GALILEO. Note that the scaling of the vertical axis is not the same for the various subplots.

NEU [mm]		GPS/float			GPS/fixed			G&G/float			G&G/fixed		
		E	N	U	E	N	U	E	N	U	E	N	U
Static		1.4	0.7	2.9	0.4	0.5	2.6	0.8	0.4	1.7	0.3	0.3	1.5
Kinematic w/o ZTD	median	10.8	11.7	24.3	8.7	11.0	22.9	6.1	7.3	14.5	5.7	7.1	14.1
	mean	11.0	13.9	25.0	9.3	13.0	23.9	6.3	7.5	14.7	5.8	7.2	14.4
	min	7.7	8.8	15.1	6.7	8.1	14.1	4.8	5.5	10.6	4.3	5.6	10.3
	max	24.8	29.3	55.9	23.5	28.9	55.2	9.3	10.5	20.8	8.5	10.3	20.6
Kinematic w/ ZTD	median	13.0	14.9	73.1	10.5	13.4	70.6	6.6	7.7	35.7	6.0	7.4	35.0
	mean	15.4	19.2	126.8	12.7	17.4	122.1	6.7	7.9	37.8	6.2	7.6	37.2
	min	8.5	9.4	34.1	6.7	8.2	32.5	4.8	5.9	25.7	4.3	5.6	25.3
	max	282.1	198.0	8830	278.1	194.2	8712	10.4	12.0	119.4	9.4	11.7	117.9

Table 5: Standard deviation of the position parameters (in mm).

ZTD [mm]	Kinematic/float		Kinematic/fixed		Static/float		Static/fixed	
	GPS	G&G	GPS	G&G	GPS	G&G	GPS	G&G
median	19.1	7.9	18.3	7.8	4.5	2.9	4.5	2.8
mean	43.3	9.2	41.7	9.0	5.5	3.1	5.3	3.1
Min-max	5.6-3943	4.9-52.2	5.3-3891	4.8-51.6	2.3-18.3	1.8-9.0	2.3-18.2	1.8-9.0

Table 6: Standard deviation of the Zenith Total Delay (in mm).

St.Dev.Ratio	GPS				GPS&GALILEO			
	E	N	U	ZTD	E	N	U	ZTD
Static w/ ZTD	0.30	0.80	0.89	0.99	0.31	0.75	0.88	0.98
Kinematic w/o ZTD	0.81	0.93	0.94	-	0.93	0.97	0.97	-
Kinematic w/ ZTD	0.81	0.90	0.97	0.96	0.91	0.96	0.98	0.98

Table 7: Ratio of standard deviation ambiguity fixed versus ambiguity float (based on the median).

We have chosen to present the results in Table 5 and 6 in terms of standard deviations. This is of course dependent on what we assumed for the standard deviation of the observations. For single point positioning it is quite common to present the results in terms of Dilution of Precision (DOP). In order to get DOP-like values instead, although not applicable to single point positioning, the standard deviations should be divided by the standard deviation of the single difference phase observable, which is $\sqrt{2}*2.98*3$ mm=12.6 mm (we ignore the contribution of the code observations which has a standard deviation of 126 cm). The standard deviations should not be taken too literally, and only be used for inter-comparisons between corresponding solutions. For instance, we know that the standard deviations in North, East and Up for the static solutions are too optimistic because we ignored several relatively small error sources (like orbits), which become important for parameters that are averaged over long time spans like the static position parameters.

In Table 8 and Fig. 3 the GPS and GPS&GLONASS solutions are compared side by side. In Table 8 the ratio of the standard deviation of the GPS&GLONASS and GPS solutions is given, using the median of the standard deviation for the kinematic parameters. The improvement is quite consistent, although it looks like the height is improved slightly more than the other position parameters. In Table 8 also the theoretical improvement is given, computed by dividing the square root of the degrees of freedom from GPS&GALILEO and GPS (see Table 4). If only the additional observations would have been taken into account, the ratio

would be 0.66 (if we would have just doubled the observations this would be √½=0.71). The actually observed improvement for in the static height is a little better than expected and the improvement in the ZTD parameters is close to the theoretical prediction. However, the improvement in the kinematic position parameters is smaller than may be expected from the theoretical prediction. Instead of expressing the improvement as a ratio of two (median) standard deviations, one can also express it as a percentage, which is defined as $(1-\sigma^2_{G\&G}/\sigma^2_{GPS})*100\%$. This improvement factor reflects the improvement in terms of variance and the higher the number the better. The improvement factor is defined in such a way that for simple models doubling the number of observations would result in a 50% improvement. The actually observed improvement in the height is thus 64% for the static solutions, 71% for the kinematic solution without ZTD and 63% for the kinematic solution with ZTD. The improvement in ZTD is 68% and 77% for the static and kinematic solutions respectively.

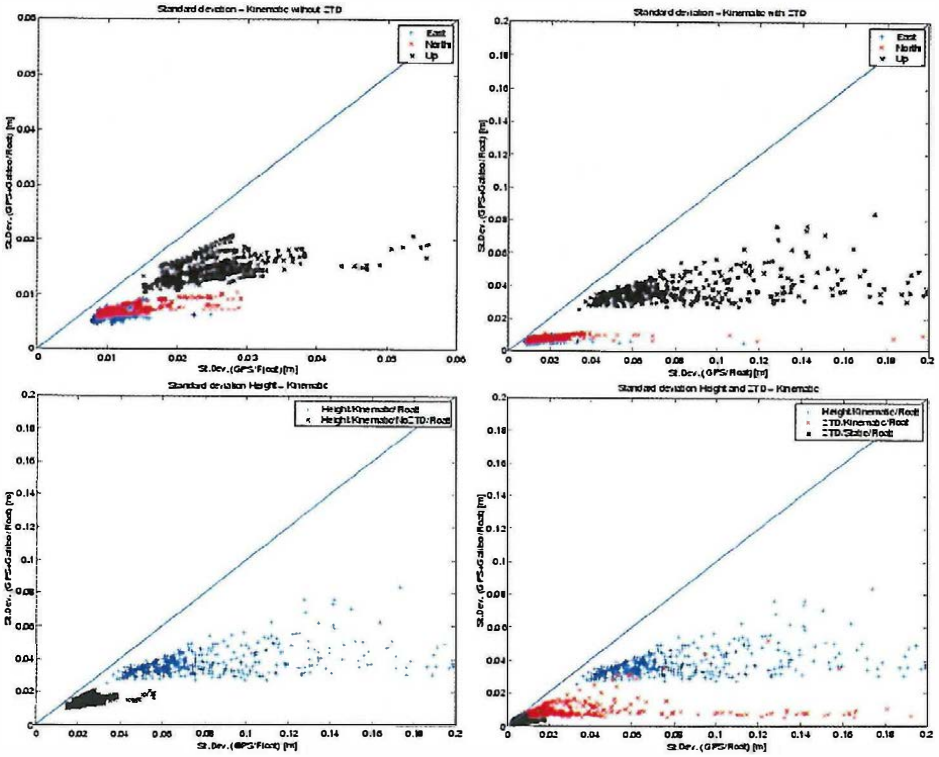

Fig. 3: Standard deviation for GPS&GALILEO (vertical axis) versus GPS only (horizontal axis). The top row shows the standard deviation in East, North and Up components for the kinematic solution without ZTD (top left) and with ZTD (top right). On the bottom row the Up component with and without estimation ZTD is shown in a single plot (bottom left), and the standard deviation of the Up component with ZTD estimated, the standard deviation of the ZTD from the kinematic solution, and the standard deviation of ZTD from the static solution is shown (bottom right). In all cases we solved for independent receiver clock errors and float ambiguities for GPS and GALILEO.

St.Dev.Ratio	Float Ambiguities				Fixed Ambiguities				Theoretical benchmark
	E	N	U	ZTD	E	N	U	ZTD	
Static w/ ZTD	0.61	0.65	0.59	0.64	0.64	0.61	0.58	0.63	0.62
Kinematic w/o ZTD	0.56	0.62	0.60	-	0.65	0.64	0.62	-	0.51
Kinematic w/ ZTD	0.50	0.52	0.49	0.41	0.57	0.55	0.50	0.42	0.43

Table 8: Ratio of standard deviation G&G versus GPS (based on the median).

The results in Table 8 give only a very limited view of the difference in performance for the kinematic solutions since the median almost completely ignores the extremes. A more powerful impression of the improvement may be obtained from Fig. 3. Along the vertical axis in Fig. 3 the standard deviation of the GPS&GALILEO solution is plotted versus the standard deviation of the GPS only solution along the horizontal axis (note that the axis are not over the full range of the data). It is apparent that the higher the standard deviation for GPS, the more it is improved by GPS&GALILEO. Clearly, the precision in North, East and Up of the combined GPS&GALILEO solutions is much better, especially for the height component in the kinematic solution with ZTD parameters. However, the height component for the kinematic solution with ZTD parameters is still much worse than the North and East components. The introduction of ZTD parameters has a major effect on the precision of the height component, as can be observed from Fig. 3c, but the ZTD parameters themselves are quite good, as can be seen from Fig. 3d where the improvement in height is compared against the improvement in ZTD for the kinematic and static solutions. It is also clear that the precision of the ZTD parameters is better than the precision of the height. So, in case of GPS&GLONASS kinematic solution with ZTD's, the North, East and ZTD parameters can be quite useable, whereas the height itself may be not. With GPS only neither parameter would be useable, unless we turn ZTD estimation off.

In this paper we only considered two extreme cases of handling the troposphere delays. Either we introduced a zenith delay parameter for every epoch, or we introduced none at all. These are limiting cases, which are mainly of interest for study purposes, e.g. it allows us to directly compare standard deviations of the height with the ZTD. The difference between these two approaches is shown in Fig. 4. In reality ZTD parameters will be introduced in batches of 6-120 minutes (2-40 epochs) or will be smoothed, so one may expect a situation somewhere in between the two plots in Fig. 4. Furthermore, it is clear from Fig. 4 that whether or not the ZTD is estimated, this hardly affects the standard deviation of the North and East component; the main effect is on the height parameters.

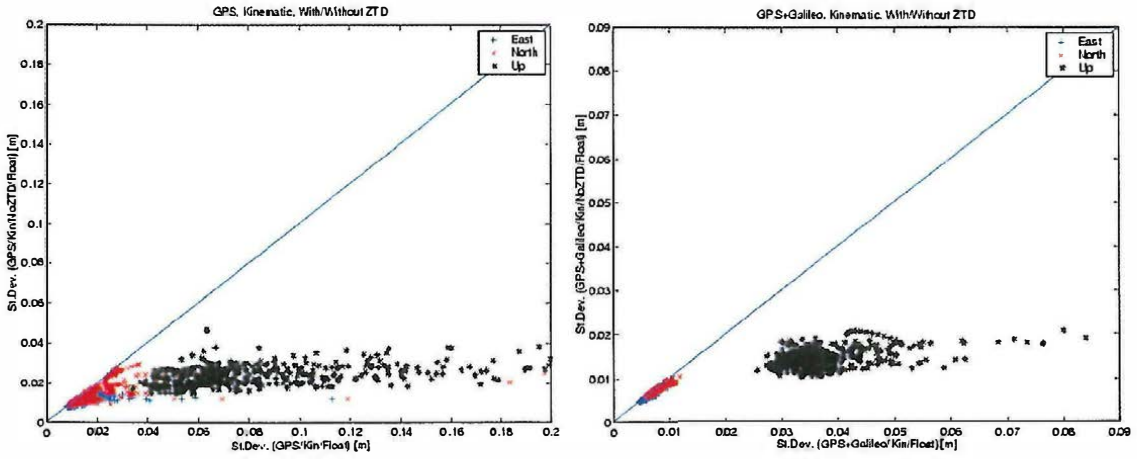

Fig. 4: Standard deviation of the position for the kinematic solution without ZTD parameters (vertical axis) versus with ZTD parameters (horizontal axis), on the left for GPS and on the right for GPS&GALILEO.

The method used for estimating ZTD is valid under the assumption that the atmosphere is layered and horizontal symmetric, and that the actually observed slant delays can be mapped to the zenith direction using dry and wet mapping functions. However, this assumption is not always valid, for example when a cold front passes the observation sites the water vapour shows strong horizontal gradients. In order to overcome this assumption horizontal gradient parameters may be estimated in addition to ZTD, or slant delays can be estimated instead. In order to derive slant delays it is also necessary to model the carrier phase multipath at the stations. In the previous section it was shown that the combined use of GPS and GALILEO improves the estimates of ZTD. Similar benefits from a dual GNSS constellation can be expected for the estimation of slant delays, gradient parameters and multipath, although we have not yet verified this experimentally. This will not only result in a better knowledge about the distribution of water vapour over the observing site, but

will also lead to improved geodetic parameters. In the case of GPS&GALILEO we simply have more redundancy left to model additional effects and error sources.

Although the ZTD is a nuisance parameter for precise positioning, the Zenith Total Delay (ZTD) estimated from ground-based GPS networks is a useful observation of Integrated Water Vapor (IWV) for Numerical Weather Prediction (NWP) and climate applications. As we have shown, with GPS&GALILEO the precision of the ZTD parameters, and thus IWV, is improved considerably, especially for moving receivers. This makes it possible to collect water vapor information from ships and buoys on the oceans where observations of water vapor have always been sparse.

6. CONCLUSION

Modernised GPS and GALILEO will provide several new and highly interesting signals to the high precision user. Using the new signals on L5 instead of L2 resulted in a 24% improvement in the precision (in terms of variance) of the ionosphere free linear combination, and 30% in case all three available frequencies are used. This is on top of the improvement in accuracy for the observations because of the improved signal structure.

Even more impressive is the effect of having additional satellites. If the receiver tracks both the GPS and GALILEO constellation, the precision of the height for a mid-latitude station is improved by about 64% for a static receiver, and in the median between 75% and 63% for a kinematic receiver depending whether zenith delay parameters are estimated or not. This is more than one may expect from just the additional observations. The improvement in ZTD is in the median 68% for a static receiver and 77% for a kinematic receiver. The higher the standard deviation for GPS, the more it is improved by GPS&GALILEO. The improvement due to ambiguity fixing is rather small. This is due to the long observation time span. The main improvement is in the horizontal coordinates for a static receiver, in particular the East component. When ZTD parameters are estimated for a moving receiver the precision of the height component is reduced strongly, although the North and East components are hardly affected. The precision of the height is much worse than the North and East components for a moving receiver, even in the GPS&GALILEO case, but surprisingly, the precision of the ZTD parameters themselves is quite good. This makes it possible to use GPS&GALILEO on ships and buoys to estimate primarily ZTD and collect water vapor information for meteorology for the oceans and seas, where these observations have always been sparse.

The results are derived for quite a conservative situation, in which we estimate the station position, satellite clock errors, independent GPS and GALILEO receiver clock errors, tropospheric delays and the initial phase ambiguities for every satellite. The use of a dual GNSS constellation will not only result in a better accuracy for the unknown parameters, but also the increased redundancy will make it possible to introduce more parameters, such as tropospheric gradients and/or slant delays, resulting in an improved modeling of the atmosphere, which in turn results in an improved accuracy of the estimated height parameters.

REFERENCES

[1] Eissfeller, B., C. Tiberius, T. Pany, R. Biberger, T. Schueler and G. Heinrichs, Real-Time Kinematic in the Light of GPS Modernization and Galileo, , in *Proceedings of the ION-GPS-2001*, September 2001.

[2] European Commission, "GALILEO: The European Program for Global Navigation Services", Available from http://ravel.esrin.esa.it/docs/GalileoBrochure.pdf

[3] Hein, G.W., J. Godet, J-L Issler, J-C Martin, R. Lucas-Rodriguez, and T. Pratt, The GALILEO Frequency Structure and Signal Design, in *Proceedings of the ION-GPS-2001*, September 2001.

[4] Parkinson, B.W., J.J. Spilker Jr., *The Global Positioning System – Theory and Applications*, AIAA, Washington, DC, 1996.

[5] Salgado, G.,.S. Abbondanza, R. Blondel and S. Lannelongue, Constellation and Availability Concepts for Galileo, in *Proceedings of the ION-NTM-2001*, January 2001, pp. 778-786.

[6] Spilker Jr., J.J., and A.J. van Dierendonck, Proposed New Civil GPS Signal at 1176.45 MHz, in *Proceedings of the ION-GPS-1999*, Nashville, September 1999.

STABILITY OF COORDINATES OF THE SLR STATIONS ON THE BASIS OF LAGEOS-1 AND LAGEOS-2 LASER RANGING IN 2000

Stanisław Schillak[1], Edwin Wnuk[2]

[1]Space Research Centre, Polish Academy of Sciences AstrogeodynamicObservatory Borowiec,

ul Drapałka 4, 62-035 Kórnik, Poland; Fax: +48-61-817-0219 e-mail: sch@cbk.poznan.pl
[2]Astronomical Observatory of the A. Mickiewicz University ul. Słoneczna 36, 60-286 Poznań, Poland
Fax: +48-61-829-2772 e-mail: wnuk@amu.edu.pl

ABSTRACT

The determination of the stations coordinates and the control of their stability is one of the most important task in the satellite geodesy and geodynamics. This paper presents results of position determinations for all active SLR stations in 2000 calculated in the ITRF2000 system on the basis of data provided by the LAGEOS-1 and LAGEOS-2 laser ranging. The calculations were performed under the usage of the GEODYN II program. Coordinates of the stations were determined from monthly arcs for the year 2000. Typical RMS errors of the (O-C) values for the monthly orbital arcs were on a level of 1.8 cm. The final stability of the geocentric coordinates of SLR stations per one year for all components varies from 0.4 cm to 4 cm.

Key words:

satellite geodesy, geodynamics, satellite laser ranging, satellite orbit determination

1. INTRODUCTION

The continuous monitoring of coordinates on the Earth surface with millimetre accuracy is the important task for control of the global, regional and local crustal deformations, or ground displacement due to seismic or volcanic activity. The control of stations coordinates in the longer period of time also is important for better understand the effects which change station position like atmospheric loading, underground water displacement, station vertical movement, or for study the changes in the position of the Earth mass centre (Pavlis, 2002). Realisation of these tasks needs accurate method of coordinates determination and their stability. In the previous papers (Kuźmicz-Cieślak *et al.,* 2000, Schillak, 2000, Schillak *et al.,* 2001, Wnuk *et al.,* 2002) the authors determined the stability of the coordinates of the Borowiec SLR station and all SLR stations in 1999 in the ITRF97 coordinates system. This paper contains the coordinates stability for all the active laser stations in 2000 determined in the ITRF2000 system (ITRF, 2001). The mean accuracy of the SLR measurements for LAGEOS-1 and LAGEOS-2 is on the level of 1-2 cm for most of the observing stations and for some stations it reaches the sub-centimetre level (ILRS, 2001). An essential factor, necessary for correct interpretation of the results in geodetic and geodynamic applications, is the estimation of the quality of the determined coordinates. The analysis of the stability of stations coordinates, presented in this paper, was performed on the basis of the LAGEOS-1 and LAGEOS-2 observations performed in the year 2000. The selected 16 stations have been assumed as a basis group for the orbit determination, the other 22 SLR stations were used only for calculating their coordinates stability.

2. DETERMINATION OF THE COORDINATES

The determination of SLR stations coordinates was performed by the NASA GEODYN II orbital program (McCarthy *et al.,* 1993) on the ALPHA workstation at the Astrogeodynamic Observatory in Borowiec. The description of forces, constants and estimated parameters is given in Table 1.

Force Model
Earth gravity field: EGM96 20x20 (Lemoine *et al.,* 1998) Earth and ocean tide model: EGM96 Third body gravity: Moon, Sun and all planets – DE200 Solar radiation pressure; C_R coefficient = 1.14 Earth albedo Dynamic polar motion Solar and magnetic flux Relativistic correction Thermal drag
Constants
Gravitational constant times the mass of the Earth (GM): $3.986004415 \times 10^{14}$ m^3/s^2 Speed of light: 299792.458 km/s Semi-major axis of the Earth (Ae): 6378.1363 km Inverse of the Earth's flattening (1/fe): 298.2564 Tide amplitudes – k_2, k_3 and phase k_2 respectively: 0.3, 0.093, 0.0
Reference Frame
Inertial reference system: true of date defined at 0^h of the first day of each month of 2000 Stations coordinates and stations velocities: ITRF2000 solution, epoch 1997.0 (ITRF, 2001) Precession: IAU 1976 Nutation: IAU 1980 Polar motion: Bulletin B IERS (IERS, 2001) Tidal uplift; Love model H2 = 0.609, L2 = 0.0852 Pole tide
Estimated parameters
Satellite state vector Station geocentric coordinates Acceleration parameters along-track, cross-track and radial at 5 days intervals
Satellites: LAGEOS-1 and LAGEOS-2
Centre of Mass Correction: 25.1 cm (McCarthy, 1992) Cross section area: 0.2827 m^2 Mass: LAGEOS-1; 409 kg, LAGEOS-2; 405 kg
Measurement Model
Observations; two minutes normal points from Eurolas Data Center Laser pulse wavelength: 532 nm (Zimmerwald 423 nm) Tropospheric refraction: Marini/Murray model (Marini and Murray, 1973) Editing criteria; 5σ for individual points of arc (σ - standard deviation of the orbital arc for a given station) 2.5 σ_P for points in the pass (σ_P – standard deviation of the pass) 3σ_{RB} for passes (σ_{RB} - standard deviation of the range biases per month) cut-off elevation 10 deg.
Numerical Integration
Integration; Cowell's method Orbit integration step size: 30 sec Arc length; one month

Table 1. GEODYN-II – Force model and parameters

The determination of the geocentric coordinates for each station was carried out in two steps. At first the independent monthly orbital arcs of LAGEOS-1 and LAGEOS-2 for 16 selected fixed stations with fixed coordinates in ITRF2000 system (Table 2) were determined. In the second step on the base of the O-C residuals from both satellites the geocentric coordinates X, Y, Z of the individual station were calculated. In addition satellite state vector and 9 parameters of general acceleration at 5 days intervals were

estimated. The fixed stations have been chosen on the base of their high quality of the coordinates in ITRF system, good quality and quantity of the data. The orbits calculated from the results provided by the fixed stations were each time supplemented with the results obtained at one station not included among the fixed stations whose coordinates were to be determined (16+1). This method ensures the minimum effect of the errors introduced by the less accurate stations on the coordinates determined.

STATION	ILRS SOD	X [m]	Y [m]	Z [m]
McDonald	70802419	-1330021.4404	-5328403.3271	3236481.6790
Yarragadee	70900513	-2389008.1303	5043331.8388	-3078526.4440
Greenbelt	71050725	1130720.1577	-4831352.9638	3994108.5091
Monument Peak	71100411	-2386279.4259	-4802356.5473	3444883.3081
Papeete	71240802	-5246409.3220	-3077286.4951	-1913815.1363
Arequipa	74031303	1942808.9308	-5804072.1597	-1796916.2176
Zimmerwald	78106801	4331283.6760	567549.7430	4633140.2670
Borowiec	78113802	3738332.8340	1148246.4910	5021816.0350
Grasse SLR	78353102	4581691.6410	556159.5390	4389359.4910
Potsdam	78365801	3800639.6760	881982.0400	5028831.6840
Simosato	78383602	-3822388.3630	3699363.5670	3507573.1390
Graz	78393402	4194426.5170	1162694.0330	4647246.6500
Herstmoceux	78403501	4033463.7120	23662.4780	4924305.1710
Grasse LLR	78457801	4581692.1810	556196.0240	4389355.0720
Mount Stromlo	78498001	-4467063.6480	2683034.4800	-3667007.3710
Wettzell	88341001	4075576.8500	931785.4560	4801583.5590

Table 2. Coordinates of the fixed 16 basis stations for the epoch 1997.0 – ITRF2000

Two-minute normal points of LAGEOS-1 and LAGEOS-2 have been taken from the Eurolas Data Center. The station coordinates determined for the markers (stations 7080, 7090, 7105, 7110, 7124, 7403) were connected to the reference point of a given station according to the data from Eccentricity Information (NASA, 2002). A summary of the results of orbital arcs for the 16 selected stations is presented in Table 3.

MONTHS 2000	NUMBER OF NORMAL POINTS	ARC RMS mm
JANUARY	8867	19.5
FEBRUARY	7742	16.4
MARCH	7062	16.5
APRIL	7202	18.5
MAY	10924	19.1
JUNE	9813	18.3
JULY	7755	17.6
AUGUST	10508	16.6
SEPTEMBER	9450	17.2
OCTOBER	7158	17.0
NOVEMBER	7371	16.4
DECEMBER	8310	18.0
MEAN PER ONE ARC	8514	17.6

Table 3. Orbital arcs for fixed stations from LAGEOS-1 and LAGEOS-2

3. RESULTS

The results of the first step are presented in Table 4. Range biases and arc RMS for each station are mean values of results from monthly orbital arcs. These results show very good agreement between

both satellites, mean value of the all stations of range bias for LAGEOS-1 is equal to 7.2 mm, for LAGEOS-2 7.1 mm and for RMS 32 mm and 31 mm respectively. The monthly LAGEOS-2 RMS for 28 stations are smaller than for LAGEOS-1. It is probably result of different inclination of these satellites and non-homogeneous accuracy of gravity field tesseral coefficients. Further study of this effect would be very important.

ILRS SOD	STATION	NUMBER NP		RANGE BIAS mm		ARC RMS mm	
		LAG-1	LAG-2	LAG-1	LAG-2	LAG-1	LAG-2
18645401	MAIDANAK	218	562	115.3	97.2	128	102
18685901	KOMSOMOLSK	48	12	1.2	23.2	67	56
18734901	SIMEIZ	98	26	40.8	23.2	62	60
18844401	RIGA	521	780	-9.9	-13.1	38	32
18931801	KATZIVELY	49	296	22.4	6.8	45	34
70802419	MC DONALD	2055	3231	-3.3	-3.6	18	16
70900513	YARRAGADEE	6687	6979	-1.7	-0.8	15	13
71050725	GREENBELT	3771	3769	-3.3	-4.6	17	16
71100411	MONUMENT PEAK	4149	4922	-4.8	0.8	18	17
71240801	PAPEETE	1384	1535	2.9	4.6	17	14
72102313	HALEAKALA	135	117	-6.9	2.4	15	19
72312901	WUHAN	379	932	0.4	7.7	34	31
72371901	CHANGCHUN	995	1266	-10.3	-5.9	24	26
72496101	BEIJING	561	580	4.2	2.8	38	26
73287101	KOGANEI	849	592	-21.9	-5.9	34	23
73357201	KASHIMA	1208	974	-20.7	-14.0	28	28
73377301	MIURA	634	785	-19.3	-12.6	27	21
73397401	TATEYAMA	1623	1547	3.4	2.9	19	20
73438401	BEIJNG-TROS	354	103	33.9	50.8	57	66
74031303	AREQUIPA	963	778	18.8	8.2	24	17
75010602	HARTEBEESTHOEK	272	471	17.8	9.8	32	22
75486201	CAGLIARI	0	75	-	24.5	-	49
78067601	METSAHOVI	679	84	-7.0	-17.5	23	24
78106801	ZIMMERWALD	3611	2629	-6.5	-5.5	20	19
78113802	BOROWIEC	834	831	7.9	9.8	18	19
78208201	KUNMING	1218	1147	68.2	56.4	84	72
78244502	SAN FERNANDO	1737	1714	28.0	33.3	53	54
78314601	HELWAN	32	18	6.4	-1.5	47	32
78353102	GRASSE SLR	3351	3150	4.2	1.8	16	14
78365801	POTSDAM	993	1090	0.4	1.9	17	15
78372805	SHANGHAI	718	1064	0.5	8.7	26	24
78383602	SIMOSATO	1636	1342	16.9	32.4	30	40
78393402	GRAZ	4476	4213	9.1	7.3	17	15
78403501	HERSTMONCEUX	5449	4110	-0.8	-2.9	16	16
78457801	GRASSE LLR	2124	1864	-2.1	-3.2	17	15
78498001	MOUNT STROMLO	7131	7451	-0.7	-0.8	16	13
79394101	MATERA	263	307	-7.3	-26.7	80	87
88341001	WETTZELL	3150	2504	-10.3	-12.0	25	24

Table 4. Results of the orbital arcs in 2000 – all stations

The appropriate stability s_X, s_Y, s_Z for each coordinate *X, Y, Z* over a period of 12 months of the year 2000 was found from the formula:

$$s_X = \sqrt{\frac{\sum_{i=1}^{n}\left(X_i - \overline{X}\right)^2}{n-1}}, \tag{1}$$

and similarly for s_Y and s_Z, where $\overline{X}, \overline{Y}, \overline{Z}$ are the mean values per year. The total stability *S* of the coordinates in 2000 for the given station was calculated from the formula:

$$S = \sqrt{\frac{s_X^2 + s_Y^2 + s_Z^2}{3}} \tag{2}$$

The coordinates stability and standard deviation of coordinates determination for every station in 2000 is presented in Table 5. The results of stations stability from 1999 (Schillak *et al.,* 2001) are included in this table for comparison of stability from both years. A very good agreement was obtained for the solutions of 1999 and 2000. The mean value for all stations of the differences of stability in 1999 and 2000 is equal –0.7 mm. Significant improvement of coordinates stability for several stations (Zimmerwald (4.0 mm), Papeete (7.9 mm), Simosato (8.9 mm), Metsahovi (8.4 mm) and Kunming (10.2 mm)) has been detected in comparison to 1999. The basis stations stability in 2000 is between 4 and 13 mm. The coordinates stability for the remaining 17 stations have values from 13 mm to 42 mm. For five stations the stability was not determined because the number of accepted monthly data archives was smaller than three.The results of coordinates determination contain systematic deviations. It is impossible to include all effects, which can to change station position on the level of several milimetres. The main elements of error budget can be divided into four sources; instrumental systematic errors of the SLR systems, station position uncertainty (lack of atmospheric and ocean loading, underground water effect, Earth center of mass position, inaccuracies of terrestrial reference frame model of fixed stations, inaccuracies of solid Earth tides and polar motion), orbital uncertainty (inaccuracies of the all perturbations effects, satellite acceleration model, satellites geometry and coverage of the data, atmospheric correction), fixed stations distribution and number of fixed stations. The very good agreement between range accuracy and coordinates stability for each station, and small standard deviation of coordinates determination (Table 5) show very important role of instrumental biases, other systematic biases on the level of several milimetres can to be detected only for the best SLR stations.

No.	STATION	ILRS SOD	MONTHS 1999		MONTHS 2000		Ş 1999	Ş 2000	σ 2000
			ACC	DEL	ACC	DEL	(mm)	(mm)	(mm)
1	HERSTMONCEUX	78403501	12	0	12	0	4.9	3.9	1.4
2	MOUNT STROMLO	78498001	12	0	12	0	5.0	4.2	1.3
3	GRAZ	78393402	12	0	12	0	5.9	5.1	1.5
4	GRASSE SLR	78353102	12	0	12	0	6.4	5.1	1.6
5	YARRAGADEE	70900513	12	0	12	0	6.6	5.5	1.3
6	GREENBELT	71050725	11	0	12	0	4.9	5.7	1.7
7	ZIMMERWALD	78106801	12	0	11	1	10.0	6.0	2.2
8	MC DONALD	70802419	12	0	12	0	7.0	7.0	1.9
9	GRASSE LLR	78457801	11	0	11	0	9.1	7.0	2.4
10	PAPEETE	71240801	8	0	10	0	15.5	7.6	2.5
11	MONUMENT PEAK	71100411	12	0	12	0	8.7	9.4	1.4
12	BOROWIEC	78113802	12	0	12	0	9.2	9.4	4.5
13	AREQUIPA	74031303	10	1	8	0	10.0	9.4	3.3
14	POTSDAM	78365801	12	0	12	0	9.4	10.0	3.7
15	WETTZELL	88341001	12	0	12	0	7.3	10.2	2.1
16	SIMOSATO	78383602	7	1	12	0	22.4	13.5	3.0
17	HARTEBEESTHOEK	75010602	-	-	5	1	-	9.4	3.4
18	CHANGCHUN	72371901	9	1	12	0	15.1	13.6	3.6
19	WUHAN	72312901	-	-	8	1	-	15.0	4.2
20	MIURA	73377301	5	4	4	1	18.0	15.1	4.6
21	KASHIMA	73357201	9	1	10	0	12.6	15.4	4.6
22	METSAHOVI	78067601	6	2	6	2	23.8	15.4	5.1
23	HALEAKALA	72102313	7	2	4	0	15.5	15.6	6.0
24	SHANGHAI	78372805	11	1	12	0	14.3	18.0	4.4
25	KOGANEI	73287101	11	1	6	1	10.7	20.8	4.0
26	BEIJING	72496101	7	4	10	1	19.0	21.6	4.3
27	TATEYAMA	73397401	9	2	10	0	14.5	22.1	3.6
28	RIGA	18844401	10	2	11	1	16.8	26.4	5.7
29	SAN FERNANDO	78244502	9	0	12	0	21.0	28.6	2.8
30	KATZIVELY	18931801	3	0	5	3	27.3	29.0	9.7
31	MAIDANAK	18645401	10	2	10	2	19.1	29.8	7.0
32	MATERA	79394101	12	0	9	1	17.1	30.3	5.7
33	KUNMING	78208201	3	6	8	1	51.9	41.7	3.4
34	HELWAN	78314601	4	2	2	3	21.2	-	-
35	KOMSOMOLSK	18685901	8	1	2	1	31.8	-	-
36	CAGLIARI	75486201	7	3	0	3	42.8	-	-
37	SIMEIZ	18734901	-	-	2	2	-	-	-
38	BEIJNG-TROS	73438401	-	-	2	1	-	-	-

Table 5. Coordinates stability for the SLR stations in 1999 (ITRF97) and 2000 (ITRF2000) (**ACC –** accepted, **DEL** – deleted).

An example is Herstmonceux station (7840). The topocentric coordinates North, East and Up for this station with reference to ITRF2000 are presented on Figure 1, where ΔN, ΔE, ΔU are mean values for each component, S is stability (Eq. 1,2) per one year. One-percentage confidence intervals, it means

three standard deviations of coordinates determination are used on these figures. The small 5 mm shift in comparison to ITRF2000 is visible for North-South component.

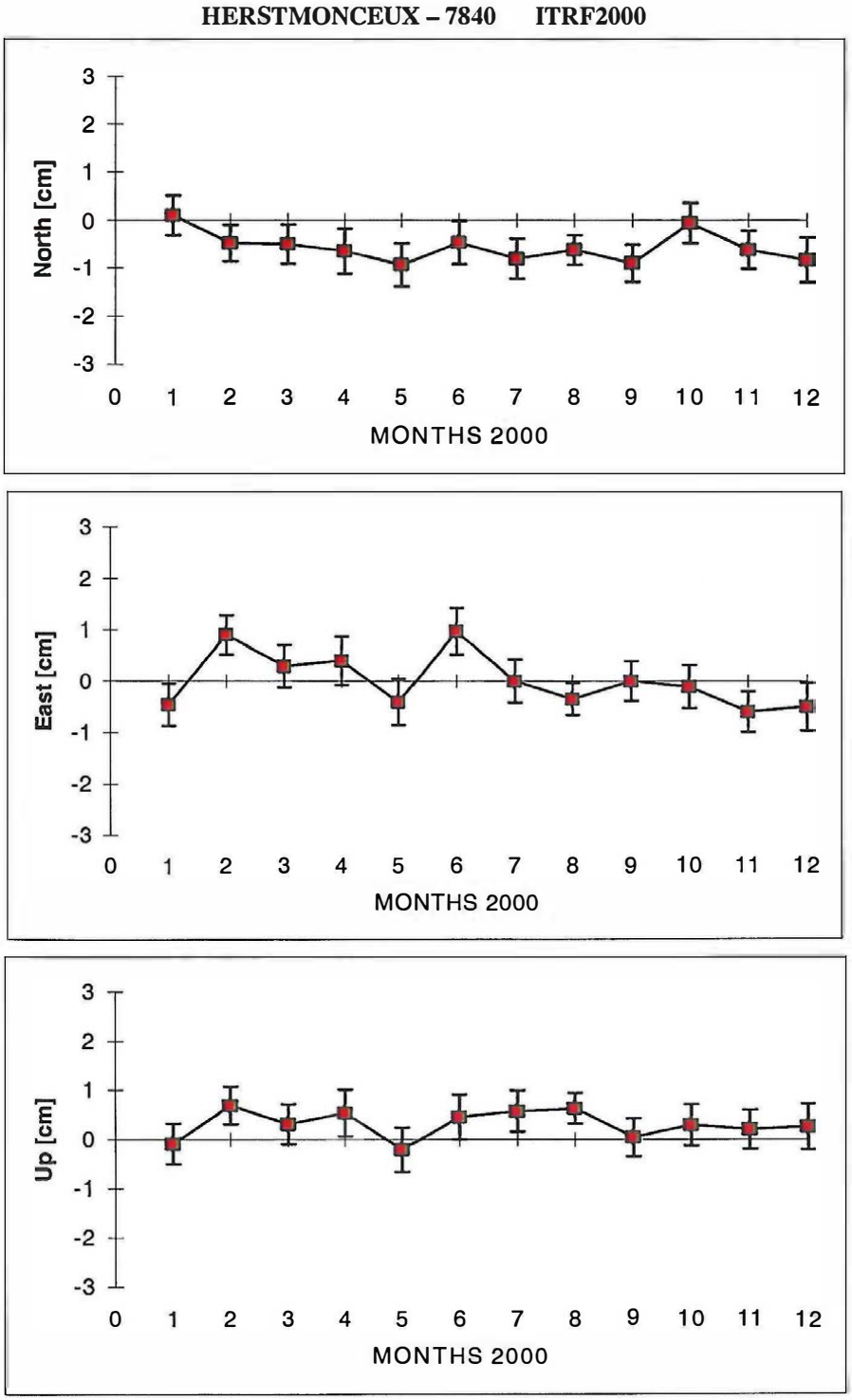

Figure 1. Herstmonceux (7840) coordinates in 2000 (0 – ITRF2000).

The results of the Keystone Project VLBI group show a significant 5 cm jump in baseline length between the stations Kashima and Tateyama over the period June-August 2000 (KSP, 2002). Unfortunately both SLR stations Kashima and Tateyama had intermittent activity in that time. The data for these stations are obtained for the periods January-May and August-December 2000. The results of the baseline

length determination from SLR data are presented on Figure 2. The baseline length (D) was calculated from:

$$D = \sqrt{\Delta X^2 + \Delta Y^2 + \Delta Z^2} \qquad (3)$$

where: ΔX, ΔY, ΔZ are differences between Kashima and Tateyama geocentric coordinates.

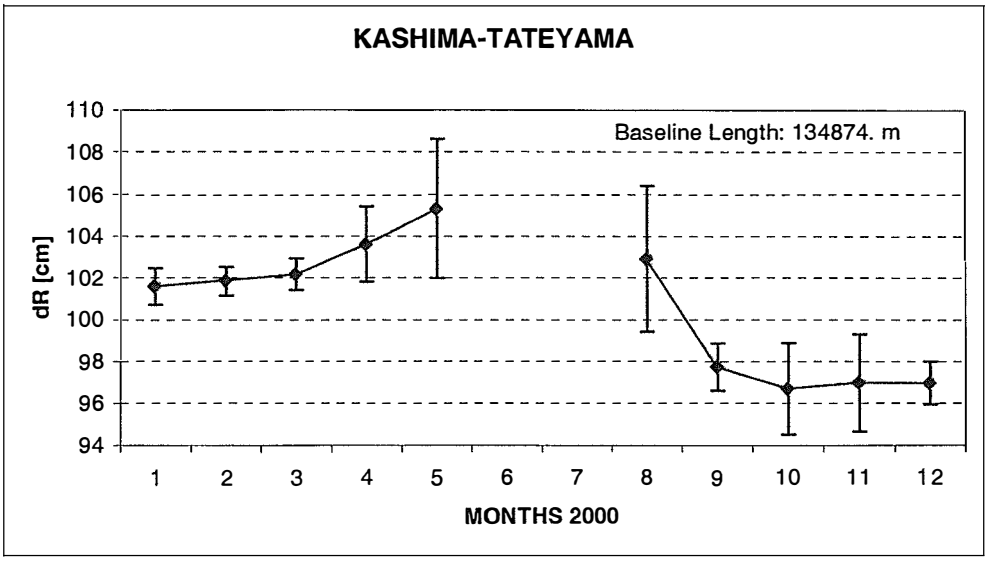

Figure 2. Baseline lengths between SLR stations Kashima and Tateyama in 2000.

The standard deviation for the coordinate determination in May and August is relatively poor due to the small number of normal points in these months for both stations. The difference between mean baseline lengths of the first and second half of the year was similar to the VLBI results, equal to 4.7±3.0 cm for all 10 months in 2000 and 5.2±1.0 cm without uncertain months May and August. The coordinates of Kashima SLR station presented on Figure 3 show only small (below 2 cm) change in East-West component. The SLR station Tateyama (7339) has two populations with difference 5.5±1.3 cm in North-South (ΔN) and 2.9±2.1 cm in East-West (ΔE) components (Figure 4), the first population for the period January-May and the second one for August-December. The vertical component (ΔU) is stable (0.8±1.6 cm). These results confirm 5 cm real movement of Tateyama station in July-August 2000 in direction North-East (Figure 5), (Yoshino *et al.*, 2002).

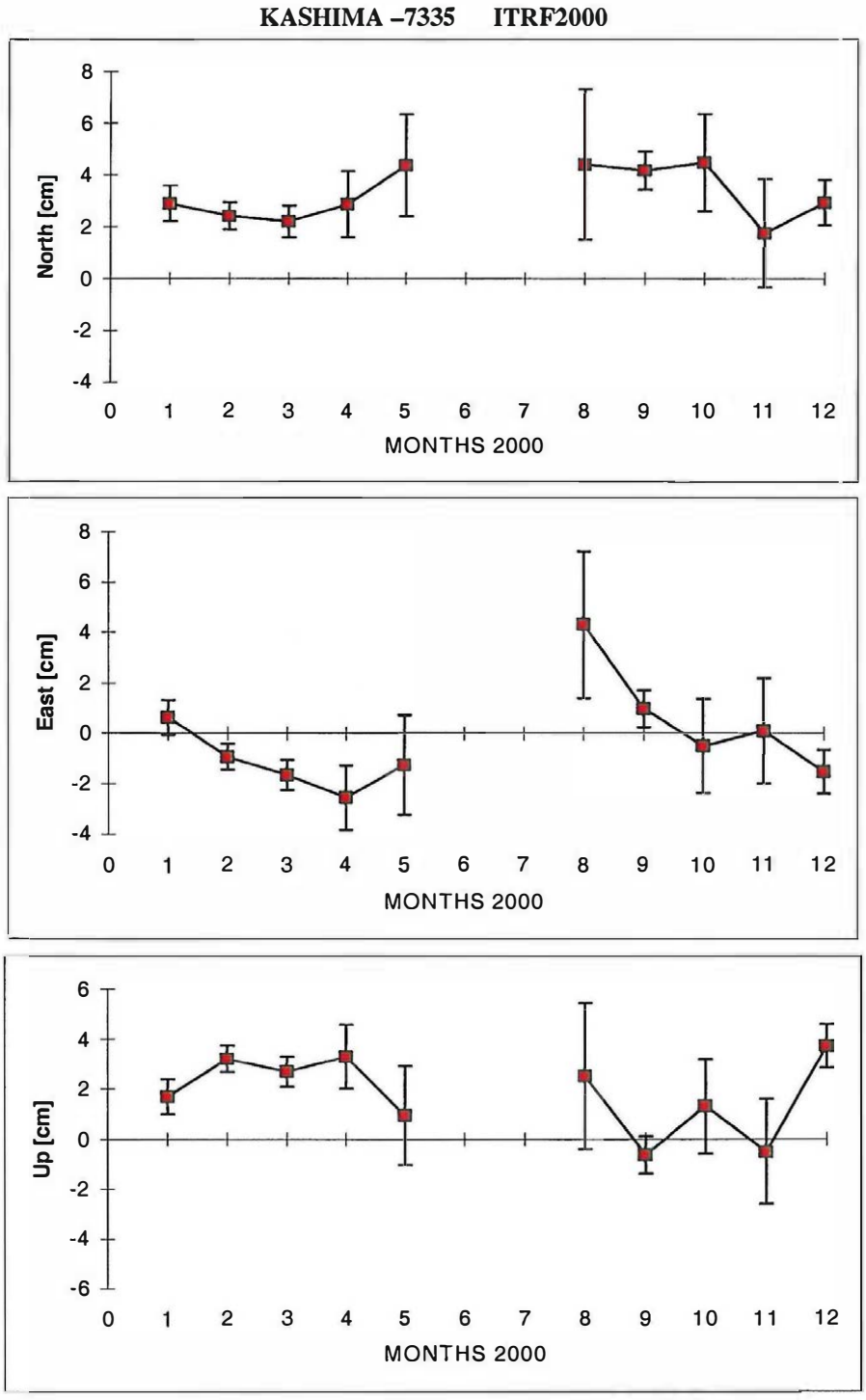

Figure 3. Kashima (7335) coordinates in 2000 (0 – ITRF2000).

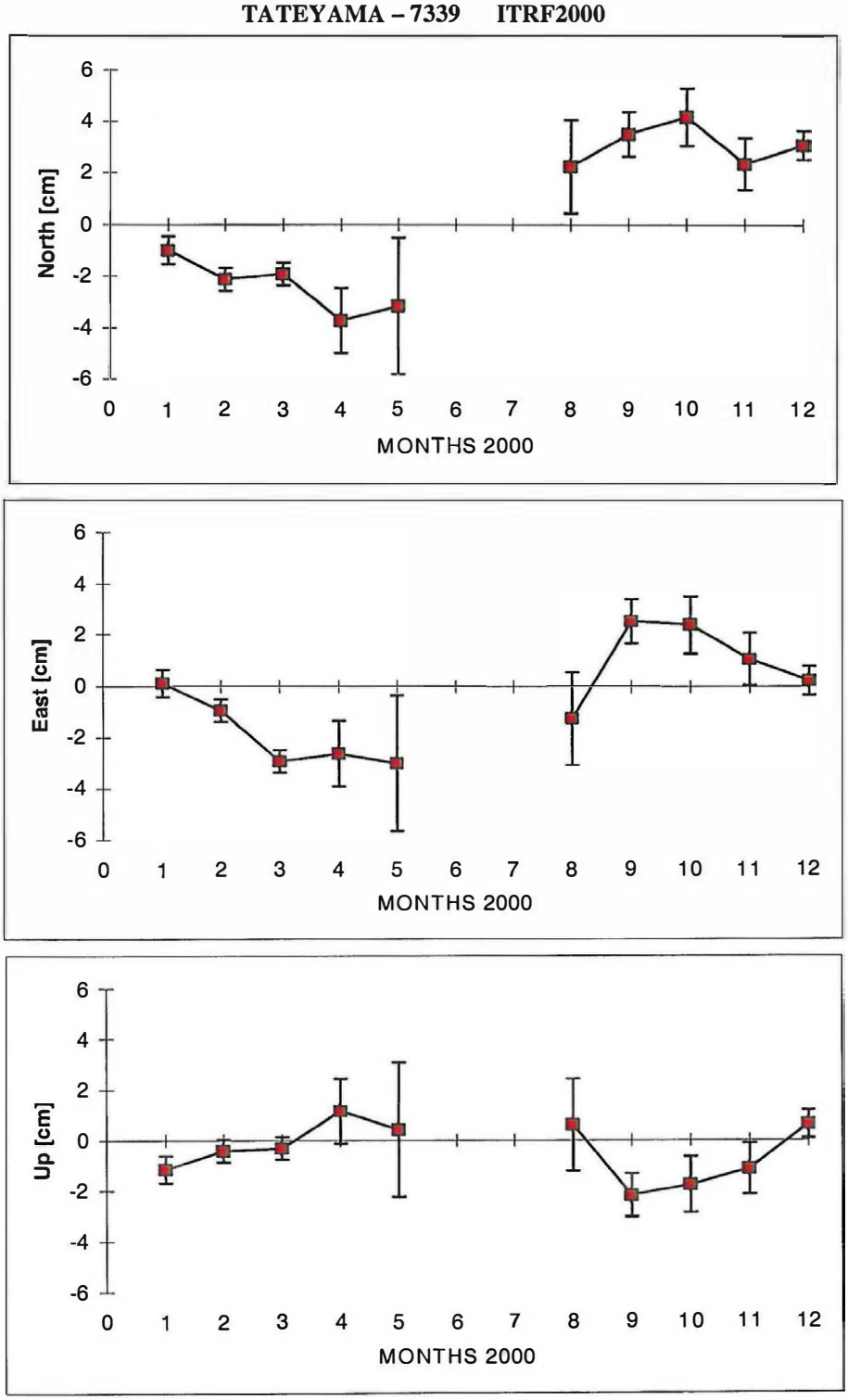

Figure 4. Tateyama (7339) coordinates in 2000 (0 – ITRF2000).

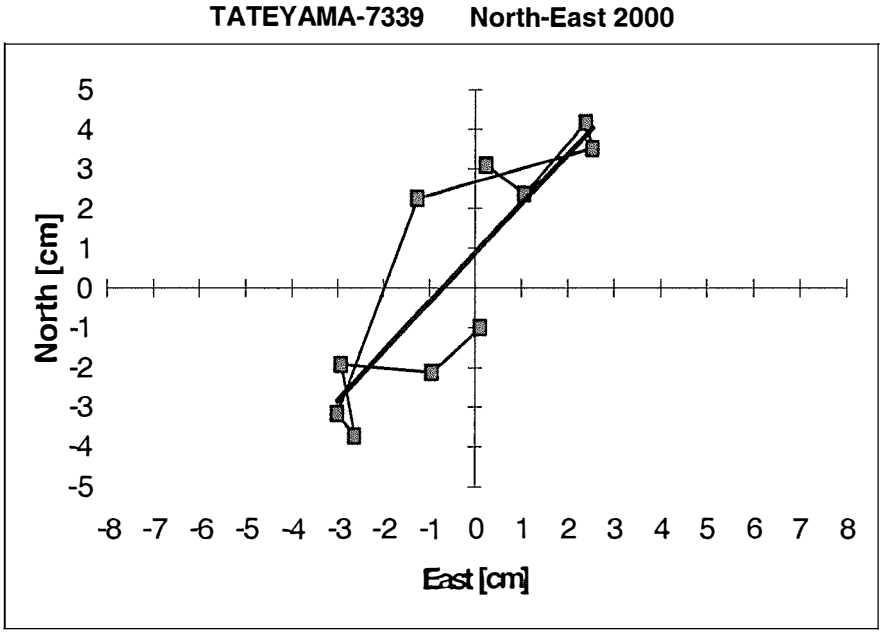

Figure 5. Horizontal position of Tateyama SLR station in 2000.

4. CONCLUSIONS

The method of coordinates determination presented in this paper shows very realistic results on the level of several millimetres. The good agreement between the mean values for all stations of range biases for LAGEOS-1 (7.2 mm) and for LAGEOS-2 (7.1 mm), and orbital RMS from orbital arcs of LAGEOS-1 (32 mm) and LAGEOS-2 (31 mm) confirms this conclusion. The determination of a real movement of the Tateyama station (52 mm) is in good agreement with the VLBI Kashima-Tateyama baseline determination (50 mm) and also confirm the good accuracy for the coordinate determination. The stability of coordinates is a very good parameter for the estimation of SLR station quality. The results presented in this paper show that the SLR stations coordinates stability in 2000 was on the level from 0.4 cm to 1 cm for the best 15 stations, for remaining stations the stability was in the range 1-4 cm. The main reason of the worse stability for these stations is small number of the normal points due to weather conditions (daily passes are needed) and technical problems (breaks in activity). The number of normal points or passes and their good distribution in time is the main factor, which limit the quality of the final result (Kuźmicz-Cieślak and Schillak, 2002). The accuracy of the orbit determination on the level of 1.8 cm per one month is similar to the range accuracy of the fixed stations equal to 1.6 cm (ILRS, 2002). This high accuracy of the orbit determination was achieved by including accelerations in the three directions. This method assures very good agreement of the fixed stations orbital arc RMS with the real distances to the satellite for the same stations determined by ILRS and can be used without any disturbances for the determination process of coordinates. The usage of a long one-month arc is vital for a small error of the stations coordinate determination due to the high number of normal points and more stable distribution of the points and the stations. The presented method based on the orbit determination from a group of fixed good stations is a better solution for the control of the SLR station coordinates stability than a method based on the orbit determination for all stations (Kuźmicz-Cieślak and Schillak, 2002). The repetition of the same configuration of the stations per one month is in this case more probably. The determination of coordinates should be performed for the data from several years with very careful control of the data for individual stations. This analysis will be performed in the near future for the SLR data from 1999 to 2001 in the ITRF2000 coordinates system.

ACKNOWLEDGMENTS

The authors wish to thank NASA geodesy group from the Goddard Space Flight Center, Greenbelt, for providing us with the GEODYN program. We are very grateful to Despina Pavlis for her help in explaining us the complexity of GEODYN. Also, we like to thank Danuta Schillak from Borowiec Astrogeodynamic Observatory for their assistance in calculations and preparing the data for the program GEODYN-II.

This work has been supported by the State Committee for Scientific Research (KBN) under grant No. 9T12E 024 19.

REFERENCES

IERS (2001) *Bulletin B IERS,* http://hpiers.obspm.fr/iers/bul/bulb/

ILRS (2001) *SLR Global Performance Report Card, Period January 1, 2000 through December 30, 2000,* http://ilrs.gsfc.nasa.gov/stations/performance_statistics/perf_2000q4.html

ITRF (2001) *ITRF2000 Station Positions at Epoch 1997.0 and Velocities, SLR Stations,* http://lareg.ensg.ign.fr/ITRF/ITRF2000/results/ITRF2000_SLR.SSC

KSP (2002) *Key Stone Project,* http://ksp.crl.go.jp/ksphome.html

Kuźmicz-Cieślak M., Schillak S., Wnuk E. (2000). *Stability of Coordinates of the SLR Stations on a Basis of Satellite Laser Ranging,* Proc. 12th International Workshop on Laser Ranging, Matera, 13-17.11.2000, ed. G.Bianco, V.Luceri, Matera, Italy.

Kuźmicz-Cieślak M., Schillak S., (2002), *The Accuracy of Station Positions Determined from Inhomogeneous Laser Ranging Data,* Artificial Satellites, Vol. 37, No. 2, Warsaw, Poland, pp.51-70.

Lemoine F.G., Kenyon S.C., Factor J.K., Trimmer R.G., Pavlis N.K., Chinn D.S., Cox C.M., Klosko S.M., Luthcke S.B., Torrence M.H., Wang Y.M., Williamson R.G., Pavlis E.C., Rapp R.H., and Olson T.R. (1998). *The Development of the Join NASA GSFC and the National Imagery and Mapping Agency (NIMA) Geopotential Model EGM96,* NASA/TP-1998-206861.

Marini J.W., Murray C.W. (1973). *Correction of Laser Range Tracking Data for Atmospheric Refraction at Elevations Above 10 Degrees,* NASA Goddard Space Flight Center, Preprint X-591-73-351, Greenbelt MD.

McCarthy D.D. (1992). *IERS Standards 1992,* IERS Technical Note 13, Obs. De Paris, Paris.

McCarthy J.J., Moore D., Luo S., Luthcke S.B., Pavlis D.E., Rowton S., Tsaousi L.S. (1993). *GEODYN-II,* Vol. 1-5, Hughes STX Systems Corporation, Greenbelt, MD.

NASA (2002) *Eccentricity Information for SLR Occupations,* ftp://cddisa.gsfc.nasa.gov/pub/slrocc/slrecc.txt

Pavlis E., (2002), *Monitoring the Origin of the TRF with Space Geodetic Techques,* Proc. 13th International Workshop on Laser Ranging, Washington, 7-11.10.2002, (in press).

Schillak S. (2000). *Determination of the Borowiec SLR Coordinates,* Proc. 12th International Workshop on Laser Ranging, Matera, 13-17.11.2000, ed. G.Bianco, V.Luceri, Matera, Italy.

Schillak S., Kuźmicz-Cieślak M., Wnuk E., (2001), *Stability of Coordinates of the SLR Stations on a Basis of LAGEOS-1 and LAGEOS-2 Laser Ranging in 1999,* Artificial Satellites, Vol.36, No.3, Warsaw, Poland, pp. 85-96.

Wnuk E., Schillak S., Kuźmicz-Cieślak M. (2002). *Stability of Coordinates of the Borowiec SLR Station (7811) on the Basis of Satellite Laser Ranging,* Adv. Space Res., Vol. 30, No. 2, pp. 413-418.

Yoshino T., Kunimori H., Katsuo F., Amagai J., Kiuchi H., Otsubo T., Kondo T., Ichikawa R., Takahashi F., (2002), *Comparison of the Baseline between the Keystone Sites by Different Space Geodetic Techniques,* IVS 2002 General Meeting Proceedings, Tsukuba, Japan, Feb. 4-7. 2002, ed. N.R.Vandenberg and K.D.Baver.

Triple laser ranging collocation experiment at the Grasse observatory, France

Joëlle Nicolas, Pascal Bonnefond, Olivier Laurain, Philippe Berio,
Pierre Exertier, and François Barlier

Observatoire de la Côte d'Azur, Avenue Nicolas Copernic, F-06130 Grasse, France.
Contact: Joelle.Nicolas@obs-azur.fr, tel.: 33.493405381, fax: 33.493405333.

Abstract

At the Grasse observatory, in the southeast of France, we had the opportunity to collocate 3 independent laser ranging systems within about 20 m from September to November 2001. These 3 instruments are: a classical Satellite Laser Ranging (SLR) station, a Lunar Laser Ranging (LLR) station, and the French Transportable Laser Ranging Station (FTLRS). The prime objective of this experiment was to qualify, to the millimeter level, the new performance of the FTLRS, after its phase of upgrades. This validation was of great importance prior to its departure to Corsica, where the FTLRS was to be used to calibrate the altimeter and to validate the orbits of the oceanographic satellite Jason-1 during its initial validation phase starting in early 2002. A secondary objective was to determine the absolute and relative instrumental biases between the SLR, the LLR and the FTLRS systems, which are presented in this paper. Our analysis shows the millimeter consistency between the 3 OCA laser stations, which demonstrates the precision and the accuracy of the SLR technique. Then, our study shows the comparison between the 3 Grasse stations and 2 other European laser systems (Graz and Herstmonceux). As a by-product, we also underscore a systematical error of about 2 cm based on the mean of TOPEX/Poseidon laser residuals for some European stations.

Keywords:

Space geodesy, Satellite Laser Ranging, collocation experiment, satellite altimetry.

1. Introduction

In Satellite Laser Ranging (SLR), a network of terrestrial stations accurately measures the round trip time of flight of ultra-short optical pulses to retro-reflector equipped satellites, including the Moon. From these accumulated time-of-flights, for a given satellite, centimeter level orbits can be determined. SLR, Global Positioning System (GPS), and Doppler Orbitography and Radiopositioning Integrated by Satellite (DORIS) are the three most used accurate techniques in precise orbit determination with SLR exhibiting the best in absolute accuracy in relating an orbit to the geocenter. SLR is also used to validate GPS and DORIS determined orbits. The space geodetic data analysis gives crucial information of our planet Earth. There is a number of science by-products of precise SLR orbits including but not limited to (1) the determination of SLR site positions and velocities and Earth orientation parameters; (2) the definition of scale and origin of the terrestrial reference frame; (3) the measurement of temporal variations of the Earth's gravity field; and (4) the accurate calibration of radar altimeters (e.g. TOPEX/Poseidon, Jason-1, ERS, and ENVISAT) and separation of long term changes in instrumental drift from secular changes in ocean heights.

Since the 1980s, SLR, GPS, DORIS, and Very Long Baseline Interferometry (VLBI) have been the 4 most successful space geodetic techniques due to their precision and accuracy. Indeed, the past decades have shown an impressive improvement of these ground-based techniques. These improvements have directly opened new scientific application fields. In geosciences for instance, this concerns the accurate study of the sea level change or the crustal deformations induced by the atmospheric, oceanic and hydrologic loading effects. But, such studies linked to very small signals (few millimeters) are only feasible if the different space geodetic techniques are currently capable of detecting millimeter changes in the station heights. The SLR technique must reach this level of accuracy.

When a given site has two or more of these geodetic techniques present, then that site is considered collocated. Since each technique has its strengths and weaknesses, collocated sites enable the accurate comparison and combination of techniques. Collocation experiments permit to check the accuracy of the different instruments and to find relative biases between different techniques or different instruments based on the same technique. Grasse (France) is a good example of such a collocated site.

The OCA (Observatoire de la Côte d'Azur) at Grasse is at an altitude of 1300 m, located in the southeast of France on the French Riviera in the southern Alpine chain, 30 km from the Mediterranean Sea. The OCA is a fundamental observatory where several continuously operating space geodetic techniques including a SLR system, a combination SLR/Lunar Laser Ranging (LLR) system, and a permanent GPS receiver. Repeated absolute gravity measurements are also performed at the OCA with a transportable FG5 (Niebauer T.M. et al., 1995). The OCA has 30 years of progressive experience in SLR/LLR, and in collaboration with the CNES (Centre National d'Etudes Spatiales), the IGN (Institut Géographique National), and the INSU (Institut National des Sciences de l'Univers), has developed a very compact and highly transportable laser ranging system named FTLRS (French Transportable Laser Ranging Station) (Nicolas J. et al., 1999); (Nicolas J. et al., 2000).

The FTLRS (see Fig. 1) was designed for quick installations of a site for short duration campaigns and in particular to support altimeter calibration and orbit validation experiments. The system capabilities were greatly enhanced between 1997 and 2001 to meet the 1 cm accuracy level, and much better if possible, and to track the LAGEOS -1 and -2 satellites at an altitude of 6000 km. This accuracy level is mandatory for the Jason-1 validation phase. LAGEOS tracking capability is also a key requirement, especially for a mobile system, since LAGEOS -1 and -2 data are primarily used in accurate SLR station position determination. In its new configuration in the summer of 2001, the FTLRS began observations at Grasse on ground targets and on satellites. Initial performance results, prior to the collocation experiment with the Grasse SLR and LLR systems, were excellent (Nicolas J. et al., 2001) and the FTLRS successfully demonstrated the following:

- LAGEOS -1 and -2 tracking new capability,
- millimeter level calibration stability from ground test results, and
- single shot satellite precision exceeding 1 cm from laboratory tests.

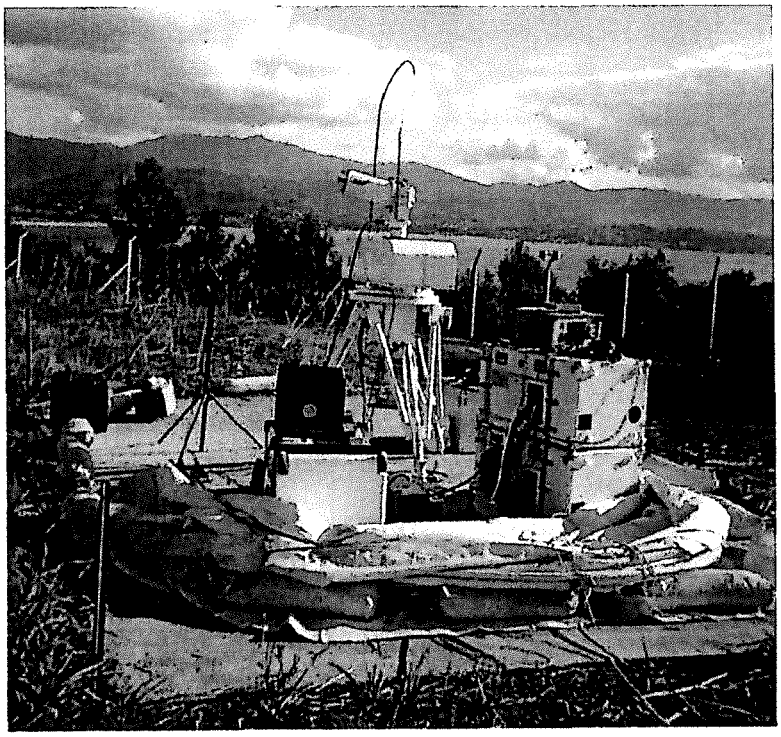

Figure 1: The FTLRS at Ajaccio, Corsica, 2002.

Nowadays, the FTLRS is the smallest existing laser ranging system in operational mode since summer 2001, with such a high accuracy level.

The collocation between these 3 laser ranging systems was conducted between September and November 2001 (see Fig. 2). Collocation is the best way to determine relative and absolute instrumental biases at the 1 millimeter level, because the largest SLR error sources (mainly the orbit), and the light propagation atmospheric delay error can be eliminated. This experiment was used to verify the new performance of the FTLRS, prior to its departure to Corsica in 2002 in support of the Jason-1 altimeter calibration and orbit validation phase (Ménard Y. et al., 1994); (Exertier P. et al., 2001); (Ménard Y. et al., 2001). Herein we present the results of this triple collocation experiment. We describe the data set and the analysis techniques, and then we summarize and discuss the results.

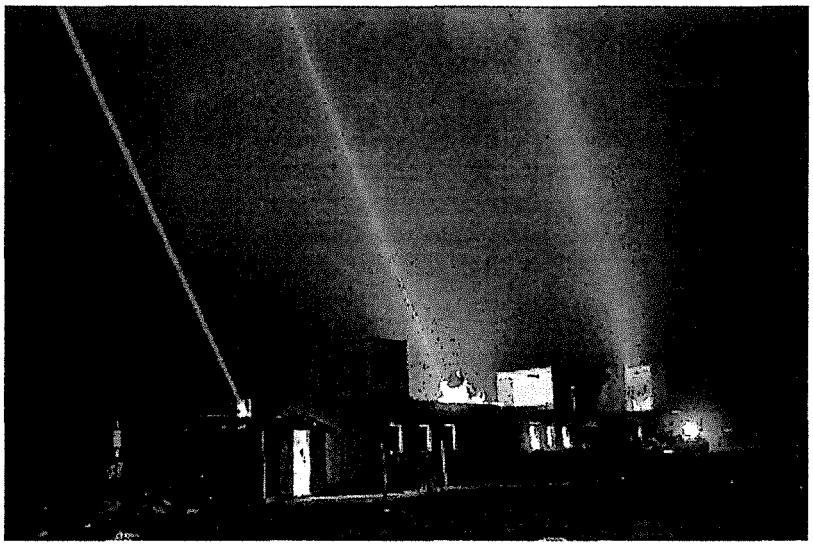

Figure 2: The 3 OCA laser ranging station during the collocation campaign simultaneously tracking the LAGEOS satellites. From the left to the right: the French Transportable Laser Ranging Station (FTLRS), the Satellite Laser Ranging (SLR) station, and the Lunar Laser Ranging (LLR) station.

2. Data and methodology

2.1. Data

For this collocation experiment, the 3 laser stations of the OCA observed common passes of satellites between September and November 2001. We used the observations of:

- the classical Satellite Laser Ranging (SLR) which observes all satellites equipped with laser retroreflectors,
- the Lunar Laser Ranging (LLR) station which also observes regularly the highest laser satellites such as LAGEOS or ETALON, and GPS and GLONASS satellites (Barlier F. et al., 2001). We used the high satellite observations of the LLR since this station is of great quality (Samain E. et al., 1998).
- the FTLRS which can now observe all the satellites up to 6000 km high, that is to say LAGEOS satellites.

We used the common observations of the 3 stations on LAGEOS -1 and -2 satellites, since these are the only common targets reachable for the 3 instruments. Indeed, the LLR system has not the technical ability to track satellites lower than LAGEOS. We analyzed 12 passes of LAGEOS –1 and 15 passes of LAGEOS –2.

We also used the LAGEOS -1 and -2 observations from Graz (Austria) and Herstmonceux (UK) stations to compare the Grasse stations to these two other systems of recognized great quality. This

comparison is based on all the LAGEOS data measured and acquired during the collocation experiment.

We finally studied the common passes between the FTLRS and the SLR station on lower satellites and especially data of TOPEX/Poseidon (T/P) at about 1300 km high. This study was performed to check the capability of the FTLRS to track Jason-1 before its launch (7th December 2001) since, for its phase of validation, Jason-1 was on the same orbit as the T/P one. But this study was not used to validate the accuracy of the FTLRS.

2.2. LAGEOS -1 and -2 analysis

We performed two kinds of analysis based on the two different data sets of the LAGEOS observations described above. The first analysis, used specifically for the Grasse stations, was based only on the common normal points between the 3 OCA laser systems. In the second analysis, we used all the data (normal points) of all the passes of the entire period (Sept. – Nov. 2001) and from the Grasse stations as well as from other European instruments.

The following method was used for our both analyses. First, we computed 10-day arcs of LAGEOS reference orbits using the GINS software with the ITRF2000 terrestrial reference frame (Altamimi Z. et al., 2002), the GRIM5-S1 gravity field (Biancale R. et al., 2000), and the standard IERS96 conventions (McCarthy D., 1996). We performed this orbit computation with the data of about 10 SLR stations, but without the data of the Grasse laser ranging stations. We have chosen to use only the data from stations performing a large number of great quality observations based on the ILRS (International Laser ranging Service) criteria. We also took care of the geographical distribution of this sub-network on the Earth surface. We did not use the data of the Grasse systems to ensure the independence of our collocation analysis results from the orbit computation. These orbits had a mean 1-σ rms of 2.3 cm for LAGEOS –1 and of 2.2 cm for LAGEOS –2 (laser residuals from 1 cm to 3.5 cm for LAGEOS –1 and from 1 cm to 3.1 cm for LAGEOS –2). Then, we used these reference orbits to compute laser residuals for each arc of each LAGEOS satellite and for each one of the 3 French laser systems. For this computation, we used the ITRF2000 coordinates for the SLR station and the ITRF2000 tie for the LLR station. For the FTLRS, we used the local tie performed very accurately at the level of few millimeters by the IGN in 1999 (Germain T., 1999). For the LLR coordinates, the agreement between the ITRF2000 and the IGN ties is at the level of few millimeters.

For our first analysis, based on the common observations on LAGEOS -1 and -2 satellites between the 3 OCA stations, we used only the common normal points between these 3 systems (there is one normal point every 120 s for the LAGEOS satellites). There are about 150 common normal points for both LAGEOS satellites. We computed the laser residuals for each laser system pass-by-pass, and the corresponding residual differences between the different instruments. Then, from the laser residuals, we estimated the mean laser residual over the 3 months for each station with a LAGEOS -1 and -2 combined solution weighted by the normal point number. The mean laser residual differences correspond to the difference between the instrumental biases of the stations. We finally compared these mean laser residuals computing the differences of the instrumental biases of the 3 Grasse stations. Since this analysis was based on data acquired nearly at the same time with the 3 stations (to within 120 s), the differences would essentially be due to instrumental reasons and this analysis allowed us to compare directly the instrumental performance of each considered station, and especially to validate the new performance of the FTLRS. Indeed, for common normal points on a given satellite, all the corrections (atmosphere, relativity, and geophysical effects such as tides or loading phenomena) are identical for the collocated stations and the differences in the station-satellite ranges are only due to instrumental differences (laser, tracking, timing, detection, ground calibration…) and to initial station coordinate eccentricities.

For our second analysis to enlarge this FTLRS validation, we compared the mobile station in its new configuration and the best European stations using the same method. But we used all the normal points of the entire considered period, and not only the common normal points between the different instruments, since it was no longer the context of a collocation experiment. The LAGEOS -1 and -2 normal points used are of about 350 for the FTLRS and more than about 2500 for the other stations. This comparison analysis was based on the same reference orbits previously computed. Then, we computed laser residuals for each laser system. This analysis gave us the station quality comparison between the 3 OCA laser systems, the Graz, and the Herstmonceux stations.

3. LAGEOS -1 and -2 data analysis results and discussion

3.1. Analysis of the common observations of the 3 OCA stations

The analysis of the common normal points of the 3 Grasse laser stations on LAGEOS -1 and -2 satellites was performed with the above described method. These results are based on 57 common normal points between the 3 OCA laser instruments on LAGEOS -1 and on 93 common normal points on LAGEOS -2 acquired between September and November 2001.

Pass-by-pass laser residuals exhibit interesting features. Generally, the LLR residuals are positive of about 1-2 cm and the FTLRS residuals are around zero. The SLR residuals are often between the curves of the two previous systems, but closer to the FTLRS one. As an example, Fig. 3a and 3b illustrate the stability of the laser residual differences for a LAGEOS -1 pass of the 12th September 2001 and for a LAGEOS –2 pass of the 10th October 2002. The overall stability is at the 6 mm level for LAGEOS -1 and at the 4 mm level for LAGEOS -2. Nevertheless, the laser residual differences between the three stations are more stable that the individual laser residuals of each station pass-by-pass. Indeed, the absolute value of the residuals shows a 2-3 cm level of variability. It would mainly correspond to the orbit errors and to coordinate variations due to effects which were not taken into account in our computations (e.g. atmospheric loading).

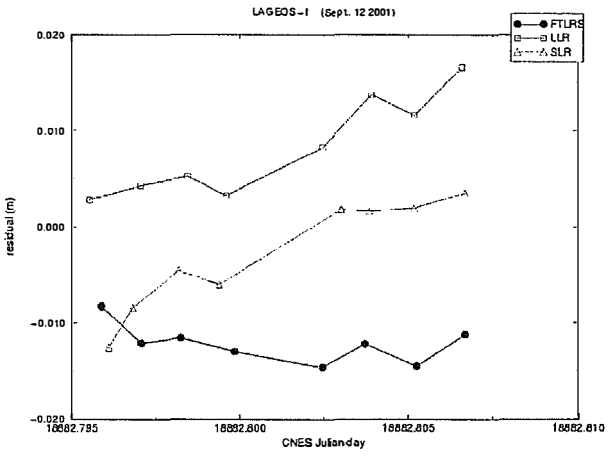

(3a)

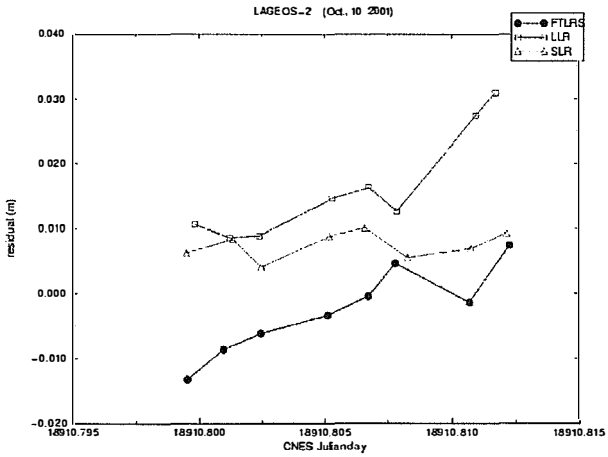

(3b)

Figure 3: Laser residuals (in meters) of the normal points of the three OCA laser systems.
(a) LAGEOS -1 pass of the 12th September 2001 (CNES Julian Day 18881);
(b) LAGEOS -2 pass of the 10th October 2001 (CNES Julian Day 18910).

The results of the mean residuals for the Grasse instruments are indicated in Table 1. The analysis of the common LAGEOS observations gave the following instrumental bias differences between the 3 Grasse laser stations:

- a bias difference of 5 mm between the fixed SLR station and the FTLRS,
- a bias difference of 18 mm between the LLR station and the FTLRS,
- and a bias difference of 13 mm between the LLR and SLR fixed stations.

Station	LAGEOS -1	LAGEOS -2
FTLRS	4 ± 2	1 ± 1
SLR	9 ± 2	7 ± 1
LLR	23 ± 1	20 ± 1

Table 1: Mean residual from reference orbits over 3 months (Sept. – Nov. 2001) for the 3 Grasse laser ranging stations: the fixed Satellite Laser Ranging station (SLR), the French transportable Laser Ranging Station (FTLRS), and the Lunar Laser Ranging station (LLR) based on the common normal points analysis. The values are given in millimeters.

These biases are obtained from a combination of LAGEOS -1 and -2 solution weighted by the normal point number, and the uncertainty on these biases is of 1 mm.

These results can be satisfactorily interpreted at the level of few millimeters as shown below and indicate the good quality of the performance of the FTLRS in its new configuration.

3.2. Discussion

Finally, this study shows the success of the FTLRS improvements. It also shows that today the satellite laser ranging technique reaches the level of a few millimeters.

Nevertheless, behind this few millimeter level reality, differences exist between the 3 Grasse laser stations in terms of mean laser residuals that we have to explain. In fact, there are instrumental explanations for these differences.

First of all, the range measurement differences can be linked to the fact that the array laser satellite signature, and particularly the satellite center of mass correction, depends on the detection level of the laser returns. We are currently performing computations on this point to determine the difference between the SLR and the LLR Grasse station measurements, since the first one is in a multi-photon detection and the second one is in a single photon electron detection. These computations of the LAGEOS satellite signature corrections are mainly based on raw data analysis and on geometrical considerations of the laser pulse impact on the satellite. The biases obtained from this analysis and from the method described above are very close and a first estimate shows a difference of about 3 mm between the SLR and the LLR station ranges caused by a difference in the LAGEOS satellite signature due to a different detection level (Nicolas J. et al., 2002). There is also a difference of 3 mm between the center of mass correction values between the LLR (244 mm) and the SLR (247 mm), whereas the standard value amounts to 251 mm.

There exists another important difference between the LLR and the two other OCA Grasse stations. Indeed, for the LLR station measurements, there is a well identified center edge effect (Schreiber U. and K.H. Haufe, 1998) on the photodiode delay of about 9 mm linked to the velocity aberration of LAGEOS satellites. Indeed, the tunings of the LLR instrument for the Moon tracking induce that the photons are always detected at the edge of the photodiode. The measured ranges are too long for the LLR station. This center edge effect would be at the level of 1 mm for the FTLRS and at the level of 5 mm for the SLR station.

Other sources of inaccuracy such as ground calibration value measurement and the local survey tie measurement accuracy would also contribute in the computed range biases between the 3 Grasse laser ranging stations, but at a level less than a few millimeters and less than the 2 first causes

previously given. For instance, with the 3 mm bias due to the center of mass correction and with the 4 mm center edge effect value difference (9 mm for the LLR and 5 mm for the SLR), we obtain a difference of 7 mm between the LLR and the SLR systems, whereas we found a difference of 13 mm. Thus, assuming an error of 2-3 mm for the calibration and as well as for the coordinate determination of each station, we can finally explain at the millimeter level the mean laser residual differences between the 3 OCA laser stations computed from the common normal points. All these results are very encouraging to ensure an accuracy at the level of few millimeters for these stations.

3.3. Comments on the particular case of TOPEX/Poseidon

We got a by-product of this collocation study with the analysis of the TOPEX/Poseidon (T/P) common passes between the FTLRS and the SLR fixed station. The purpose of this analysis was to validate the FTLRS capability for the oceanographic missions such as T/P. The idea was to check if we could use consistently both the OCA SLR system and the FTLRS on this kind of satellite.

For this analysis, we used the same method as the one used with the LAGEOS data except for the reference orbits. Indeed, for this part we used the reference orbits regularly computed by CNES (Nouël F. et al., 1994), (Barotto B. and J.P. Berthias, 1996) from which we computed mean laser residuals over the entire considered period common normal points. Then, we compared the results obtained with this T/P analysis and the LAGEOS -1 and -2 combined solutions previously obtained. Thus, it allowed us to conclude concerning the part of the instrumental bias coming from the station and the one coming from the satellite itself. We could only perform this analysis with the FTLRS and the fixed SLR data since the LLR station is unable to track satellites lower than 6000 km high. Thus, the LLR system is not concerned by this part of our analysis. The aim of this study was to check the tracking capability of the FTLRS for this kind of orbit since the observations of this mobile station are a key point in the altimeter calibration and in the orbit validation campaign (CAL/VAL) of Jason-1 performed in 2002. Indeed, during this phase Jason-1 and T/P would have the same trajectory, Jason-1 being only 1 minute ahead T/P. This study also allowed us to check if there were a problem with the particular retroreflector array of T/P since it is the only satellite with a ring of retroreflectors. Indeed, from many years a problem seemed to exist, especially for the European stations, a problem until now possibly interpreted as geographically correlated errors (Bonnefond P. et al., 1999). This is an important point for the T/P calibration and also for the Jason-1 altimeter cross calibration with the T/P one.

We benefited thus of the collocation configuration between the FTLRS and the SLR stations to consider the common passes on TOPEX/Poseidon (T/P). Fig. 4 shows laser residuals from a reference CNES orbit on a T/P pass observed by different European stations. It illustrates the good consistency between the T/P observations of these 4 stations.

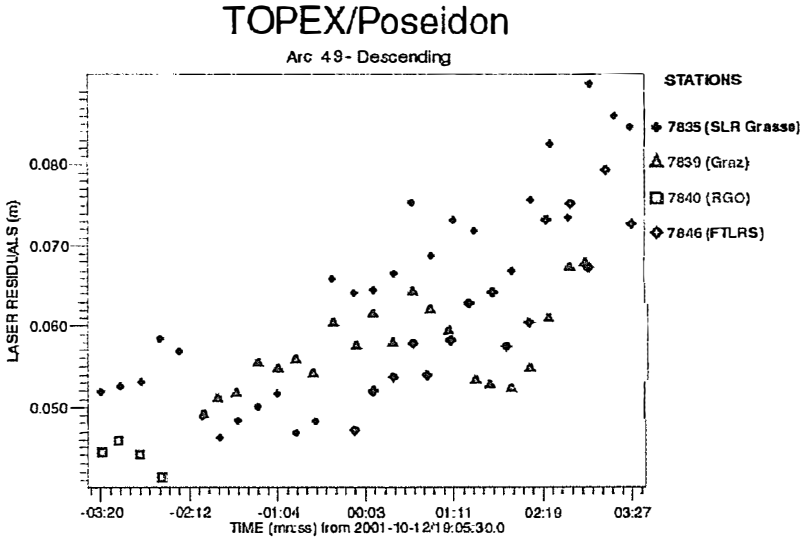

Figure 4: Laser residuals from a CNES reference orbit for TOPEX/Poseidon observations obtained simultaneously by 4 European stations: the FTLRS and the SLR in France, the Graz station in Austria and the Herstmonceux station in UK.

We analyzed the 957 common normal points between the OCA SLR system and the FTLRS. Their analysis over the 3 months from a reference CNES orbit gives a mean laser residual weighted by the normal point number of (2.3 ± 0.1) cm for the FTLRS and of (2.8 ± 0.1) cm for the Grasse SLR station. Then, we compared these results with the ones obtained with the common normal point analysis on LAGEOS satellites. The mean laser residuals from a combined LAGEOS -1 and -2 solution are of (4 ± 1) mm for the FTLRS and of (8 ± 1) mm for the SLR station (see Table 2). The T/P and LAGEOS analysis comparison indicates a systematic difference of about 5 mm between the FTLRS and the SLR stations which confirms the agreement between these two stations at this level. It also shows the stability of the quality of the FTLRS whatever the altitude of the observed satellites. We can say that the FTLRS has now the same level of quality as the OCA SLR station which confirms the success of the FTLRS improvements.

	LAGEOS -1		LAGEOS -2		Combination
Station	Stability (mm)	Mean residual (mm)	Stability (mm)	Mean residual (mm)	Mean residual (mm)
FTLRS	11	6 ± 1	7	3 ± 1	4 ± 1
SLR	7	9 ± 1	5	7 ± 1	8 ± 1
LLR	7	16 ± 1	6	17 ± 1	16 ± 1
Graz	7	4 ± 1	4	4 ± 1	4 ± 1
Herstmonceux	14	2 ± 1	5	2 ± 1	2 ± 1

Table 2: Stability and mean residuals for the entire period (Sept. – Nov. 2001) for LAGEOS -1 and -2 satellites for the different laser stations. The LAGEOS -1 and -2 combined residuals were computed from a weighted solution with the normal point number. The values are indicated in millimeters.

This analysis also indicates a systematic difference of about 2 cm between T/P and LAGEOS mean residuals, which is a significant result. This difference cannot be due to the station performance since we found the same bias result for two independent stations. Moreover, since this difference is not observed on the analysis of the Jason-1 first results and since these 2 satellites are on the same orbit, we can assume that this difference is properly linked to the T/P satellite itself, and not to the laser stations. T/P is a very particular target for satellite laser ranging because of its ring retroreflector array of about 85 cm diameter (see Fig. 5) placed around the altimeter antenna (Schwartz J., 1990); (Neubert R., 1995). Moreover, this difference is observed for the Herstmonceux station and for the Graz one at different levels, but not for the American laser ranging stations. The 2 cm bias may be due to the T/P retroreflector array model which seems to be incorrect in the case of some European stations. We are currently investigating to understand this difference. Indeed, the FTLRS, the SLR, the Graz and the Herstmonceux stations use a C-SPAD detector (Kirchner G. et al., 1997) whereas all the American ones use a photo-multiplier. The T/P retroreflector array model developed seems to be well fitted for this kind of detector used by the American but not for the European stations. Indeed, the model used has been developed especially for the stations equipped with photo-multiplier receivers whereas European stations commonly use photodiodes. This point, actually under investigation, is crucial for the T/P calibration data analysis.

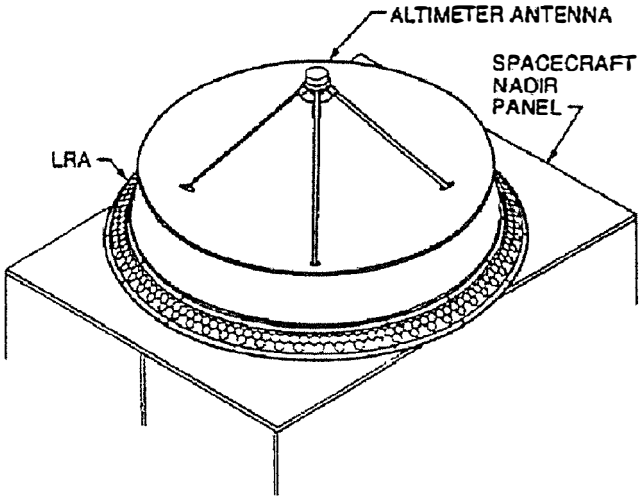

Figure 5: TOPEX/Poseidon laser retroreflector array (Schwartz J., 1990).

Finally, these results indicate that the T/P satellite signature is the same for the OCA SLR system and for the FTLRS. It shows that these two stations deliver consistent data at a sub-centimeter level. Thus, it confirms that the FTLRS performance meet the requirements of the CAL/VAL experiment of the T/P – JASON-1 tandem mission in 2002 in Corsica.

3.4. Global analysis

The common normal point analysis was then completed with the comparison over the entire considered period (September – November 2001) between the 3 OCA laser systems with a global analysis. For this global analysis, we used all the data available for the considered period. It allowed to have a better statistics (more data). Then, as an illustration, we compared the FTLRS with the Graz (Austria), and with the Herstmonceux (UK) stations, which are two European laser ranging stations of very high quality.

We first studied the stability of the mean laser residual computed each 10-day arc for each LAGEOS satellite and for each station. The number of normal points of each arc and the mean laser residuals are indicated on the Fig. 6. We defined the bias stability as the standard deviation of the mean of residuals computed arc-by-arc on the 10-day LAGEOS orbits over the entire collocation experiment duration, with respect to the mean of residuals over the 3-month experiment which we called bias. Then, we computed for each satellite and for a combined solution the mean bias for the whole collocation period for each station. The results are summarized in millimeters in Table 2.

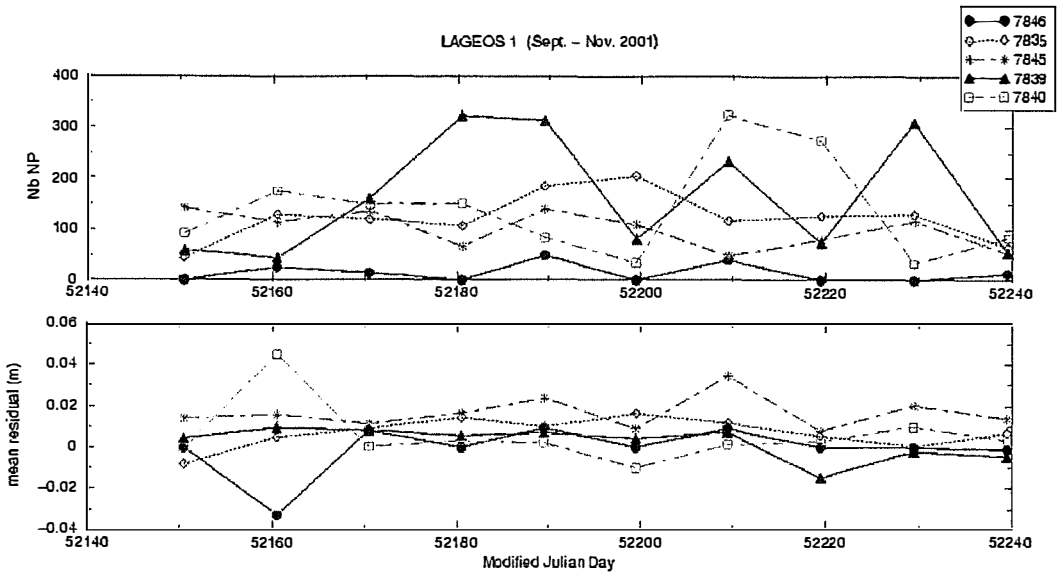

(6a)

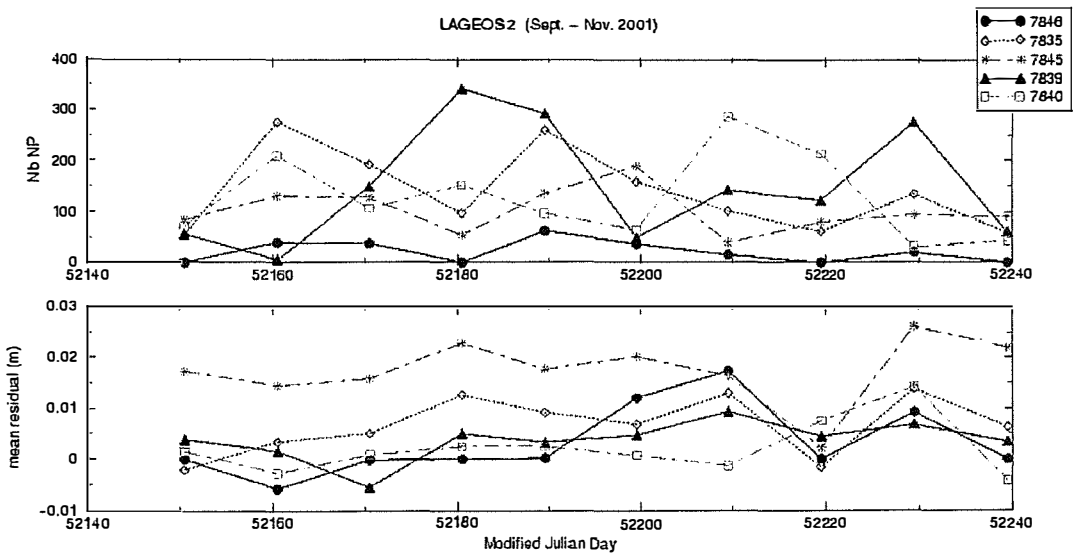

(6b)

Figure 6: Number of normal points and mean residual (in meters) for each LAGEOS 10-day arc and each laser station with respect to the date (in Modified Julian Day) during the entire collocation experiment (Sept. to Nov. 2001). 7846 stands for the FTLRS at Grasse, 7835 for the OCA SLR station, 7845 for the OCA LLR system, 7839 for the Graz station, and 7840 for the Herstmonceux station. (a) Results of LAGEOS -1 analysis; (b) Results of LAGEOS -2 analysis.

Finally, we computed the mean instrumental bias differences between the different instruments for a normal point number weighted LAGEOS -1 and -2 combined solution over the entire period. We found the following bias differences for the mobile station:

- a bias difference of (0 ± 1)mm between the FTLRS and the Graz station,
- a bias difference of (3 ± 1)mm between the FTLRS and the Herstmonceux station.

The comparison between the FTLRS results with other European reference laser stations gave a bias of few millimeters between the FTLRS and the Graz and the Herstmonceux SLR stations, which is a good result. These results confirm that this analysis does not change the bias difference values. It is mainly due to the high orbit quality, to the high coordinate quality, and to the mean consistency of the atmospheric perturbations at the European scale over a 3-month period.

4. Conclusion

In conclusion of this triple collocation experiment, the new performance of the FTLRS is validated at the level of few mm. Indeed, today we can say that this station in its new configuration has an accuracy level of a few millimeters according to the mean laser residuals based on LAGEOS data analysis. This result, which is very good in terms of SLR standards, indicates the success of the improvements of this instrument. It also confirms that this mobile system now meets the conditions required for the Jason-1 calibration and validation experiment, that is to say the 1-cm accuracy level. This result can be also extended to the ENVISAT calibration phase.

Our study shows also that the mean laser residual differences between the different OCA laser systems are explained at the millimeter level. It emphasizes the importance of different parameters to obtain such a few mm accuracy level for the laser ranging technique:

- the dependence of the satellite signature on the detection level,
- the center edge effect of the photo-detector,
- the geodetic local survey for coordinates determination and the ground calibration value measurement.

Another point, not discussed above, could also play a role in the final accuracy: it is the normal point computation method. In our analysis, the normal point computation for the 3 Grasse stations was performed with exactly the same method. But it is not the case when we compare the results with other laser stations which have their own normal point computation method. Even if it is almost the same, there are some differences which can induce visible differences at the accuracy level reached nowadays. Thus, the mode of data editing is another important factor in the process, and we have still to look later very carefully at this question.

Our results indicate that the FTLRS in its new configuration reaches the quality level of the best European stations, and thus that the mobile station can have a good place in the ILRS network. This is a very important result, and notably for the Jason-1 CAL/VAL experiment.

Another important by-product is the difference of 2 cm between LAGEOS and T/P mean laser residuals for both the FLTRS and the Grasse fixed SLR station, bias which is specific to the T/P satellite. It would be probably linked to a non-correct retroreflector array correction model used for some European laser stations. Computations are in progress on this particular point. So we confirm the T/P retroreflector array correction problem for the European stations, problem which was already suspected, but never proved.

Since the new performances of the FTLRS are validated, this station can be routinely used. The FTLRS has successfully performed the CAL/VAL campaign in Corsica from January to September 2002. Future campaigns are already planned, such as a campaign in Gavdos island (Crete) from March to June 2003 for Jason-1 and ENVISAT calibration and validation experiment (Mertikas S. et al., 2002) and a campaign in Normandy in France for ocean loading effect measurements in 2004.

Acknowledgments

We are grateful to F. Pierron in charge of the SLR and FTLRS instruments. We also thank J.-F. Mangin, who is in charge of the LLR station, for his computations of the LAGEOS satellite signature. Special recognition is given to all the observers who contributed to the data acquisition during this collocation experiment which considerably increased the tracking observation planning. The authors whish to acknowledge helpful discussions with E. Samain. We also thank J.-L. Hatat for his help and for his beautiful picture of the 3 stations simultaneously tracking a LAGEOS satellite.

The FTLRS experiment is supported by CNES, IGN, INSU, CNRS, and OCA. The SLR and the LLR stations are respectively supported by CNES and INSU. This work was supported by CNES, CNRS, INSU and the French Ministry of Research.

References

Altamimi Z., P. Sillard and C. Boucher, 2002. ITRF2000: a new release of the International Terrestrial Reference Frame for Earth science applications. Journal of Geophysical Research, 107, B8,

Barlier F., C. Berger, P. Bonnefond, P. Exertier, O. Laurain, J.F. Mangin and J.M. Torre, 2001. Laser-based validation of GLONASS orbits by short-arc technique. Journal of Geodesy, 75, pp. 600-612.

Barotto B. and J.P. Berthias, 1996. First results of reduced dynamics with DORIS on T/P and SPOT. Journal of guidance, control, and dynamics, Vol. 19, N° 6, pp. 1296 - 1302.

Biancale R., G. Balmino, J.M. Lemoine, J.C. Marty, B. Moynot, F. Barlier, P. Exertier, O. Laurain, P. Gegout, P. Schwintzer, C. Reigber, A. Bode, R. König, F.H. Massmann, J.C. Raimondo, R. Schmidt and S.Y. Zhu, 2000. A new global Earth's gravity field model from satellite orbit perturbations: GRIM5-S1. Geophys. Res. Lett., 27, N° 22, pp. 3611-3614.

Bonnefond P., P. Exertier and F. Barlier, 1999. Geographically correlated errors observed from a laser-based short-arc technique. J. G. R., 104 (7), pp. 15885-15893.

Exertier P., P. Bonnefond, J. Nicolas and F. Barlier, 2001. Contributions of Stallite Laser ranging to past and future radar altimetry missions. Surveys in Geophysics, Vol. 22, Nos. 5-6, pp. 491-507.

Germain T., 1999. Rattachement métrologique des axes Laser Lune, Laser satellite et laser satellite mobile, Rattachement altimétrique de dalles proches du réfectoire, Rattachement altimétrique de points de gravimétrie. Rapport IGN, IGN.

Kirchner G., F. Koidl, J. Blazej, K. Hamal and I. Prochazka, 1997. Time walk compensated SPAD : Multiple Photons Versus Single Photon Operation. Proceedings of SPIE Laser Radar Ranging and atmospheric Lidar Technique, EUROPTO Series. Ed. U. Schreiber and Ch. Werner, Vol. 3218, pp. 106-112.

Mccarthy D., 1996. IERS Conventions (1996). IERS Technical Note. Observatoire De Paris, 21,

Ménard Y., B. Haines and W.C.F.T.J.-C. Team, 2001. Jason-1 CALVAL Plan. CNES, NASA, and JPL, CNES, NASA, and JPL.

Ménard Y., E. Jeansou and P. Vincent, 1994. Calibration of TOPEX/Poseidon altimeters at Lampedusa : Additional results at Harvest,. J. Geophys. Res., 99 (C12), pp. 24487-24504.

Mertikas S., E. Pavlis, Tziavos, Drakopoulos, Pesec, Forsberg, Kahle and P. Exertier, 2002. Establishment of a European radar altimeter calibration and sea-level monitoring site for Jason, Envisat and EURO-GLOSS. Contract No: EVR1-CT-2001-40019.

Neubert R., 1995. Satellite signature model, application to LAGEOS and TOPEX. EUROLAS Meeting.

Nicolas J., P. Exertier, P. Bonnefond, F. Pierron, Y. Boudon, J.F. Mangin, F. Barlier, M. Kasser and J. Haase, 1999. Stability control and range biases on the French laser ranging stations. Proceedings of EUROPTO - SPIE Laser Radar Ranging and Atmospheric Lidar Technique II. Ed. U. Schreiber and Ch. Werner, Vol. 3865, pp. 27-32.

Nicolas J., J.-F. Mangin, G. Métris and F. Barlier, 2002. Difference of LAGEOS satellite response from raw data analysis of the collocation experiment between the Grasse Satellite and Lunar Laser Ranging stations. 13th International Laser Ranging Workshop "Towards Millimeter accuracy".

Nicolas J., F. Pierron, M. Kasser, P. Exertier, P. Bonnefond, F. Barlier and J. Haase, 2000. French transportable Laser Ranging Station : scientific objectives, technical features, and performance. Applied Optics, Vol. 39, No. 3, pp. 402-410.

Nicolas J., F. Pierron, E. Samain and F. Barlier, 2001. Centimetre accuracy for the French Transportable Laser Ranging Station (FTLRS) through sub-system controls. Surveys in Geophysics, Special Issue on Evolving Geodesy, Vol. 22, Nos. 5-6, pp. 449-464.

Niebauer T.M., G.S. Sasagawa, J.E. Faller, R. Hilt and F. Klopping, 1995. A new generation of absolute gravimeters. Metrologia, 32, 159-180.

Nouël F., J.P. Berthias, M. Delouze, A. Guitart, P. Laudet, A. Piuzzi, D. Pralines, C. Valorge, C. Dejoie, M.F. Susini and D. Tubariau, 1994. Precise Centre National d'Etudes Spatiales orbits for TOPEX/Poseidon : is reaching 2 cm still a challenge ? J. Geophys. Res., 99 (C12), pp. 24405-24419.

Samain E., J.F. Mangin, C. Veillet, J.M. Torre, P. Fridelance, J.E. Chabaudie, D. Feraudy, M. Glentzlin, J.P. Van, M. Furia, A. Journet and G. Vigouroux, 1998. Millimetric Lunar Laser Ranging at OCA. Astronomy and Astrophysics Supplement Series, 130, pp. 235-244.

Schreiber U. and K.H. Haufe, 1998. Timewalk in Avalanche Photodiode. Proceedings of the 11th International Workshop on Laser Ranging. published by the Bundesamt für Kartographie und Geodäsie, Frankfurt am Main, W. Schlüter, U. Schreiber and R. Dassing, 2, pp. 445-451.

Schwartz J., 1990. Pulse spreading and range correction analysis for satellite laser ranging. Applied Optics, Vol. 29, N° 25, pp. 3597-3602.

One way laser ranging in the solar system
The TIPO Project (Télémétrie InterPlanétaire Optique)

E. SAMAIN

Observatoire de la Côte d'Azur, 2130 route de l'observatoire, 06460 Caussols, France
(E-mail : etienne.samain@obs-azur.fr)

Abstract.

The Tipo project, Télémétrie InterPlanétaire Optique (InterPlanetary Optical Telemetry), is a one-way laser ranging experiment proposed in the frame of the first Mars Sample Return mission scheduled for 2007. A clock, a time tagging unit and a photo-detection system are implemented on board the spatial vehicle that will orbit around Mars. The principle of the experiment lies on the measure of the propagation duration of laser pulses emitted from an Earth laser station in the Martian orbiter direction. These laser pulses are timed on Earth and on board the orbiter, respectively in the time scale of the terrestrial clock and in the time scale of the orbiter clock. The distance between the Earth and the orbiter is computed from the difference between the start time and the arrival time on board. Since the link budget depends on the distance to the power two as compared to the power four for the classical two-ways laser ranging, measurements in the range of the solar system can be envisioned. Such a laser ranging telemetry has never been realised and has many technological and scientific applications. The instrumental description and the objectives of the experiment will be presented here.

Keywords:

Satellite laser ranging, TIPO, one way laser ranging, Solar system

1. Introduction

The usual Laser Ranging is based on the time propagation measurement of a light pulse emitted from a terrestrial laser station, reflected by a retro-reflector located on the target, and received by the same laser station (Degnan, 1993, Samain et al, 1998). In this scheme we have two solid angles, one at the emission, and another one at the reflection. Because of these solid angles, the link overall efficiency depends on the fourth power of the distance. The farthest distance currently reachable is the distance between the Earth and the Moon. In this case the ratio between the number of photons emitted per pulse (~ 10^{18}) and the number of photons received after reflection on the Lunar retro reflector (~ 0.01) is in the range of 10^{20}. Larger distance measurements can be envisioned by using a one way laser ranging technique with a link budget decreasing only as the square of the distance (Degnan et al, 1996, Veillet, 1994).

2. Instrumentation

2.1 Principle

The purpose of the project is to measure the distance between a laser station, located on the Earth, and a spacecraft in the solar system. The spacecraft has to be equipped with an ultra-stable clock, a photodetection device and an event timer linked to the clock. These equipments represent the TIPO payload. The Earth station is composed of a laser, a telescope, an ultra-stable clock and an event timer. The start times of the light pulses emitted by the laser station are recorded in the time scale of the terrestrial clock and the arrival times of the pulses on board of the spacecraft are recorded in the time scale of the space clock (Figure 1). The data corresponding to the arrival times on board of the spacecraft are transmitted later to the Earth with a classical microwave link. At the lowest level, propagation delay and distance between the Earth and the spacecraft are deduced from the differences between the arrival and departure times. Obviously the behaviour of the on-board clock is

a major factor in the accuracy of the experiment. This point is discussed in the next sections. Observations with several Earth laser stations permit to measure the angular position of the spacecraft and then to be able to locate the spacecraft in the plane perpendicular to the line of sight.

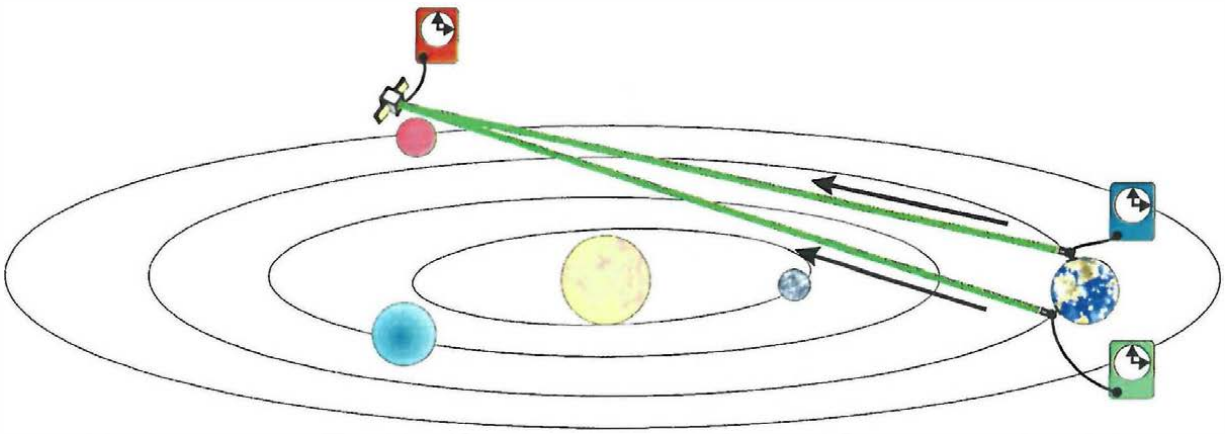

Figure 1: Tipo Principle. The distance between the Earth and the spacecraft is deduced from the differences between the arrival and departure times.

2.2 Mission

The spacecraft foreseen for the TIPO project is the CNES Mars 2007 Orbiter. This orbiter is an element of the PREMIER program (Programme de Retour d'Echantillons Martien et Installation d'Expérience en Réseau). PREMIER includes the development of a network of four Mars ground stations (NetLanders) (Marshal et al., 1999) aimed at performing geophysical measurements and the development of the orbiter vehicle of the future Mars Sample Return (MSR) mission to be performed in cooperation with the NASA. The aims of the CNES Mars 2007 orbiter are :

- Transport and deployement of the four NetLanders,
- Relay between the NetLanders and the Earth
- Rendez-vous in orbit
- Orbital science

The orbital science will be performed by a scientific payload involving several instruments and TIPO should be one of them. The volume and the mass of this Scientific payload should be respectively < 300 liters and < 120 kg.

2.3 Experimental description

The project is made of a space segment and a ground segment. The ground segment is an usual laser station operating in a one way mode. Figure 2 is a synoptic of this instrumentation.

The laser shots are synchronised to the clock in order to be able to generate pseudo random codes. These codes are required to improve the signal to noise ratio of the on-board detection. They will also permit to identify the echoes corresponding to different laser stations operating simultaneously.

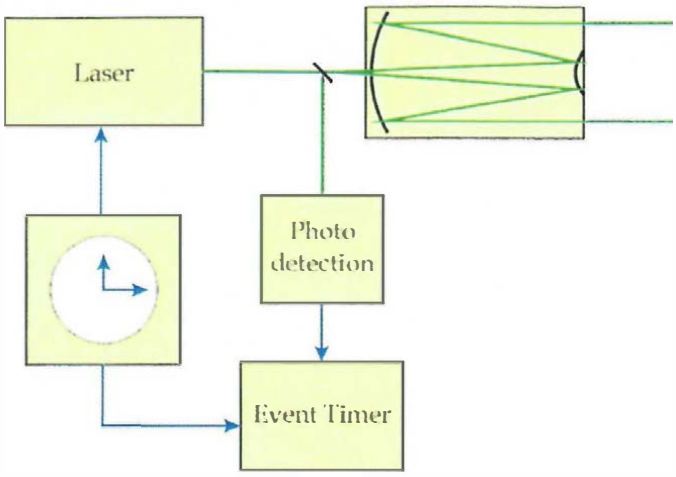

Figure 2: Synoptic of a one way laser ranging station. It is a classical laser ranging station without any reception channel.

The nominal laser rate is 10 Hz, the wavelength is 532 nm and the divergence beam is in the range of 5 arc seconds. The space segment includes an electronic module linked to an optic detection device (Figure 3). The on board detection optic is a telescope having an aperture of 100 mm. This telescope is pointed in the Earth direction with an accuracy of 0.2°. The space clock is an ultra-stable rubidium clock (Delporte, 2000) having a time stability σ_x in seconds of :

$$\tau < 1444\,\mathrm{s} : \sigma_x = 3.9 \cdot 10^{-13} \sqrt{\tau}$$

$$1444 < \tau < 10000\,\mathrm{s} : \sigma_x = 1.2 \cdot 10^{-14} \tau\ ,$$

where τ is the integration duration. The time stability of the clock can be maintained at the level of $\sigma_x = 3.9 \cdot 10^{-13} \sqrt{\tau}$ if the frequency drift of the oscillator can be removed.

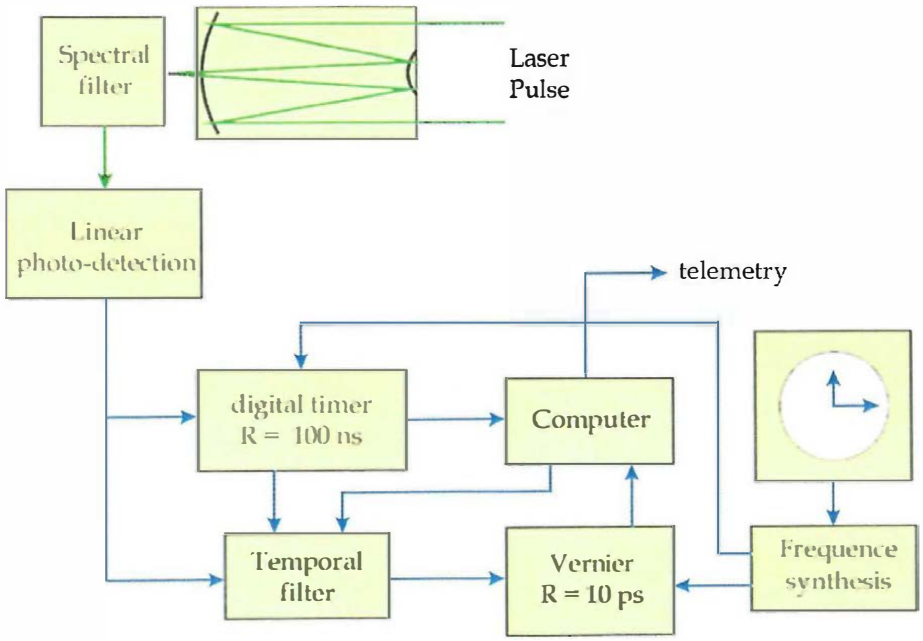

Figure 3: Synoptic of the space instrumentation.

This subtraction is possible only if the long-term behaviour of the oscillator is known. This behaviour can be measured with an external two-way microwave link (used for telecommunication and navigation) or extracted from the signature induced by the motion of the spacecraft. The global weight of the space instrumentation is roughly 11 kg, the power consumption is 30 W, and the volume is 8 liters.

2.4 Signal to noise ratio

Based on a Mars-Earth scenario, the link budget and noise evaluations give a signal to noise ratio between 0.8 and 5, depending on the distance between the Earth and the spacecraft. The photons number received on-board the spacecraft is below 100 per square meter and per pulse. This signal to noise ratio value implies to have an asynchronous temporal filter device. For this reason light pulses are emitted with a pseudo random code. A first acquisition phase during a few ten seconds permits to predict the arrival time of the next light pulses. This prediction allows the positioning of a detection gate around the expected arrival time of the next light pulse. This asynchronous detection mode allows a dramatic improvement of the signal to noise ratio.

2.5 Performances

The radial measurement performances of this one-way laser ranging are mainly driven by the time stability and the frequency accuracy of the on-board oscillator. The accurate distance between the Earth and the spacecraft can be obtained if the clock is able to “keep” the time during the cruise phase. In the Mars-Earth scenario this cruise phase duration is of the order of one year and getting a ranging accuracy at the meter level would imply a relative frequency accuracy of both the space and the ground clocks at the 10^{-16} level (Salomon et al, 2001). This kind of clock accuracy is not yet available but it should be obtained in the near future (Laurent et al, 1990, Salomon et al., 1996, Lea et al, 1994). In the frame of the TIPO project, the small space rubidium oscillator proposed will not permit to obtain such an accuracy and the accurate distance between the Earth and the spacecraft will not be measured. On the other hand, the very good short time stability of this oscillator allows determination of very precise distance variation for observation duration shorter than one day. The global error budget of the TIPO experiment shows that a centimetric precision should be obtained for radial distance variation integrated during less than 10 000 s.

The determination of the spacecraft position in the plane perpendicular to the line of sight relies on a differential measurement between light pulses coming from several laser stations. In this case, the time stability of the space clock is not involved and the performances of the position determination depend mainly on the time synchronisation of the Earth laser station. With a time synchronisation at the level of 30 ps, the angular accuracy is in the range of a few nano radians which implies a determination with an accuracy of a few hundreds of meters in the frame of the Mars-Earth distance.

3. Science

3.1 Introduction

The direct results of the measurement is set of times read out on the ground and on-board clocks. Times of flight of the light pulses are extracted from this data. Ultimately, this information is related to the distance, the refractive index of the medium and the local gravity field.

3.2 Measurement of the general relativity parameters γ

The γ parameter is deduced from the variation of the propagation duration of the light pulses which is induced from the gravity field modification along the line of sight (Ni, 1994, Ni, 1996, Mignard 2001) (Shapiro delay). The gravity field involved is induced by the sun and the gravity field variation is induced by the displacement of the beacon in the field of the sun. The Shapiro delay is maximum when the distance between the beam and the sun is minimum. In this case, the delay is in the range of 120 μs. The sensitivity of the measure is maximum when the derivative of the Shapiro delay is

maximum, that is to say, during the conjunction phase of Mars with the sun. A first conjunction will be obtained in December 2008 and another one in 2010. A first error budget estimation indicates that an improvement better than one order of magnitude should be reached.

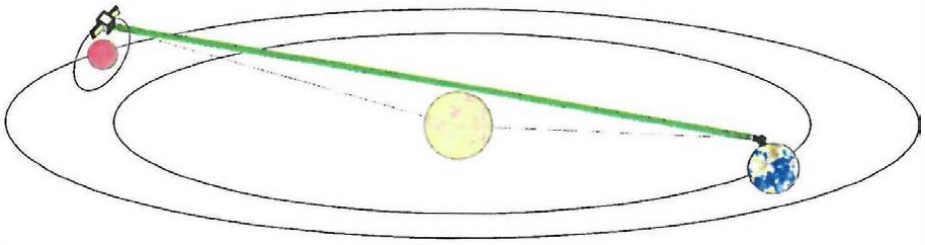

Figure 4: Spahiro Delay. This parameter is deduced from the variation of the propagation duration of the light pulses which is induced from the gravity field modification along the line of sight.

3.3 Martian and solar atmospheres

During occultation phases of the orbiter by Mars, the light beam through the atmosphere and generate a time propagation modification. The delays involved reach a few nano seconds when the distance between the light beam and the planet surface tends towards zero. The duration of the measurement is in the range of a few tens seconds. If the spacecraft orbit is known during this duration, the analysis of time propagation variation permits to extract atmospheric parameters.

This kind of analysis can also be achieved during solar occultation to extract some solar atmosphere characteristics.

3.4 Gravity field, orbitography

Gravity field studies of the Mars planet are split in two parts. The first one deals with short wavelength for the study of small structures such as volcanoes, mascon,.... . The second one deals with large wavelength at the scale of the planet for the determination of Mars mass. As compared to the terrestrial laser ranging, the short term stabilities are quit similar but the coverage is very different : it is local but distributed all over the world (40 laser stations) for the Earth laser ranging and global (complete tracking of the orbiter between the occultation phase) for TIPO.

3.5 Interplanetary medium

The large difference between the optical carrier of TIPO and the microwave carrier used for navigation and communication permits to improve the determination of Total Electronic Content (TEC) along the line of sight Mars-Earth. It is a differential measurement between optical signals coming from TIPO and microwave signals.

3.6 Navigation

TIPO is able to give a radial distance variation at a centimetre level for a time integration of 10 000 s and to give an accurate position in a plane perpendicular to the line of sight with an accuracy of a few hundreds of meters. This telemetry can be obtained during the cruise phase (from the Earth to Mars) and during the orbiting period. About forty laser stations in the world could potentially participate to this project. This large ground coverage counterbalance the reliability of the measurement induced by the fact that the technique is weather depend. The principle of the TIPO project is different from the classical microwave dopler technique using the great antenna of the Deep Space Network (DSN) and this independence should improve the global reliability of the means of navigation.

4. Conclusions, prospective

This experiment as never been realised. The spectacular improvement in the ultra-stable clocks domain, and the improvements expected in the near future will permit to dramatically improve the telemetry performances. Space qualified clocks (under development) having a frequency accuracy in the range of 10^{-16} will allow accurate measurement at a sub-metric level and differential measurements over a few days at a millimetric level. This one-way telemetry should become an excellent technique for measurements at the solar system scale and should give access to many scientific experiments such as :

- Equivalence principle (Touboul et al, 2001)
- Einstein effect
- γ measurement at a 10^{-7} level
- Mass determination of planets, asteroids (Su et al, 1999)
- Navigation

References

Degnan J., 1993, Contributions of space Geodesy to geodynamics : Technology Geodynamics, 25, 133-162

Degnan J. et al, 1996, Proceedings of 10th International Workshop on laser ranging Instrumentation, 24-31.

Delporte J. Brunet M., Tournier T., 2000, Complete evaluation of a PerkingElmer RAFS in the Galileo context, Proceedings of EFTF, Turin.

Laurent P. et al, 1990, Proceedings of the 25th rencontre de Moriond, ed Frontières.

Lea S. N. ett al, 1994, Physica Scripta, T51, 78-84.

Marshal O. et al., 1999, American Institute of aeronotics and astronotics Inc., CNES.

Mignard F. 2001, Fundamental physics with GAIA, J. Phys. IV France 1.

Ni W. T., Wu A. M., Shy J. T., 1994, Proceedings of the seventh Marcel Grossmann Meeting on general relativity, Standford, California 1519-1521.

Ni W. T., Sandford M.C.W., Veillet C. Wu A. M., Fridelance P., Samain E., Spalding G., Xu X., 1996, National Tsing Hua university preprint GP-074.

Salomon C. et al., 1996, ESA symposium proceedings on space utilisation, 289-294.

Salomon C. et al, 2001 C.R. Acad Sci Paris, t. 2 Série IV, 1313-1330.

Samain E. et al, 1998, Astron. Astrophys. Suppl. Ser. 130, 235-244

Su Z. Y. et al, 1999, Planetary ans space science 47, 339-343.

Touboul P. Rodrigues M., Metris G. Tatry B. ,2001, C.R. Acad. Sci. Paris, t.2, série IV, 1271-1286.

Veillet C., 1994, SORT, A proposal in the discipline area of fundamental physics in response to ESA's call for mission concepts for the follow up to horizon 2000.

Is there any frequency dependent time lag between atmospheric and geodetic excitation functions?

Wiesław Kosek[1], Waldemar Popiński[2], Harald Schuh[3], Michael Schmidt[4]

[1] Space Research Centre, Polish Academy of Sciences, Warsaw, Poland,
e-mail: kosek@cbk.waw.pl
[2] Department of Standards, Central Statistical Office, Warsaw, Poland,
e-mail: w.popinski@stat.gov.pl
[3] Institute of Geodesy and Geophysics, University of Technology, Wien, Austria,
e-mail: hschuh@luna.tuwien.ac.at
[4] Deutsches Geodätisches Forschungsinstitut (DGFI), München, Germany,
e-mail: schmidt@dgfi.badw.de

ABSTRACT

The purpose ot these investigations is to find frequency dependent time lags between complex-valued polar motion and its atmospheric excitation using the wavelet and Fourier transform techniques. The wavelet transform with Morlet analysing function (**MWT**) (Chui 1992), harmonic wavelet transform (**HWT**) (Newland 1998) and the Fourier transform band pass filter (**FTBPF**) (Popiński and Kosek 1995) techniques are applied. All these methods enable changing the frequency resolution of the coherence, cross-covariance and time lag functions. These functions are computed from the wavelet transform coefficients representing two time series in time-frequency domain (Popiński and Kosek 1994) or from the outputs of the FTBPF. The frequency dependent time lags computed for oscillations with periods ranging from 3 to 250 days correspond to maxima of the modules of cross-covariance functions between the polar motion and atmospheric excitation functions. The statistical errors of the computed coherence and time lag functions were determined in the Monte-Carlo experiment using white noise data. The coherences are significant for all short period oscillations. Time lag functions were obtained for oscillations with periods of about -50, -85 and 115 days.

1. DATA SETS

Atmospheric excitation functions $\chi_1^{w+p+ib}, \chi_2^{w+p+ib}$ - equatorial components of the effective atmospheric angular momentum (EAAM) reanalysis data in 1958.0-2002.2 from the U.S. NCEP/NCAR, the top of the model is 10 hPa (Barnes et al. 1983; Salstein et al. 1986; Kalnay et al. 1996; Salstein and Rosen 1997; AER 2002),

Geodetic excitation functions ψ_1, ψ_2 - computed from the IERSC04 x, y pole coordinates data in 1962-2002 (IERS 2002) using the time domain Wilson and Haubrich (1976) deconvolution formula (Chandler period equal to $1/F_C = 435\ days$, quality factor $Q_C = 100$).

2. THE FREQUENCY DEPENDENT CROSS-COVARIANCE AND TIME LAG FUNCTIONS

Frequency dependent cross-covariance function between complex-valued time series $x(t)$ and $y(t)$, $t = 0,1,...,N-1$,

$$\hat{C}_{xy}(\beta,a) = \sum_{k=0}^{N-1} \hat{X}(k,a)\overline{\hat{Y}(k+\beta,a)},$$

N - number of data, $\hat{X}(k,a)$, $\hat{Y}(k,a)$ - MWT or HWT coefficients or the FTBPF outputs.

Frequency dependent time lag function

$$\hat{\beta}(a) = \arg\max_{\beta \in D} \left| \hat{C}_{xy}(\beta, a) \right|,$$

the maximum is determined over some finite set $D = \{-K, -K+1, \ldots, K-1, K\}$ of time shifts β.

Coherence between $x(t)$ and $y(t)$

$$\hat{\gamma}_{xy}(a) = \frac{\left| \hat{C}_{xy}(0, a) \right|}{\sqrt{\hat{\sigma}_x^2(a) \hat{\sigma}_y^2(a)}},$$

where $\hat{\sigma}_x^2(a) = \sum_{k=0}^{N-1} \left| X(k,a) \right|^2$, $\hat{\sigma}_y^2(a) = \sum_{k=0}^{N-1} \left| \hat{Y}(k,a) \right|^2$.

3. MORLET WAVELET TRANSFORM (MWT) COEFFICIENTS

Continuous Wavelet Transform (CWT) of a signal $x(t)$ (Chui 1992):

$$\hat{X}(k,a) = \mid a \mid^{-1/2} \int_{-\infty}^{\infty} x(t) \overline{\varphi}((t-k)/a) dt,$$

where $\varphi(t) = \frac{1}{\sqrt{2\pi}} \exp(ipt) \left[\exp(-t^2/2\sigma^2) - \sqrt{2} \exp(-t^2/\sigma^2) \exp(-p^2\sigma^2/4) \right]$ is the Morlet wavelet function (Schmitz-Hübsch and Schuh 1999), σ, k, $a \neq 0$ are decay, translation and dilation parameters, respectively. $p = 2\pi$.

Continuous Fourier Transform (CFT) of the Morlet wavelet

$\breve{\varphi}(\omega) = \sigma \left[\exp(-(\omega - p)^2 \sigma^2 / 2) - \exp(-(\omega - p)^2 \sigma^2 / 4) \exp(-p^2 \sigma^2 / 4) \right]$. Coefficients $\hat{X}(k,a)$ involve CFT of the signal $\breve{x}(\omega)$ and the wavelet function

$$\breve{\varphi}(\omega): \hat{X}(k,a) = \frac{1}{2\pi} \mid a \mid^{1/2} \int_{-\infty}^{\infty} \breve{x}(\omega) \overline{\breve{\varphi}}(a\omega) \exp(ik\omega) d\omega.$$

4. HARMONIC WAVELET TRANSFORM (HWT) COEFFICIENTS

HWT coefficients of a signal $x(t)$ (Newland 1998):

$$\hat{X}(k,a) = \int_{-\infty}^{\infty} \overline{w}(t-k,a) x(t) dt,$$

$w(t,a)$ - harmonic wavelet function localised in frequency domain, a, k - period and translation parameters.

Frequency domain formula:

$$\hat{X}(k,a) = \int_{-\infty}^{\infty} \breve{w}(\omega, a) \breve{x}(\omega) \exp(ik\omega) d\omega.$$

where: $\breve{w}(\omega, a) = \begin{cases} \exp\left[-(1/a - \omega)^2 / (2\sigma^2) \right] & if \quad \mid 1/a - \omega \mid \leq \lambda, \\ 0 & otherwise, \end{cases}$ λ - window halfwidth, σ - smoothing parameter.

5. FOURIER TRANSFORM BAND PASS FILTER (FTBPF)

FTBPF output: $\widehat{X}(k,a) = FFT^{-1}\left[A(P,a)FFT\left(x(k)\right)\right]$, where a - oscillation period, FFT - Singleton (1969) Fast Fourier Transform operator

$$A(P,a) = \begin{cases} 1-\left(\dfrac{1/a-1/P}{\lambda}\right)^2 & if \quad |1/a-1/P| \le \lambda \\ 0 & otherwise, \end{cases}$$

- parabolic transfer function, λ - frequency bandwidth, P - period argument.

6. COHERENCES BETWEEN THE ATMOSPHERIC AND GEODETIC EXCITATION FUNCTIONS AND THEIR STATISTICAL ERRORS

The MWT, HWT and FTBPF coherences between atmospheric and geodetic excitation functions together with their statistical errors. The statistical errors were computed in the Monte-Carlo experiment as the mean of 500 samples of the computed MWT, HWT and FTBPF coherences between the $u(t)$ and $v(t)$ gaussian white noise data. The coherences and their statistical errors depend on the parameter values of σ, $\lambda = \sigma$ and λ in the MWT, HWT and FTBPF, respectively. The MWT statistical errors increase with the oscillation period, the HWT/FTBPF ones are almost constant (Popiński at al. 2002).

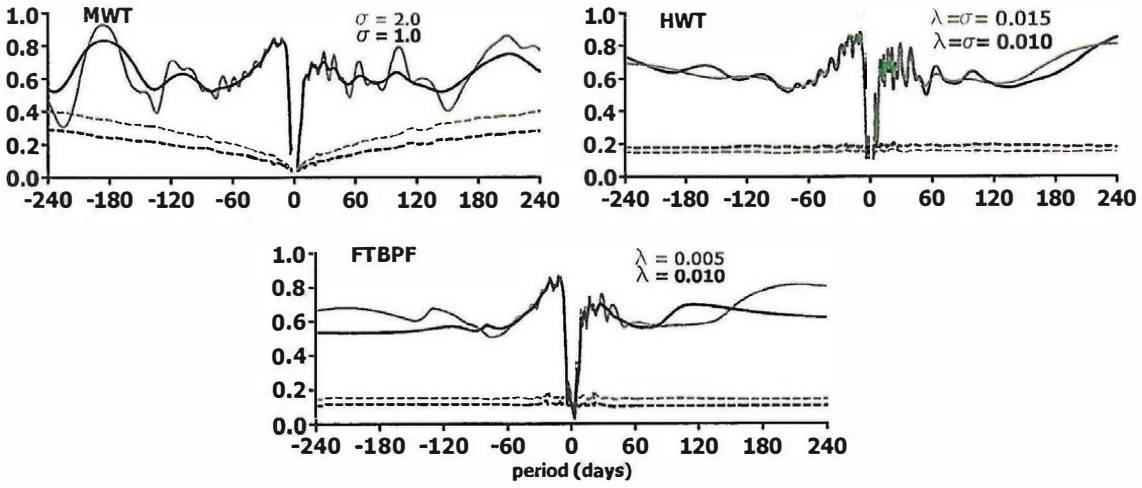

Fig. 1: The MWT, HWT and FTBPF coherence functions between the complex-valued atmospheric $\chi_1 + i\chi_2$ and geodetic $\psi_1 + i\psi_2$ excitation functions in 1986.0-2002.0 together with their statistical errors for different values of σ (MWT), $\lambda = \sigma$ (HWT) and λ (FTBPF), respectively.

7. THE CROSS-COVARIANCE AND TIME LAG FUNCTIONS BETWEEN THE ATMOSPHERIC AND GEODETIC EXCITATION FUNCTIONS AND THEIR STATISTICAL ERRORS

Figure 2: MWT, HWT and FTBPF cross-covariance and time lag functions between the atmospheric and geodetic excitation functions.

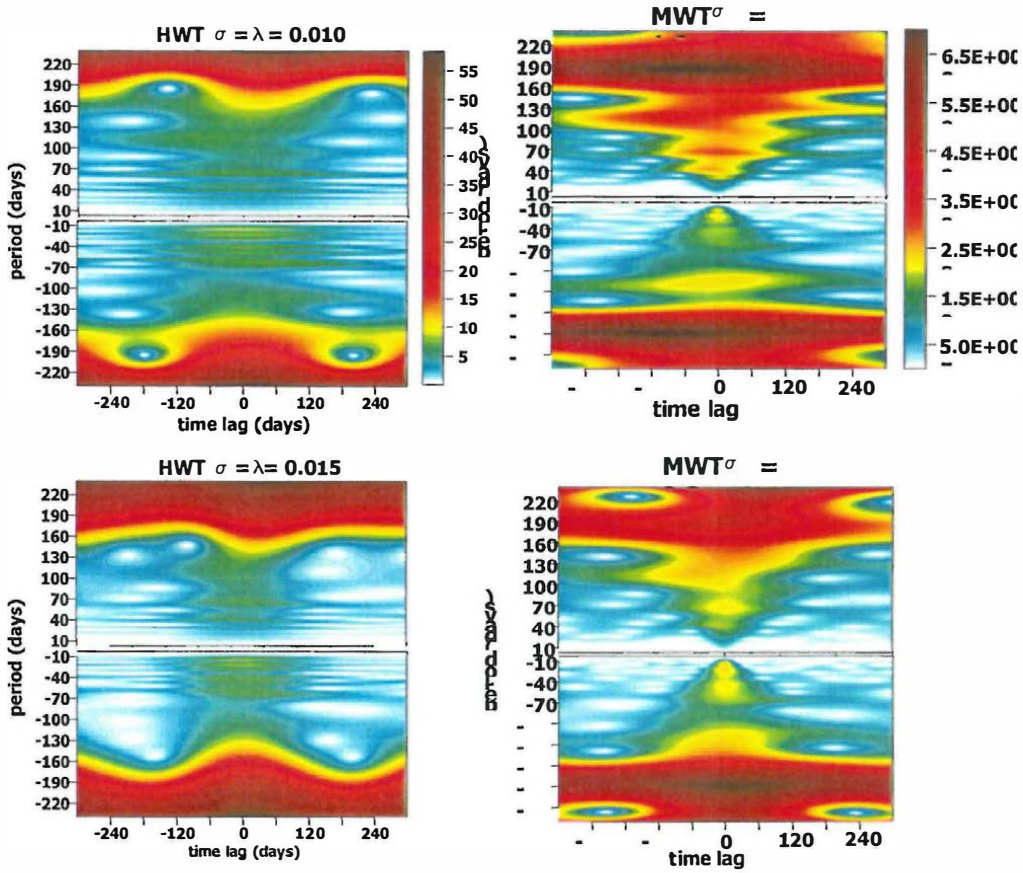

Fig. 2a,b: The MWT and HWT cross-covariance functions between the complex-valued atmospheric $\chi_1 + i\chi_2$ and geodetic $\psi_1 + i\psi_2$ excitation functions in 1986.0 – 2002.0 for different values of σ and $\lambda = \sigma$, respectively.

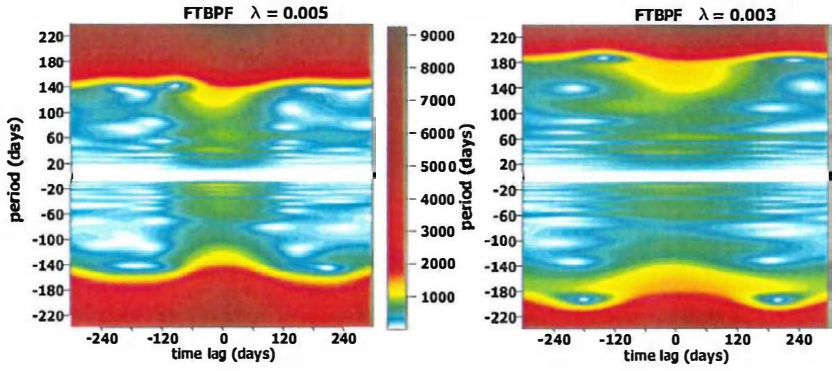

Fig. 2c: The FTBPF cross-covariance functions between the complex-valued atmospheric $\chi_1 + i\chi_2$ and geodetic $\psi_1 + i\psi_2$ excitation functions in 1986.0 – 2002.0 for different values of λ, respectively.

Figure 3: The time lag functions between the atmospheric and geodetic excitation functions. The statistical errors of the time lag functions were computed as the mean of 500 absolute values of the computed MWT, HWT and FTBPF time lag functions between the $w(t)+u(t)$ and $w(t)+v(t)$ white noise data. The increase of σ in the MWT and the decrease of $\lambda=\sigma$ and λ in the HWT and FTBPF, respectively increases the frequency resolution of the coherence and cross-covariance functions. The frequency resolution of the coherence (Fig. 1), cross-covariance (Fig. 2) and time delay (Fig. 3) functions grows faster with decrease of the period for the HWT than for the MWT and FTBPF (Popiński et al. 2001). The absolute values of the computed MWT, HWT and FTBPF time lag functions exceed the estimated statistical errors for oscillations with periods of about -50, -85, and +115 days which means that they are significant, however the precise time lag values are very difficult to determine.

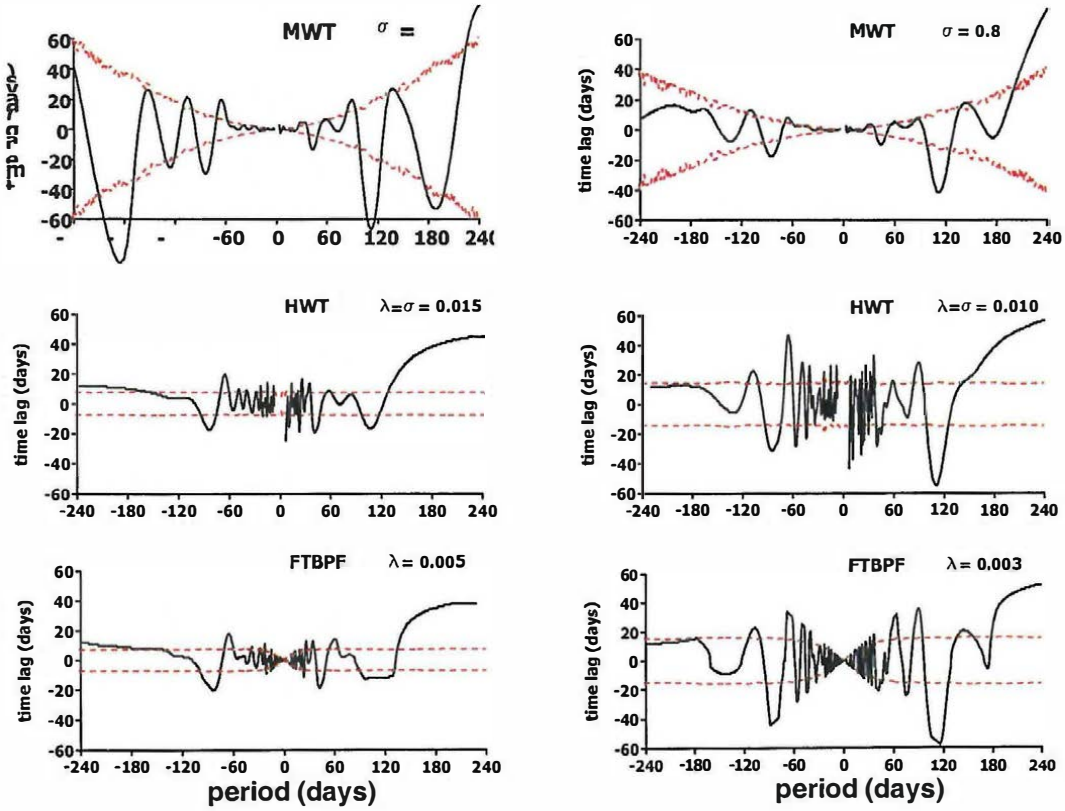

Fig. 3: The **MWT, HWT** and **FTBPF** time lag functions between the atmospheric $\chi_1+i\chi_2$ and geodetic $\psi_1+i\psi_2$ excitation functions in 1986.0 – 2002.0 together with their statistical errors (red) for different values of σ, $\lambda=\sigma$ and λ, respectively.

Figure 4: The ratio of standard deviations of the $w(t)$ and $u(t)$ (or $v(t)$) white noise data, equal to 0.9, was chosen so that the mean of 500 samples for the MWT, HWT and FTBPF coherences between $w(t)+u(t)$ and $w(t)+v(t)$ white noise data is approximately of the same order as the coherences between the atmospheric and geodetic excitation functions (Fig. 1).

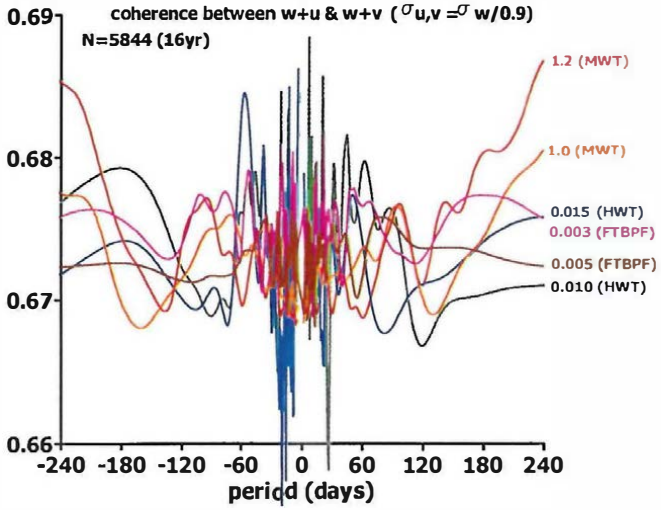

Fig. 4: The mean (from 500 samples) MWT, HWT and FTBPF coherences between $w(t)+u(t)$ and $w(t)+v(t)$ white noise data for different parameter values.

8. CONCLUSIONS

Negative values of time lags for oscillations with periods of -50, -85 and +115 days mean that these oscillations appear earlier in the atmospheric than in the geodetic excitation function.

The values of time lags differ for the applied methods and depend on their parameter values, so they are very difficult to determine precisely. In the case of oscillations with periods different from those given above the exchange of the equatorial atmospheric angular momentum and the angular momentum of the Earth seems to be immediate.

Acknowlegement.

This paper was supported by the Polish Committee of Scientific Research project No 8T12E 005 20 under the leadership of W. Kosek.

REFERENCES

AER 2002, EAAM reanalysis data of the NCEP/NCAR, anonymous ftp service: ftp.aer.com/pub/sba

Barnes R.T.H., Hide R., White A.A., and Wilson C.A. 1983, Atmospheric Angular Momentum Fluctuations, length-of-day changes and polar motion, Proc. R. Soc. London, A387, 31-73.

Chui C.K. 1992, An Introduction to Wavelets, Wavelet Analysis and its Application Vol. 1, Academic Press, Boston-San Diego.

IERS 2002, The Earth Orientation Parameters, http://www.iers.org/iers/earth/rotation/eop/eop.html.

Kalnay E., Kanamitsu M., Kistler R., Collins W., Deaven D., Gandin L., Iredell M., Saha S., White G., Woollen J., Zhu Y., Chelliah M., Ebisuzaki W., Higgins W., Janowiak J., Mo. K., Ropelewski C., Wang J., Leetmaa A., Reynolds R., Jenne R. and Joseph D.,1996, The NCEP/NCAR 40-year reanalysis project, Bull. Amer. Meteor. Soc., 77, 437-471.

Newland D.E. 1998, Time-Frequency and Time-Scale Signal Analysis by Harmonic Wavelets, in Signal Analysis and Prediction, A. Prohazka, J. Uhlir, P.J. Rayner, N.G. Kingsbury (eds), Birkhauser, Boston.

Popiński W., Kosek W. 1994, Wavelet Transform and Its Application for Short Period Earth Rotation Analysis, Artificial Satellites, Vol. 29, No 2, 75-83.

Popiński W., Kosek W., 1995. The Fourier Transform Band Pass Filter and Its Application to Polar Motion Analysis., Artificial Satellites, Planetary Geodesy No 24, Vol. 30 No 1 - 1995, 9-25.

Popiński W., Kosek W., Schuh H. and Schmidt M., 2001, Comparison of two wavelet transform coherence and cross-covariance functions applied on polar motion and atmospheric excitation, Proc. IAG 2001 Scientific Assembly, 2-7 September 2001 - Budapest, Hungary

Popiński W., Kosek W., Schuh H. and Schmidt M., 2002, Comparison of two wavelet transform coherence and cross-covariance functions applied on polar motion and atmospheric excitation, Studia geophysica et geodetica, 45, (2002), 455-468,

Salstein D.A., D.M. Kann, A.J. Miller, R.D. Rosen 1986, The Sub-bureau for Atmospheric Angular Momentum of the International Earth Rotation Service: A Meteorological Data Center with Geodetic Applications, Bull. Amer. Meteor. Soc., 74, 67-80.

Salstein D.A. and R.D. Rosen 1997, Global momentum and energy signals from reanalysis systems. Preprints of the 7th Conf. on Climate Variations, American Meteorological Society, Boston, MA, 344-348.

Schmidt M. and Schuh H. 2000a, Abilities of Wavelet Analysis for Investigating Short-Period Variations of Earth Rotation, IERS Technical Note No 28, Observatoire de Paris, 73-80.

Schmidt M. and Schuh H. 2000b, Frequency-dependent phase lags between LOD- and AAM-variations detected by wavelet analysis, poster presented at the EGS 25th General Assembly, Nice, France, 24-29 April 2000, http://www.dgfi.badw.de/dgfi/DOC/2000/schmidt_egs00.pdf

Schmitz-Hübsch H., Schuh H. 1999, Seasonal and Short-Period Fluctuations of Earth Rotation Investigated by Wavelet Analysis, Technical Report Nr. 1999.6-1, Department of Geodesy and Geoinformatics, Universität Stuttgart : "Quo vadis Geodesia ...?", Festschrift for Erik W. Grafarend on the occasion of his 60th birthday, F. Krumm, V.S. Schwarze (Eds), 421-431.

Singleton R.C. 1969, An Algorithm for Computing the Mixed Radix Fast Fourier Transform, IEEE Transactions on Audio and Electroacoustics, Vol. AU-17, No 2, 93-103.

Wilson C.R. and Haubrich R.A. 1976, Meteorological Excitation of the Earth's Wobble, Geophys. J. R. Astron. Soc., 46, 707-743.

Bisher erschienen:

Heft1: Kolloquium der Assistenten der Studienrichtung Vermessungswesen. 1970 - 1973, Dezember 1973.

Heft 2: EGGER-PERDICH-PLACH-WAGENSOMMERER, Taschenrechner HP 45 und HP 65, Programme und Anwendungen im Vermessungswesen. 1. Auflage, März 1974, Special Edition in English, Juli 1974, 2. verbesserte Auflage, November 1974.

Heft 3: Kolloquium der Assistenten der Studienrichtung Vermessungswesen 1973 - 1974, September 1974.

Heft 4: EGGER-PALFINGER-PERDICH-PLACH-WAGENSOMMERER, Tektronix-Tischrechner TEK 31, Programmbibliothek für den Einsatz im Vermessungswesen, November 1974.

Heft 5: K.LEDERSTEGER, Die horizontale Isostasie und das isostatische Geoid, Februar 1975.

Heft 6: F.REINHART, Katalog von FK4 Horrebow-Paaren für Breiten von +30 bis +60, Oktober 1975.

Heft 7: Arbeiten aus dem Institut für Höhere Geodäsie, Wien, Dezember 1975.

Heft 8: Veröffentlichungen des Instituts für Photogrammetrie zum XIII. Internationalen Kongreß für Photogrammetrie in Helsinki 1976, Wien, Juli 1976.

Heft 9: W.PILLEWIZER, Felsdarstellung aus Orthophotos, Wien, Juni 1976.

Heft 10: PERDICH-PLACH-WAGENSOMMERER, Der Einsatz des programmierbaren Taschenrechners Texas Instruments SR-52 mit Drucker PC100 in ingenieurgeodätischen Rechentechnik, Wien, Mai 1976.

Heft 11: Kolloquium der Assistenten der Studienrichtung Vermessungswesen 1974 - 1976, November 1976.

Heft 12: Kartographische Vorträge der Geodätischen Informationstage 1976, Wien, Mai 1977.

Heft 13: Veröffentlichung des Instituts für Photogrammetrie anläßlich des 80. Geburtstages von Prof.Dr.h.c.K.Neumaier, Wien, Januar 1978.

Heft 14: L.MOLNAR, Self Checking Analytical Relative Orientation and Strip Formation, Wien, Dezember 1978.

Heft 15: Veröffentlichung des Instituts für Landesvermessung anläßlich des 80. Geburtstages von Prof.Dr.Alois Bavir, Wien, Januar 1979.

Heft 16: Kolloquium der Assistenten der Studienrichtung Vermessungswesen 1976 - 1978, Wien, November 1979.

Heft 17: E.VOZIKIS, Die photographische Differentialumbildung gekrümmter Flächen mit Beispielen aus der Architekturbildmessung, Wien, Dezember 1979.

Heft 18: Veröffentlichung des Instituts für Allgemeine Geodäsie anläßlich des 75. Geburtstages von Prof.Dipl.Ing.Dr.F.Hauer, Die Höhe des Großglockners, Wien, 1981.

Heft 19: H.KAGER, Bündeltriangulation mit indirekt beobachteten Kreiszentren, Wien, April 1981.

Heft 20: Kartrographische Vorträge der Geodätischen Informationstage 1980, Wien, Mai 1982.

Heft 21: Veröffentlichung des Instituts für Kartographie anläßlich des 70. Geburtstages von Prof.Dr.Wolfgang Pillewizer: Glaziologie und Kartographie, Wien, Dezember 1982.

Heft 22: K.TEMPFLI, Genauigkeitsschätzung digitaler Höhenmodelle mittels Spektralanalyse, Wien, Mai 1982.

Heft 23: E.CSAPLOVICS, Interpretation von Farbinfrarotbildern, Wien, November 1982.

Heft 24: J.JANSA, Rektifizierung von Multispektral-Scanneraufnahmen - Entwicklung und Erprobung eines EDV-Programms, Wien, Mai 1983.

Heft 25: Zusammenfassung der Diplomarbeiten, Dissertationen und Habilitationen an den geodätischen Instituten der TU Wien, Wien, November 1984.

Heft 26: T.WUNDERLICH, Die voraussetzungsfreie Bestimmung von Refraktionswinkeln, Wien, August 1985.

Heft 27: G.GERSTBACH (Hrsg.), Geowissenschaftliche/geotechnische Daten in Landinformationssystemen - Bedarf und Möglichkeiten in Österreich, Juni 1986.

Heft 28: K.NOVAK, Orientierung von Amateuraufnahmen ohne Paßpunkte, Wien, August 1986.

Heft 29: Veröffentlichung des Instituts für Landesvermessung und Ingenieurgeodäsie, Abt. Ingenieurgeodäsie, anläßlich des 80. Geburtstages von Prof.Dipl.Ing.Dr.F.Hauer, Wien, Oktober 1986.

Heft 30: K.-H.ROCH, Über die Bedeutung dynamisch ermittelter Parameter für die Bestimmung von Gesteins- und Gebirgseigenschaften, Wien, Februar 1987.

Heft 31: G. HE, Bildverbesserung mittels digitaler Filterung, Wien, April 1989.

Heft 32: F.SCHLÖGELHOFER, Qualitäts- und Wirtschaftlichkeitsmodelle für die Ingenieurphotogrammetrie, Wien, April 1989.

Heft 33: G.GERSTBACH (Hrsg.), Geowissenschaftliche/geotechnische Daten in Landinformationssystemen - Datenbestände und Datenaustausch in Österreich, Wien, Juni 1989.

Heft 34: F.HOCHSTÖGER, Ein Beitrag zur Anwendung und Visualisierung digitaler Geländemodelle, Wien, Dezember 1989.

Heft 35: R.WEBER, Lokale Schwerefeldmodellierung unter Berücksichtigung spektraler Methoden zur Geländereduktion, Wien, April 1990.

Heft 36: o.Prof.Dr.Hans Schmid zum 70. Geburtstag. Veröffentlichung der Abteilung für Landesvermessung, Wien, Oktober 1990.

Heft 37: G.GERSTBACH, H.P.HÖLLRIEGL und R.WEBER, Geowissenschaftliche Informationsbörse - Eine Nachlese zu GeoLIS II, Wien, Oktober 1990.

Heft 38: R.ECKER, Rastergraphische Visualisierungen mittels digitaler Geländemodelle, Wien, August 1991.

Heft 39: Kartographische Forschungen und Anwendungsorientierte Entwicklungen, herausgegeben von W.Stams und F.Kelnhofer zum 80. Geburtstag von Prof.Dr.W.Pillewizer, Wien, Juli 1991.

Heft 39a: W.RIEGER, Hydrologische Anwendungen des digitalen Geländemodelles, Wien, Juli 1992.

Heft 40: K.STEINNOCHER, Methodische Erweiterungen der Landnutzungsklassifikation und Implementierung auf einem Transputernetzwerk, Wien, Juli 1994.

Heft 41: G.FORKERT, Die Lösung photogrammetrischer Orientierungs- und Rekonstruktionsaufgaben mittels allgemeiner kurvenförmiger Elemente, Wien, Juli 1994.

Heft 42: M.SCHÖNER, W.SCHÖNER, Photogrammetrische und glaziologische Untersuchungen am Gàsbre (Ergebnisse der Spitzbergenexpedition 1991), Wien, Mai 1996.

Heft 43: M.ROIC. Erfassung von nicht signalisierten 3D-Strukturen mit Videotheodoliten, Wien, April 1996.

Heft 44: G.RETSCHER, 3D-Gleiserfassung mit einem Multisensorsystem und linearen Filterverfahren, Wien, April 1996.

Heft 45: W.DAXINGER, Astrogravimetrische Geoidbestimmung für Ingenieurprojekte, Wien, Juli 1996.

Heft 46: M.PLONER, CCD-Astrometrie von Objekten des geostationären Ringes, Wien, November 1996.

Heft 47: Zum Gedenken an Karl Killian "Ingenieur" und "Geodät" 1903-1991, Veröffentlichung der Fachgruppe Geowissenschaften, Wien, Februar 1997.

Heft 48: A.SINDHUBER, Ergänzung und Fortführung eines digitalen Landschaftsmodelles mit multispektralen und hochauflösenden Fernerkundungsaufnahmen, Wien, Mai 1998.

Heft 49: W.WAGNER, Soil Moisture Retrieval from ERS Scatterometer Data, Wien, Dezember 1998.

Heft 50: R.WEBER, E.FRAGNER (Editoren),Prof.Bretterbauer, Festschrift zum 70.Geburtstag, Wien, Juli 1999.

Heft 51: Ch.ÖHRENEDER, A Similarity Measure for Global Image Matching Based on The Forward Modeling Principle, Wien, April 1999.

Heft 52: M.LECHTHALER, G.GARTNER, Per Aspera ad Astra, Festschrift für Fritz Kelnhofer zum 60. Geburtstag, Wien, Jänner 2000.

Heft 53: F.KELNHOFER, M.LECHTHALER, Interaktive Karten (Atlanten) und Multimedia – Applikationen, Wien, März 2000.

Heft 54: A.MISCHKE, Entwicklung eines Videotheodlit-Meßsystems zur automatischen Richtungsmessung von nicht signalisierten Objektpunkten, Wien, Mai 2000

Heft 55: Veröffentlichung des I.P.F. anlässlich der Emeritierung von Prof.Dr. Peter Waldhäusl, Wien.

Heft 56: F.ROTTENSTEINER, Semi-automatic Extraction of Buildings Based on Hybrid Adjustment Using 3D Surface Models and Management of Building Data in a TIS, Wien, Juni 2001.

Heft 57: D.LEGENSTEIN, Objektrekonstruktion aus perspektiven Bildern unter Einbeziehung von Umrisslinien, Wien, Mai 2001.

Heft 58: F.KELNHOFER, M.LECHTHALER und K.BRUNNER (Hrsg.), Telekartographie und Location Based Services, Wien, Jänner 2002.

Heft 59: K.BRETTERBAUER, Die runde Erde eben dargestellt: Abbildungslehre und sphärische Kartennetzentwürfe, Wien, 2002.

Heft 60: G.GARTNER, Maps and the Internet 2002, Wien 2002.

Heft 61: L.DORFFNER, Erzeugung von qualitativ hochwertigen 3D Photomodellen für Internetbasierte Anwendungen mit besonderem Augenmerk auf Objekte der Nahbereichsphotogrammetrie, Wien, Jänner 2002.

Heft 62: CHMELINA, Wissensbasierte Analyse von Verschiebungsdaten im Tunnelbau Wien 2002

Heft 63: A.NIESSNER, Qualitative Deformationsanalase unter Ausnutzung der Farbinformation, Wien 2002

Heft 64: K.BRETTERBAUER; R.WEBER, A Primer of Geodesy for GIS-Users, Wien im Herbst 2003

Heft 65: N.PFEIFER, 3D Terain Models on the basis of a triangulation, Wien, Jänner 2002.

Heft 66: G.GARTNER (Hrsg), Lacation Based Services & Telecartography, Wien, 2004.

Heft 67: I.KABASHI, Gleichzeitig-gegenseitige Zenitwinkelmessung über größere Entfernungen mit automatischen Zielsystemen, Wien, 2004.

Heft 68: J. BÖHM, Troposphärische Laufzeitverzögerungen in der VLBI, Wien, 2004.